

QC852
.C6
no. 429
ARCHIVE



USAF, NSF ATM-8419116
NSF ATM-8418204

Investigation of Tropical Cyclone Genesis and Development Using Low-level Aircraft Flight Data

by Michael G. Middlebrooke

P. I.: William M. Gray



Atmospheric Science

PAPER NO.
429

DEPARTMENT OF ATMOSPHERIC SCIENCE
COLORADO STATE UNIVERSITY
FORT COLLINS, COLORADO

INVESTIGATION OF TROPICAL CYCLONE GENESIS AND
DEVELOPMENT USING LOW-LEVEL AIRCRAFT FLIGHT
DATA

By
Michael G. Middlebrooke

Department of Atmospheric Science
Colorado State University
Fort Collins, CO 80523

May, 1988

Atmospheric Science Paper No. 429

ABSTRACT

Low-level wind and pressure observations from aircraft weather reconnaissance missions flown in the western North Pacific were composited on a polar coordinate grid. The observations are from eight years of US Air Force investigative and center-fix missions flown into both developing and non-developing tropical disturbances during the period 1977-1984. The missions were separated into various categories depending on the type of disturbance which they were flown in; e.g., genesis vs. non-genesis, or development stage 1, 2, or 3, or pre-tropical storm vs. pre-typhoon. Data composites were made for each category.

A comparison of the genesis and non-genesis composites reveals only slight differences in the sea-level pressure (SLP) and tangential wind fields out to 5° latitude (555 km) from the center. But the genesis composite is found to have significantly higher inner-core (within 1.5° of the center) radial inflow than the non-genesis composite, as well as a much stronger and better organized low-level convergence field in the same region.

The three development composites show large increases in tangential wind and vorticity near the center, along with a sharp drop in SLP, as higher stages of development are reached. At the same time, there are only slight increases in the inner-core radial inflow and associated low-level convergence field.

It is hypothesized that the stronger inner-core radial inflow and associated convergence that distinguish the genesis composite from the non-genesis are a result of environmentally forced low-level wind surges that penetrate to the center, bringing in mass and cyclonic vorticity from the outside, and initiating the cyclone formation and early development process. The wind surge then fades out, but the vortex can continue its spin-up due to the increasing vorticity and inertial stability near the center.

TABLE OF CONTENTS

1 FLIGHT DATA AND TROPICAL CYCLONE GENESIS	1
1.1 The Problem of Tropical Cyclone Genesis	1
1.2 Purpose	2
1.3 Procedures	2
2 DATA AND STRATIFICATIONS	4
2.1 Observations and Mission Profiles	4
2.2 Stratification of the Missions	9
2.2.1 Non-Developers	13
2.2.2 Developers	14
2.3 Characteristics of the Stratification Files	16
3 COMPOSITING THE DATA	17
3.1 Compositing Philosophy	17
3.2 Compositing Procedures	20
3.2.1 The Compositing Grid	20
3.2.2 Compositing the Observations	20
3.2.3 Determining System Center Location	22
3.2.4 Determining System Movement	23
3.2.5 Coordinate Systems	25
3.3 Aircraft vs. Rawinsonde Composites	25
4 GENESIS VS. NON-GENESIS	27
4.1 Data Sets Being Compared	27
4.2 Comparing the Composites	28
4.2.1 Sea-Level Pressure	28
4.2.2 Streamlines and Isotachs	29
4.2.3 Tangential Wind	29
4.2.4 Relative Vorticity	31
4.2.5 Radial Wind	36
4.2.6 Divergence	42
4.2.7 Balance Between Wind and Pressure Gradient	46
4.3 Summary of Results	50
5 DEVELOPMENT	52
5.1 Data Sets Being Compared	52
5.2 Development at Low Level	52
5.2.1 Sea-Level Pressure	52
5.2.2 Tangential Wind	54

5.2.3	Relative Vorticity	58
5.2.4	Radial Wind	59
5.2.5	Divergence	60
5.2.6	Balance Between Wind and Pressure Gradient	66
5.3	Summary of Results	66
6	PRE-STORM VS. PRE-TYPHOON	69
6.1	Data Sets Being Compared	69
6.2	Comparing PRE-STM and PRE-TY	70
6.2.1	Sea-Level Pressure	70
6.2.2	Tangential Wind and Vorticity	70
6.2.3	Radial Wind and Divergence	71
6.2.4	Balance Between Wind and Pressure Gradient	76
6.3	Summary	76
7	SUMMARY AND DISCUSSION	78
7.1	Summary of Results	78
7.1.1	Genesis vs. Non-Genesis	78
7.1.2	Development	79
7.1.3	Pre-storm vs. Pre-typhoon	79
7.2	The Presence and Probable Role of Low-Level Surges	79
7.2.1	Radial Wind, Convergence, and Low-Level Surges	79
7.2.2	Surges and Inertial Stability	81
7.3	Genesis and Development	81
8	AFTERWORD	84
A	W. M. GRAY'S FEDERALLY SUPPORTED RESEARCH PROJECT REPORTS SINCE 1967	89

Chapter 1

FLIGHT DATA AND TROPICAL CYCLONE GENESIS

1.1 The Problem of Tropical Cyclone Genesis

The basic large-scale requirements for tropical cyclone genesis are well known, and have been discussed and summarized by Gray (1968, 1975, 1979). Nevertheless, it is still not well understood why, in an environment conducive to tropical cyclone genesis, some disturbances will intensify while other apparently similar disturbances will not. Rawinsonde compositing has helped to identify some of the factors that determine whether or not genesis and development will take place (Zehr, 1976; Erickson, 1977; McBride, 1979; Gray, 1981; Lee, 1986), but this method suffers from lack of data and poor resolution within 2-3° latitude of the system center. In this report, a data source which has never been used to study tropical cyclone genesis is being brought to light. These data are from U.S. Air Force aircraft low-level reconnaissance flights into developing and non-developing tropical disturbances in the western North Pacific Ocean.

Flight data studies are not new. As far back as 1952, Hughes composited low-level data from 40 flights into 13 large typhoons in the western North Pacific. This pioneering work greatly advanced our knowledge of low-level circulation in tropical cyclones, but only fully developed typhoons were composited. Since 1952, flight data have been used extensively in case studies of individual Atlantic hurricanes, such as Hurricanes Daisy (Jordan, *et al.*, 1960; Riehl and Malkus, 1961; Colon, 1961), Cleo (LaSeur and Hawkins, 1962), Helene (Colon, 1964), Janice, Ella, and Dora (Sheets, 1967a, 1967b, 1968), and Hilda, Debbie and Inez (Hawkins and Rubsam, 1968; Hawkins, 1971; Hawkins and Imbembo, 1976). More recently, flight data have been used by Jorgensen (1984) to study four mature hurricanes, by Weatherford (1985) and Weatherford and Gray (1988a, 1988b) to

investigate structural variability in typhoons, and by Frank (1984) to composite the core of Hurricane Frederic. In all cases, however, mature typhoons or hurricanes were the subjects of study. This paper marks the first time low level (1500 feet or 457 meters absolute altitude or below) flight data have ever been used to study many cases of tropical cyclone genesis and non-genesis.

1.2 Purpose

In this study, composites were made of low-level aircraft observations from flights into western Pacific tropical disturbances so that by comparing composites of developing and non-developing disturbances, answers could be found to the following questions:

- a. What, if any, features in the low level circulation and pressure field distinguish a disturbance that will develop into a tropical cyclone from a disturbance that will not? (Chapter 4).
- b. How do the low-level circulation and pressure field change as a newly formed cyclone continues to develop? (Chapter 5).
- c. Are there any low-level differences between disturbances that will later become typhoons and disturbances that will later only become tropical storms? (Chapter 6).
- d. What, if anything, do the answers to the above questions tell us about the basic physical processes of the tropical cyclone formation and early development process? (Chapter 7).

A secondary purpose is to help fill in the data-poor region of 0-3° latitude radius from the center in earlier rawinsonde composite studies, at least at low level.

1.3 Procedures

All available low-level missions flown on tropical systems in the western North Pacific from 1977 to 1984 were used. These mission records had been previously obtained

from the National Climatic Data Center in Asheville, NC. After plotting and editing the missions, they were divided into various categories of developer and non-developer, as explained in Chapter 2. Wind and surface pressure observations from the missions were then composited within the various categories, or stratifications, as explained in Chapter 3. Composite fields were analyzed and compared with each other. The results of this study are presented in Chapters 4-7. Such data reduction procedures have been previously discussed by Weatherford (1985) and Weatherford and Gray (1988a, 1988b).

Chapter 2

DATA AND STRATIFICATIONS

2.1 Observations and Mission Profiles

All of the observations used in this report are from U.S. Air Force storm reconnaissance missions flown in the western North Pacific from 1977 to 1984. Henderson (1978) describes the WC-130 aircraft used in these missions. As he goes on to point out, there were two kinds of storm missions tasked by the Joint Typhoon Warning Center (JTWC) at Guam: investigative missions, or invests, and fix missions.

Fix missions are flown to pinpoint (or "fix") the location of a storm center already known to exist, as well as to obtain information about the surrounding winds out to 250 n m from the center. Weatherford (1985), in her study of structural variability in typhoons, describes the standard flight pattern of these missions, which has two center fixes and four radial peripheral legs (see Fig. 2.1). The missions are usually flown at the 700 mb level, but may be flown at low level (1500 feet absolute altitude or below) if the storm's maximum winds do not exceed 50 kts (25 m/s). Weatherford used only fix missions at 700 mb.

Invests are generally flown at low level, though they may on rare occasions be conducted at 850 mb or even 700 mb. In contrast to fix missions, the purpose of an invest is to determine whether or not a low-level circulation center exists in a suspect area. There is no standardized flight pattern, because there is no way of knowing in advance what the mission will find. Instead, the Aerial Reconnaissance Weather Officer (ARWO), using JTWC's tasked position as the center of the search area, must use the winds he observes and his judgment to efficiently determine whether or not a circulation center can be "closed off". Generally, if a center exists it is found using just enough observations to

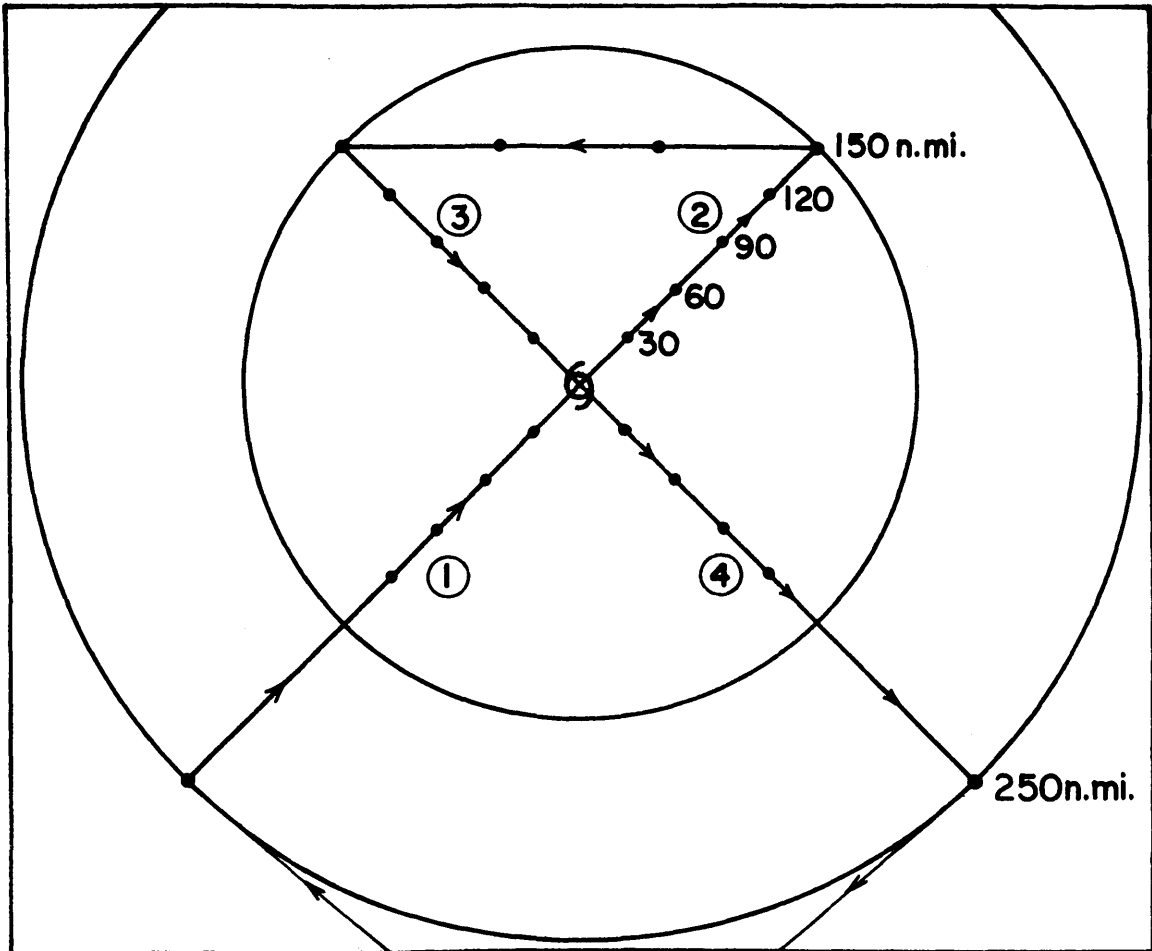


Figure 2.1: Idealized flight pattern for a 2-fix low-level mission. Dots indicate locations of observations, and the center is indicated by the tropical storm symbol. The four 150 n mi peripheral data legs are numbered to show the order in which they are flown in this example, though legs 1 and 4 can be switched if need be. But the connecting leg between legs 2 and 3 is always flown with the center on the plane's left; i.e., downwind. The overall pattern can be rotated to any desired orientation. In the real world, of course, the legs are seldom exactly straight or perpendicular to each other, and the two center fixes almost never coincide. Moreover, prior to 1984, leg 1 was normally flown at 700 mb, after which the aircraft would descend to low level for the first fix, then remain at low level for the rest of the peripheral track. Only beginning in 1984 was the entire track flown at low level on a routine basis.

define and locate it, after which a vortex fix is made and the plane returns to base. If a center cannot be found, enough observations are taken to satisfy the ARWO and JTWC that there is no closed circulation, and the plane goes home. Figure 2.2 shows a typical invest mission profile.

JTWC has three options once an invest locates an incipient circulation. Depending on how the system looks to JTWC, they may task another invest the following day, or they may start tasking fix missions at low level or 700 mb, or they may do nothing at all. In this report both invests and fix missions flown at low level are used.

Typical low-level mission profiles are shown in Figs. 2.3-2.8. Only a few observations are required to find a circulation in Fig. 2.3, while in Fig. 2.4 many more observations are needed. Note that in both cases supporting winds are found in all four quadrants in order to close off the circulation. Figure 2.5 is a low-level fix mission, with the pattern of Fig. 2.1. All three of these missions were flown on systems that developed into storms. Figures 2.6 and 2.7 are examples of missions that did not find a closed circulation, but only the first of these continued developing. In Fig. 2.8, a closed circulation was found and the center was fixed, but the system never developed.

Figures 2.3-2.8 also illustrate the distinction between open and closed missions. If a closed cyclonic circulation is found and a vortex fix is made, we have a "closed" mission. If a vortex fix cannot be made because no closed circulation can be found, the mission is "open". Figures 2.3, 2.4, 2.5, and 2.8 are closed, while Figs. 2.6 and 2.7 are open. (For a more detailed explanation of the difference between open and closed missions, as well as how circulations are or are not "closed off", see the captions to Figs. 2.3-2.8.)

As Henderson (1978) explains, the instrumentally sensed meteorological parameters at each observation are sea surface temperature, flight level temperature and dewpoint, flight level wind direction and speed, and sea level pressure, extrapolated to the sea surface from a flight level D-value. In this report, the only parameters of interest are wind velocity and pressure. The wind direction is reported to the nearest ten degrees azimuth, while the speed is reported to the nearest knot. Surface pressure is reported to the nearest millibar,

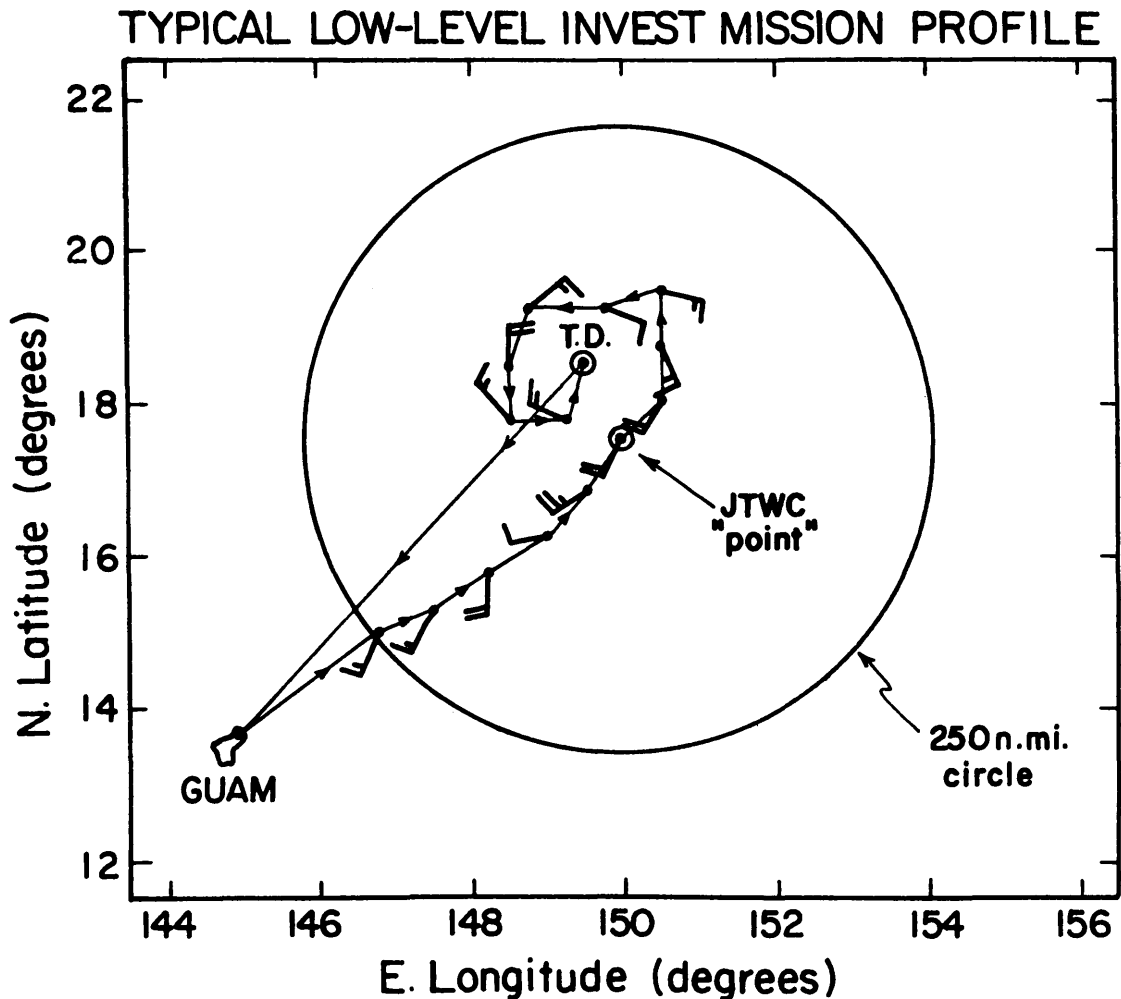


Figure 2.2: Profile of a typical low-level investigative mission flown on a disturbance near Guam. JTWC tasks the mission to fly to where it appears most likely a circulation center will be found; this is the JTWC "point". Following the tasking, the airspace between the surface and 700 mb within 250 n mi of the point is reserved for the aircraft, establishing the "250 circle". Within this altitude reservation, the aircraft may fly wherever the ARWO needs to go in order to fulfill his investigative mission. The mission is normally planned so that the plane arrives at the 250 circle near sunrise, at which point the first low-level observation is made. While taking observations at 15-minute intervals, the ARWO directs the aircraft to the point, after which he must use his judgement to decide where to go next. Here, a closed circulation is found fairly easily, and the center (marked "T.D." for tropical depression) is fixed about 65 n mi NNW of JTWC's point. Barring any further requests from JTWC, the aircraft heads back to base.

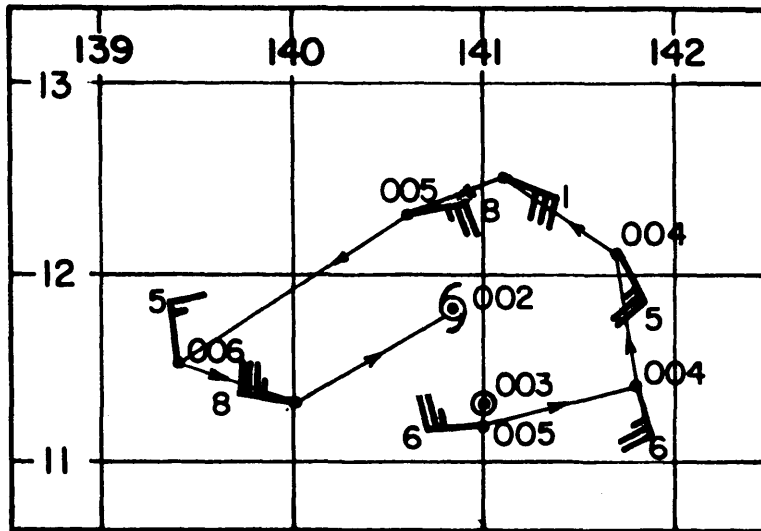


Figure 2.3: A plot of the low-level invest mission of 5-6 July 1980, flown on the disturbance that later became Tropical Storm Ida. Flight-level winds are plotted, with full barbs indicating 10 kt and half barbs 5 kt. For each wind, the tens digit of the direction, in degrees, from which the wind is blowing is given. For example, at 11.5 N, 139.4 E the wind is blowing from 350°; hence the “5”. Light-and-variable or calm winds are indicated by a circle around the observation point. Extrapolated surface pressures are plotted in whole millibars, with only the tens and units digits plotted. The light lines with arrows connecting the observations show the flight path the aircraft followed. This mission is a good illustration of a rule the ARWOs at Guam use when flying an invest: in order to “close off” a circulation, winds supporting a closed cyclonic circulation must be found in “all four quadrants”. Here, a westerly wind was found in the southern quadrant at 11.2 N, 141.0 E, followed by a southerly wind in the eastern quadrant at 12.1 N, 141.7 E, an easterly wind in the northern quadrant at 12.3 N, 140.6 E, and a northerly wind in the western quadrant at 11.5 N, 139.4 E. These winds clearly define the closed circulation, the center of which was fixed at 11.8 N, 140.8 E. The “four quadrants” can be rotated to any orientation, depending on what winds are found; eg., NW-SE and NE-SW.

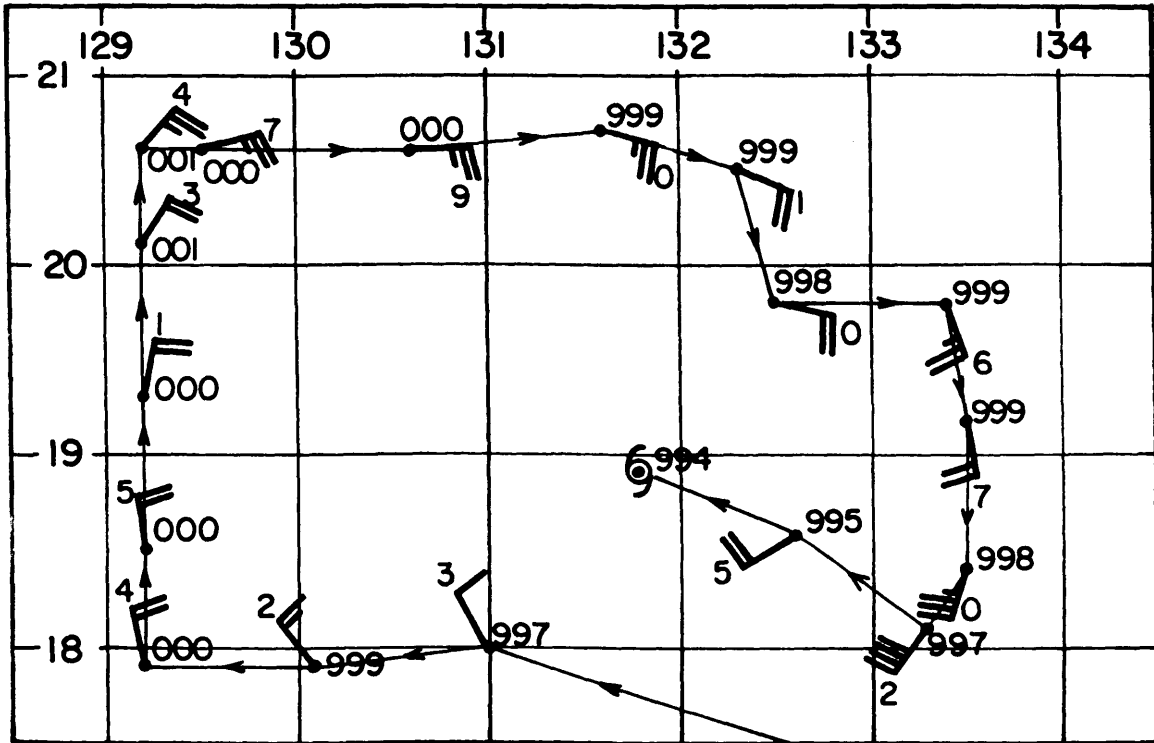


Figure 2.4: Low-level invest mission flown by the author on 16 August 1981, on the disturbance that later became Typhoon Thad. Here, the required winds were found in the SW, NW, NE, and SE quadrants before the center was fixed at 18.9 N, 131.8 E. More observations were needed here than in Fig. 2.3 for two reasons: JTWC's tasked point was well to the west of where the center was found, and the circulation was large and loosely organized.

but before being used in this study each reported pressure was corrected to account for diurnal pressure variation. The position of each observation is reported to the nearest tenth of a degree of latitude and longitude, and the observation time is noted to the nearest minute.

2.2 Stratification of the Missions

For compositing purposes, the missions are grouped together in stratification files according to characteristics they may have in common. For example, a stratification file might be made of all missions flown on northward-moving developing storms. Presumably, the composite of the missions in this file would then be compared with a composite of some

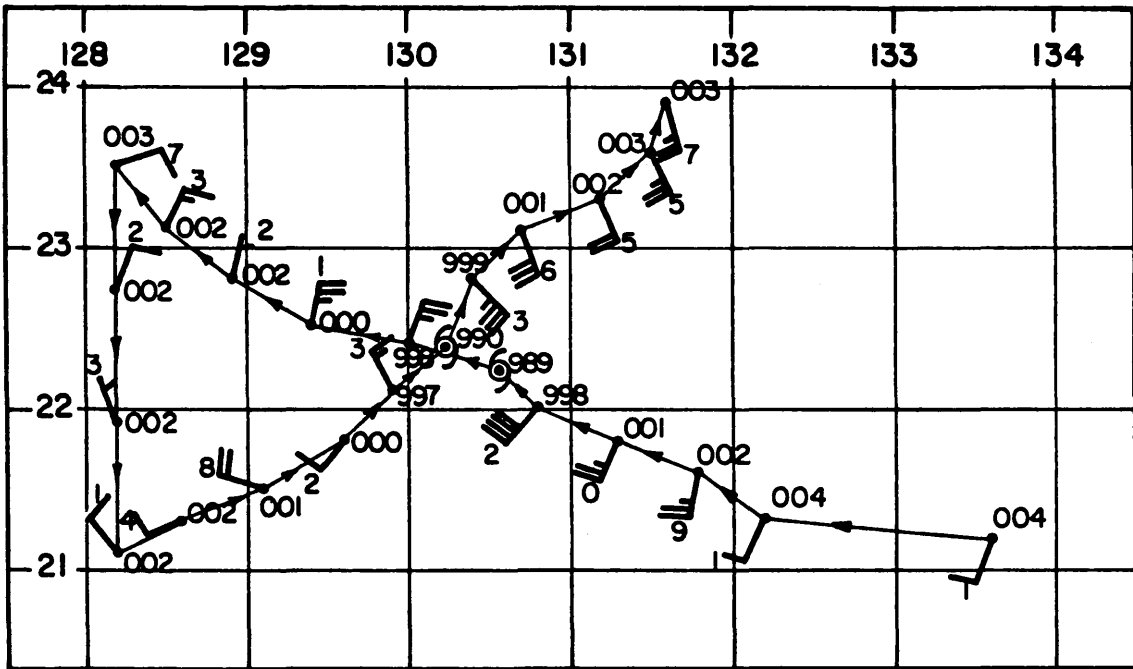


Figure 2.5: A typical low-level fix mission, flown on 20 June 1984 into Tropical Storm Wynne. The observation at 21.2 N, 133.6 E is on the 250 n mi circle. The first inbound leg into the center from the southeast only extends out 120 n mi because the center was encountered 30 n mi sooner than expected—a not uncommon event.

other file; for example, the composite of all missions from westward-moving developing storms. The files used in this report are explained below; the compositing procedure itself is reserved for the next chapter.

The two basic kinds of missions are the developers and non-developers. A developer mission is one that meets the following criteria:

- The mission was flown on a system that either already is or will become at least a named tropical storm (maximum surface winds ≥ 34 kt).
- The mission was flown while the system was developing, or at least it was not weakening at the time.

These criteria include practically all missions flown on a named storm prior to its time of maximum intensity. Note that a developer mission may be flown on anything from a 50 kt tropical storm to a disturbance lacking a closed circulation but nevertheless destined to be a named storm.

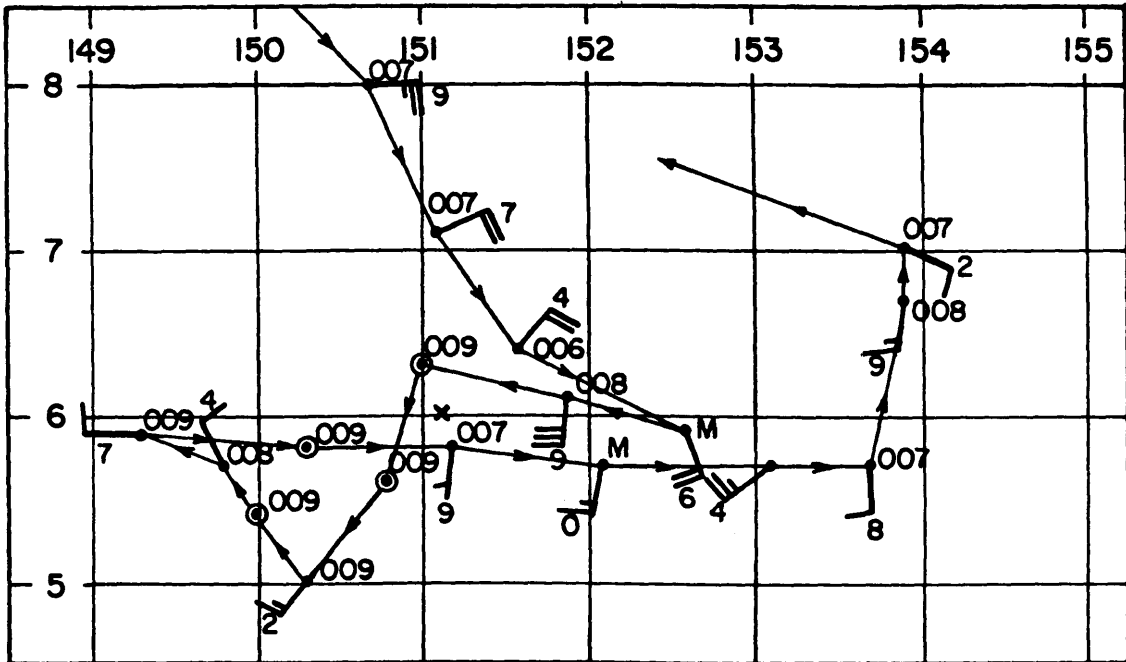


Figure 2.6: This low-level invest, flown on 18-19 September 1983, was the second mission flown into the disturbance that later became Super Typhoon Forrest. This is a good example of an “open” mission; no center fix was made because a definite closed circulation could not be found. The NW wind at 5.7 N, 149.8 E and the SW wind at 5.0 N, 150.3 E, along with the light southerly wind at 5.8 N, 151.2 E seem to be trying to outline a circulation, but the calm winds at 5.4 N, 150.0 E and 6.3 N, 151.0 E provide contrary evidence. Also, the 20 kt NE wind at 6.4 N, 151.6 E is too far east to support the other winds mentioned. Finally, no good SE wind can be found in any of the right places. The X at 6.0 N, 151.1 E represents the point about which the winds appear to be organizing.

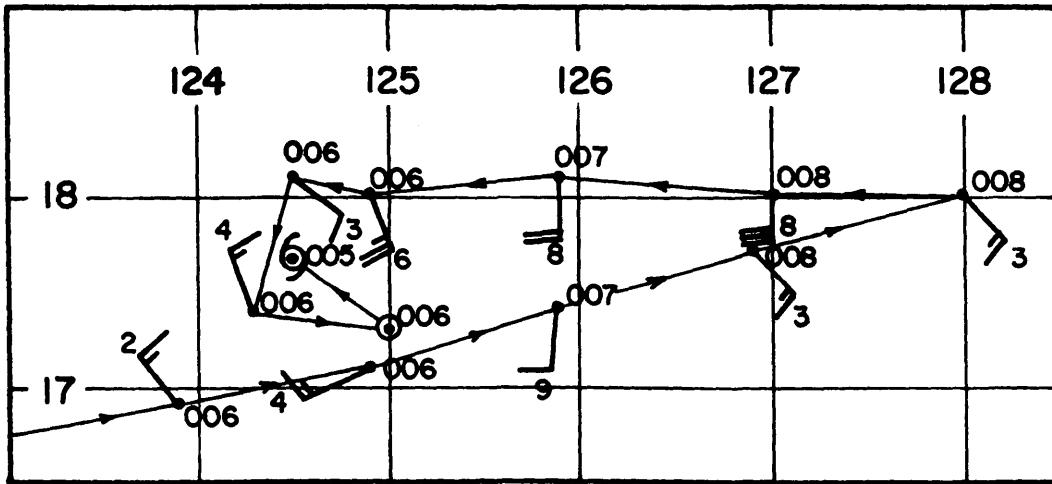


Figure 2.8: Like Fig. 2.7, this invest of 9-10 July 1981 was flown on a disturbance that never amounted to anything. Unlike Fig. 2.7, however, a closed circulation was found, and the center was fixed, making this a “closed” mission.

Non-developers include the following:

- All missions flown on systems that will never develop beyond tropical depression intensity (maximum surface winds < 34 kt). This includes actual numbered tropical depressions as well as disturbances that never even have closed circulations.
- Missions flown on a former tropical storm or typhoon that has weakened over water, is still weakening, and is near the end of its life. Such a mission may or may not find a closed circulation.

In general, if a mission does not meet the criteria of the developer, it is a non-developer.

2.2.1 Non-Developers

There are two categories of non-developers:

- Non-developer (NON-DEV): This is all non-developers as defined above.
- Non-genesis (NON-GEN): Here are all the missions flown on systems that either will never develop a closed circulation, or if they do the maximum surface wind will

never exceed 25 kt (note that this is more restrictive than the 34-knot limit for non-developers in general). This is the stratification file that would result if the following were deleted from the NON-DEV file:

1. Missions flown on weakening systems that were former named storms;
2. Missions flown on systems that were, are, or became at some later time, numbered tropical depressions with maximum surface winds in excess of 25 knots.

There is an important distinction made here between non-development in general and non-genesis in particular. Non-genesis implies that a system never develops during its entire history, whereas non-development can also include dissipating systems that were once named storms. Hence, while non-development means “not developing,” non-genesis means not only that but “never developing” as well.

2.2.2 Developers

Because the developer data set contains more than twice as many observations as the non-developer set (see Table 2.1), more stratifications are possible. Three of the files are based on degree of development, where minimum sea level pressure (MSLP) is used as a measure of how far developed the system is. Other files are based on the storm's subsequent history or on whether or not the mission found a closed circulation.

- Early Developers (D1): All missions in this file were flown on systems whose MSLP equalled or exceeded 1003 mb at the time, whether or not a closed circulation existed. The stage of development represented here is about the same as that of the non-genesis file, as far as maximum surface winds and MSLP are concerned. Most of the missions in the D1 file were flown within 24 hours of the time the disturbance first acquired a closed circulation.
- Middle Developers (D2): This represents the early tropical depression stage, with the MSLP ranging from 1002 mb to 997 mb. Whereas slightly less than half of the D1 missions found a closed circulation, about 80% of the missions in this file are

closed. However, even the 20% or so that still are not closed off usually have higher winds than their counterparts in the D1 file.

- Late Developers (D3): A late developer mission has a MSLP from as high as 996 mb, representing a strong tropical depression, to as low as 980 mb, typical of a well-developed tropical storm with maximum surface winds of 55-60 knots. The average MSLP of the file is about 991 mb, or minimal tropical storm intensity.
- Open Developers (OPEN-DEV): All developer missions that are open are included. Of the 82 missions in this file, 53 are early developers (D1), 24 are middle developers (D2), and the other 5 are late developers (D3).
- Pre-Tropical Storm (PRE-STM): For this and the next file, only missions from the D1 and D2 files are used. The Pre-Tropical Storm file contains the missions flown on systems that never intensified beyond 70 knots maximum surface wind in their lifetimes. By definition, a tropical storm has maximum surface winds of no more than 63 knots, but for this file the limit is stretched to 70 knots to provide more observations.
- Pre-Typhoon (PRE-TY): Again, only early and middle developers go into this file. Pre-Typhoon missions are those flown on systems that attained a maximum intensity of at least 75 knots maximum surface wind some time during their lifetimes. Of course, many of the typhoons represented in this file had winds much stronger than 75 knots. For both this file and the PRE-STM file, maximum surface winds were obtained from the JTWC Best Tracks published annually in their Annual Tropical Cyclone Reports (JTWC, 1977-1984). Tropical cyclone Best Tracks are discussed in more detail in the next chapter.

2.3 Characteristics of the Stratification Files

Table 2.1 lists the main characteristics of the stratification files given above. Since a given mission may appear in more than one file, adding up the number of observations or missions will not yield the totals at the bottom.

Table 2.1: Characteristics of Stratification Files.

Strat. File	LAT. (°N)	LONG. (°E)	No. Obs.	No. Missions	No. Missions Open/Closed	Speed of Movmnt.(kt)	MSLP (mb)
NON-DEV	15	139	2113	166	110/56	9.1	1003
NON-GEN	14	141	1342	111	93/18	8.7	1006
D1	12	141	1409	100	53/47	10.6	1004
D2	14	141	1640	114	24/90	9.7	998
D3	18	137	1519	123	5/118	8.2	991
OPEN-DEV	13	141	1235	82	82/0	9.5	1002
PRE-STM	15	138	1406	103	44/59	9.7	1002
PRE-TY	12	144	1643	111	34/77	10.3	1003
Totals			6681	503			
Total Developers			4568	337			
Total Non-Developers			2113	166			

Chapter 3

COMPOSITING THE DATA

3.1 Compositing Philosophy

If one wishes to conduct an observational study of how newly formed tropical cyclones develop at low level, or of the low level differences between developers and non-developers, there are not many choices open to the investigator. In a data-sparse area like the northwest Pacific, there are only two data sources: rawinsonde observations and aircraft reconnaissance observations.

The problem with rawinsonde observations is their scarcity. As Fig. 3.1 shows (Zehr, 1976), there are only about two dozen rawinsonde stations in the northwest Pacific south of 40°N. At any one time, five or six of these stations might be within 15° latitude of a storm center, and one or two might be within 5°. It is obvious from this that rawinsondes are not suitable for individual case studies of cyclone development, nor for comparisons on a case-by-case basis of developers and non-developers. However, if all the rawinsonde observations made over many years are collected, these can be composited with respect to the centers of any tropical cyclones or disturbances, provided the centers are known with sufficient accuracy. For each observation, the position of the appropriate center is determined for the time of the observation, then the bearing and range from the center to the observation is determined. Several CSU project investigators have been successful in using this technique for the study of western North Pacific tropical cyclones, such as Zehr (1976), Erickson (1977), Arnold (1977), Frank (1977), McBride (1979), and Lee (1986).

Aircraft observations are distributed much differently with respect to cyclone centers than are rawinsondes. Whereas rawinsondes go up at fixed times from fixed locations, the aircraft seek out the centers in order to cluster the observations near them. If a complete

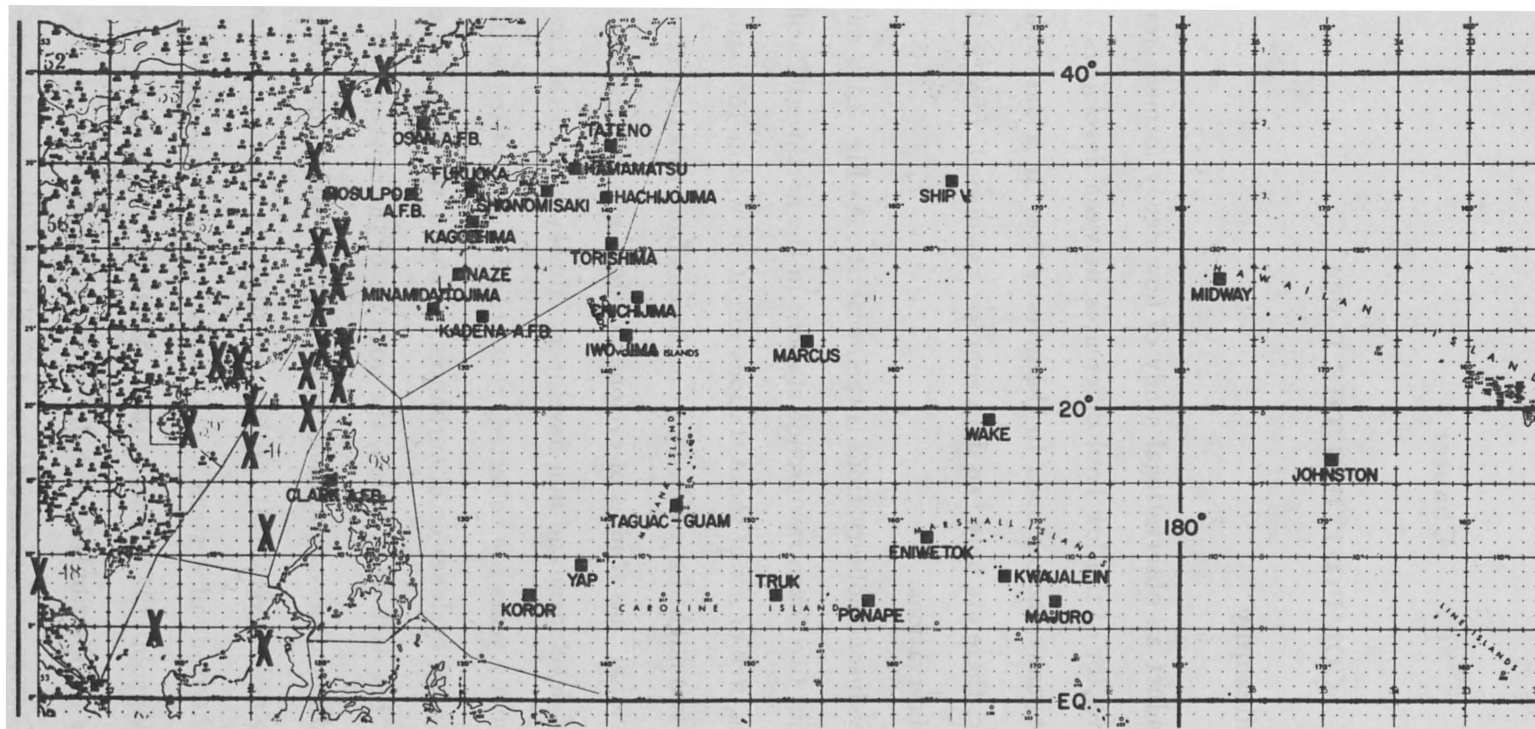


Figure 3.1: Rawinsonde data network in the western North Pacific Ocean (from Zehr,1976).

low level fix mission profile is flown (see Fig. 2.1), 24 observations are taken within 3° latitude of the center, with two of these at the center itself. Hence, limited case studies may be conducted on individual storms within 3° latitude of the center. Invests are less useful in general, since fewer observations may be taken and they tend to be distributed in an irregular fashion, but some missions might still be adequate for case studies inside 3° . Outside of 3° latitude from the center, the number of aircraft observations falls off drastically, so that outside of 5° latitude from the center they are even more scarce than rawinsonde observations.

Another approach to using low level aircraft observations, the approach used in this study, is to composite them the same way the rawinsondes are composited. As Zehr (1976) and others have pointed out, compositing has certain advantages and disadvantages common to both rawinsonde and aircraft observations.

The greatest advantage is that many observations over a period of years can be collected and located with respect to the disturbance and cyclone centers, resulting in a dense network of observations that can then be averaged in the individual grid boxes defined by an appropriate coordinate grid. From this, average fields of various meteorological parameters can be analyzed. If a large amount of data is available, the data set can be stratified according to characteristics such as intensity, movement, or structure, and comparisons can be made between the composites of different data subsets. An important advantage over case studies is that the averaging process tends to eliminate the random small-scale variations that are present whenever a system is sampled by an aircraft or a few rawinsondes. On the other hand, the more relevant meso- and synoptic-scale features that are common to all tropical systems are retained.

The averaging process mentioned above can also be a disadvantage, possibly smoothing out features that might be desirable to retain. This smoothing will depend not only on the variability of individual systems, but also on the degree of uncertainty in positioning the centers of the systems. Indeed, it must be remembered when interpreting a composite that the average cyclone depicted does not really exist, since all real systems will show

some variation from the mean. Nevertheless, if there are indeed certain features of cyclone formation that are common to all developers, or features of non-development that are common to all non-developers, these features should be present in the composites.

3.2 Compositing Procedures

3.2.1 The Compositing Grid

The compositing grid used in this study is a circular grid that uses polar coordinates, similar to the grid used by Zehr (1976). It is divided into eight octants, oriented with Octant 1 pointing due north, and into eleven radial belts, resulting in 88 grid boxes. This grid is shown in Fig. 3.2. The belt boundaries are at radii of 15 n mi, 45 n mi, 75 n mi, and so on every 30 n mi until the outer boundary of the eleventh belt at 315 n mi. The eight sectors of the innermost belt, Belt 1, are treated together as a circle 30 n mi in diameter centered at the center of the grid. Winds in this circle are ignored, but the average of all the surface pressures in this circle is assigned to the center point of the grid. For Belts 2 through 11, the grid box center points occur at radii of 30 n mi, 60 n mi, 90 n mi, on out to Belt 11 at 300 n mi. Hence, the box centers are at intervals of 0.5° latitude from the center of the grid.

3.2.2 Compositing the Observations

For each mission flown on a disturbance or cyclone, the position of the center was determined for each individual observation time in a manner that is described below. Each observation was then positioned with respect to where the center was at the time of the observation. This position, expressed as a bearing and range from the center, determined where on the compositing grid the observation fell, which in turn determined which grid box the observation was assigned to. For each grid box, the averages of the parameters to be composited were calculated from the observations in the box, and the average values were assigned to the center point of the box. Some parameters, such as surface pressure or total wind speed, could be averaged directly from the observations, while for others, such as radial wind or wind speed squared, a value was calculated from each observation, then

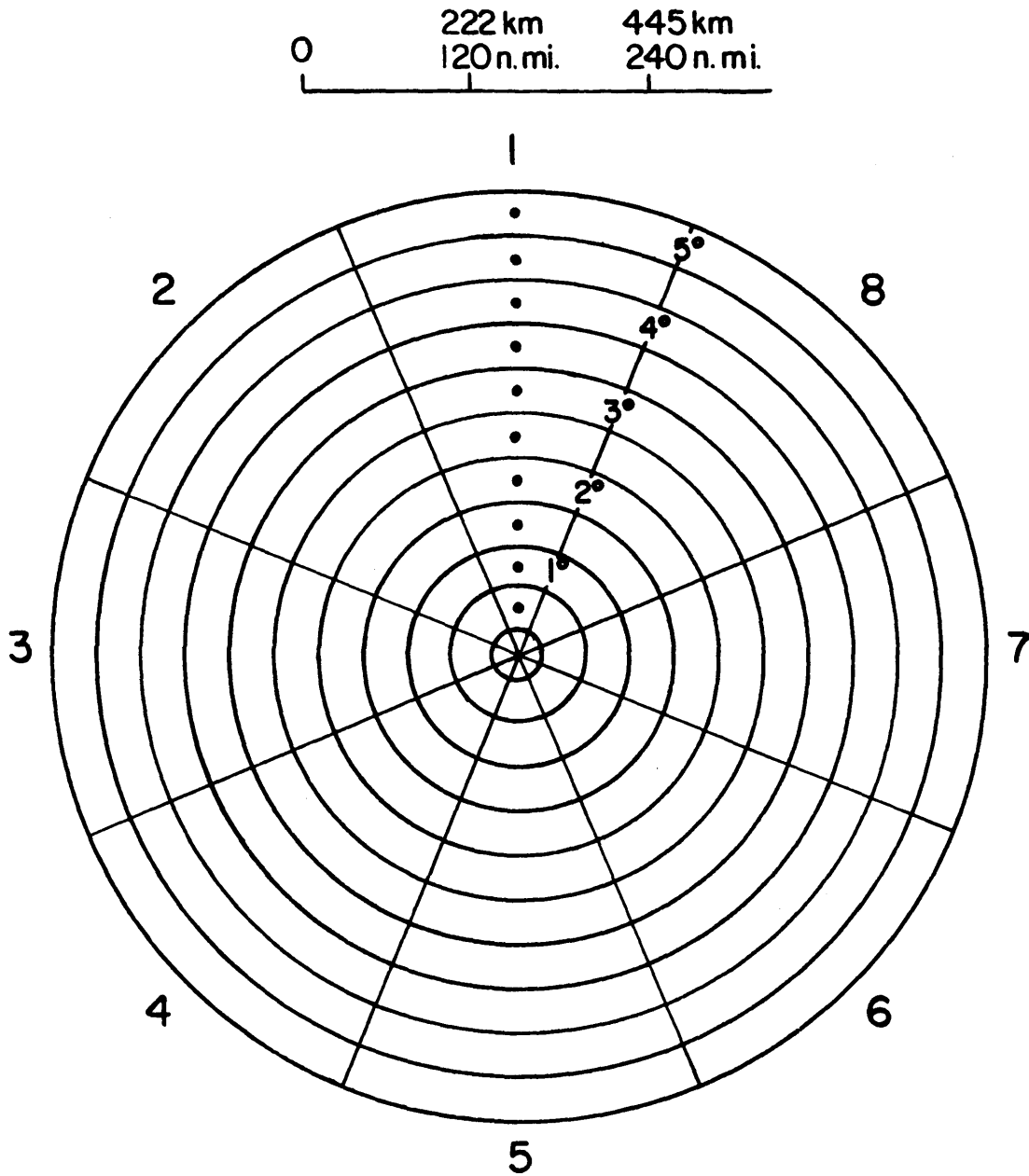


Figure 3.2: The grid used for compositing the low-level flight data. Each radial belt is 30 n mi (0.5° latitude) wide, as is the inner circle containing the center of the grid. Radii in degrees latitude are given for every other radial belt. These radii apply to the grid-box center points, examples of which appear in Octant 1. Octant 1 points north (except in the rotated coordinate system, where Octant 1 points in the direction of system motion; see section 3.2.5).

these calculated values were averaged. Yet other parameters, such as relative vorticity, were calculated using other, previously calculated, averages already at the grid box center points. Once average values were calculated for all the grid box center points, the resulting average fields were analyzed.

In addition to the grid composites, composited radial profiles were also constructed, using two methods. Unweighted belt averages were calculated by giving each of the eight boxes in the belt equal weight, simply computing the mean of the eight values. Weighted belt averages, using only in the sea-level pressure profiles given in this report, were obtained by averaging all the individual observations in each belt, equivalent to giving each box a weight according to the number of observations it contained.

3.2.3 Determining System Center Location

In order to determine the composite position of each observation in a mission, it is necessary to know where the center of the system was at any given time during the mission. If the mission contains one or more center fixes, center location is obviously an easy task. Otherwise, one or more center positions were derived for each mission, corresponding to one or more times during that mission or bracketing it. To do this, several sources were used, beginning with the observations themselves. In many cases, even though a center fix was not made, the observed winds gave a strong indication of where the center should be, and so that was enough to locate it. In cases where the observations were not enough, or where the center was outside the area where observations were taken, some centers were located by using JTWC Best Tracks, published annually in their Annual Tropical Cyclone Report. After a cyclone has completed its life cycle, JTWC determines 6-hourly positions for the cyclone's surface center for its entire lifetime. These Best Track positions are derived from an analysis of aircraft data, positions measured by satellite, land-based radar fixes, and synoptic surface observations. Indicated at each 00Z, 06Z, 12Z or 18Z position on the Best Track are the storm's maximum sustained surface winds and the speed at which the center was moving. While these Best Tracks do not always correspond exactly with aircraft center fixes, they are still very useful for locating centers.

If a JTWC Best Track was not available, which was the case for all non-developers that were not numbered tropical depressions, tropical surface analysis charts, from both the National Weather Service and the forecast office at Darwin, Australia, were used. In many cases, the streamline analysis clearly indicated the position of the center, at least on a synoptic scale. If no cyclone was analyzed on the chart, surface observations in the region, in combination with the aircraft observations, were often sufficient to locate a center with good accuracy.

It should be emphasized here that no center location was accepted unless it agreed well with the aircraft data. If, after consulting all available sources, a center could not be found that would fit the aircraft data, the mission was rejected for compositing purposes. Thus, by using aircraft data, JTWC Best Tracks, and tropical surface charts, centers suitable for compositing were derived for all the missions composited, both developers and non-developers. While many of these derived centers probably do represent actual closed circulations, there are, no doubt, many cases in which a complete closed circulation did not actually exist. In these cases, the derived center is better described as the center of action about which the observed winds appear to be organizing. Figure 3.3 shows a typical mission, in this case a developer, where it is not clear that a closed circulation exists. The circled X indicates the derived center, while the other Xs indicate locations (one from a Darwin surface analysis) that probably do not mark the point about which the winds are organizing. The assumption made here is that even in cases where a completely closed circulation may not have existed, the derived center is still suitable for compositing.

3.2.4 Determining System Movement

The centers determined by the above procedures were used not only to locate the observations with respect to the center, but also to define the movement of the system during the time period covered by each mission. Enough center positions and times were derived for each system so that its movement was well approximated during the time of each mission flown on it by simply moving the system at constant velocity between each pair of center positions. Thus, the position of the center was calculated for the time of

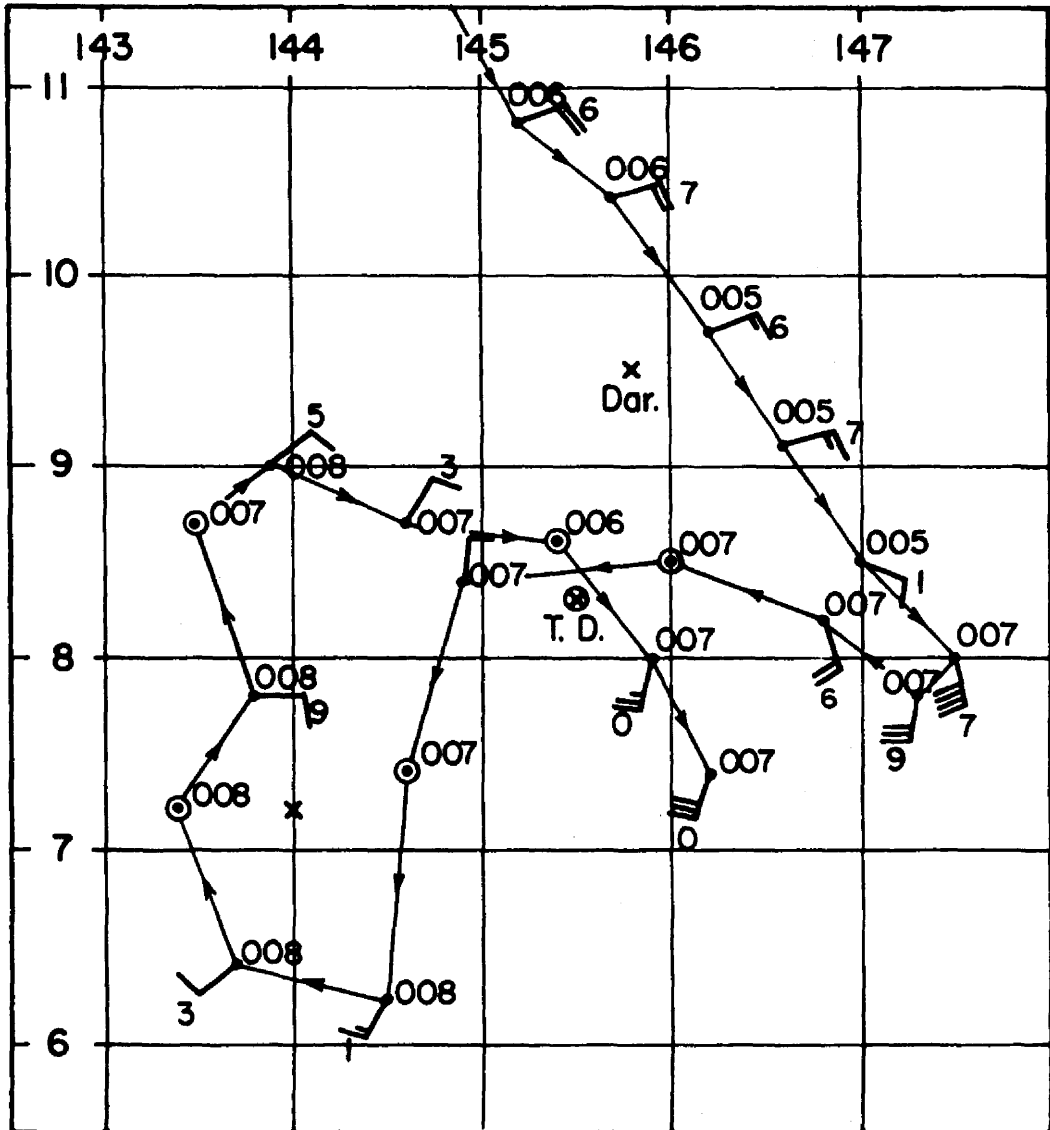


Figure 3.3: A typical open developer mission in which no center fix was made. The circled X marked "T.D." (for "tropical depression") is the derived center location. This location is strictly valid for some specific time during the mission. The X marked "Dar." is the position that was obtained from the applicable surface analysis chart from the Darwin forecast office. The unlabelled X at 7.2 N, 144.0 E is another possible, but unlikely, position for the center.

any observation by linearly interpolating between the center positions before and after the observation time, and the center's velocity was easily found by simply dividing the distance vector between the two positions by the elapsed time.

3.2.5 Coordinate Systems

Three different polar coordinate systems were used for compositing the data, though all three used the same grid:

NAT: The grid is geographic or stationary with Octant 1 pointing due north. Winds are used as measured without regard to cyclone motion.

MOT: Motion system: Octant 1 still points north, but the system motion is subtracted vectorially from each wind before it is composited, yielding relative wind, or wind relative to the moving center.

ROT: Rotated system: similar to the NAT, but before the composite is made each observation is rotated to a relative position so that the direction of motion always points towards Octant 1.

3.3 Aircraft vs. Rawinsonde Composites

When comparing the results of this study with those of earlier studies using rawinsonde composites, the important differences between the two types of composites must be kept in mind. These differences are:

- Aircraft composites have very dense data coverage near the center, within about 3° latitude, while rawinsonde composites have poor coverage near the center but much better coverage beyond 3° latitude radius. See Table 4.2 in Chapter 4 for a comparison of this report's D1, NON-GEN, OPEN-DEV, and NON-DEV data sets with some of Lee's (1986) and McBride's (1979) rawinsonde data sets.
- In earlier rawinsonde studies, circulation centers could not be determined for many of the non-genesis cloud clusters, either because the cluster had no closed circulation

or because there were not enough data to locate the center. In such cases, the center of the cluster as it appeared on satellite imagery, which may have no relation to the actual low-level circulation, was used instead (Zehr, 1976; Arnold, 1977; Lee, 1986). In this study, all centers were based on the observed low level winds.

- The non-genesis systems in this study are not comparable to the non-genesis systems of Zehr (1976) and Lee (1986). They used all the well-defined non-genesis clusters they could find, but the non-genesis cloud clusters used in this report were all selected by JTWC. Because of various operational constraints, JTWC was very selective when tasking an invest on a cloud cluster. There are many cloud clusters each year in the western North Pacific, but JTWC only tasks invests on those that seem likely to have a closed circulation and have a potential for development. Many other non-genesis clusters, some of which no doubt have a very impressive satellite signature at one time or another, are not tasked for invests because JTWC correctly sees that they will not develop. This automatically eliminates many other weaker non-genesis clusters that would have been selected by the rawinsonde compositors. Thus, the non-genesis file in this report contains a lot of missions flown on disturbances that were very close to being developers, but did not quite make it.

Chapter 4

GENESIS VS. NON-GENESIS

4.1 Data Sets Being Compared

In order to discover what differences might exist between genesis and non-genesis disturbances, composites of four mission files are compared here: D1, NON-GEN, OPEN-DEV, and NON-DEV. The early developer composite D1 represents the typical genesis disturbance, and it will be compared with NON-GEN, the typical non-genesis disturbance. This is the primary comparison being made in this chapter. As Table 2.1 in Chapter 2 shows, a little over half of the missions in the D1 file are open, but in the NON-GEN file about 84% of the missions are open. Hence, it might be argued that any differences between D1 and NON-GEN reflect the larger percentage of open missions in NON-GEN, not the difference in “genesis potential”. Considering the uncertainties in deriving centers for the open missions, this could be a strong argument. This is the reason for having the OPEN-DEV composite, in which all of the missions are open. If a characteristic that differentiates D1 from NON-GEN is also seen in OPEN-DEV, the argument that the difference is genesis-related is much stronger. The main reason for including the NON-DEV composite is to test the validity of the distinction made in Chapter 2 between non-development and non-genesis.

In this and the following chapters, both grid composites and composited radial profiles are shown (see Chapter 3).

4.2 Comparing the Composites

4.2.1 Sea-Level Pressure

Composite radial profiles of sea-level pressure are presented in Fig. 4.1. Diurnal correction has been made to all profiles. The profiles for D1 and NON-GEN are nearly identical, never differing by as much as a millibar all the way out to 5° latitude from the center. The OPEN-DEV curve is two to three millibars lower, since it includes some D2 and D3 missions, but it otherwise looks much the same as D1 and NON-GEN. Since NON-DEV also includes some missions with lower pressures, its profile is similarly shifted down a millibar or so. All four curves show nearly the same pressure gradient, except that OPEN-DEV and NON-DEV have slightly steeper gradients within a degree of the center. Certainly, there is nothing in these profiles to distinguish genesis from non-genesis disturbances.

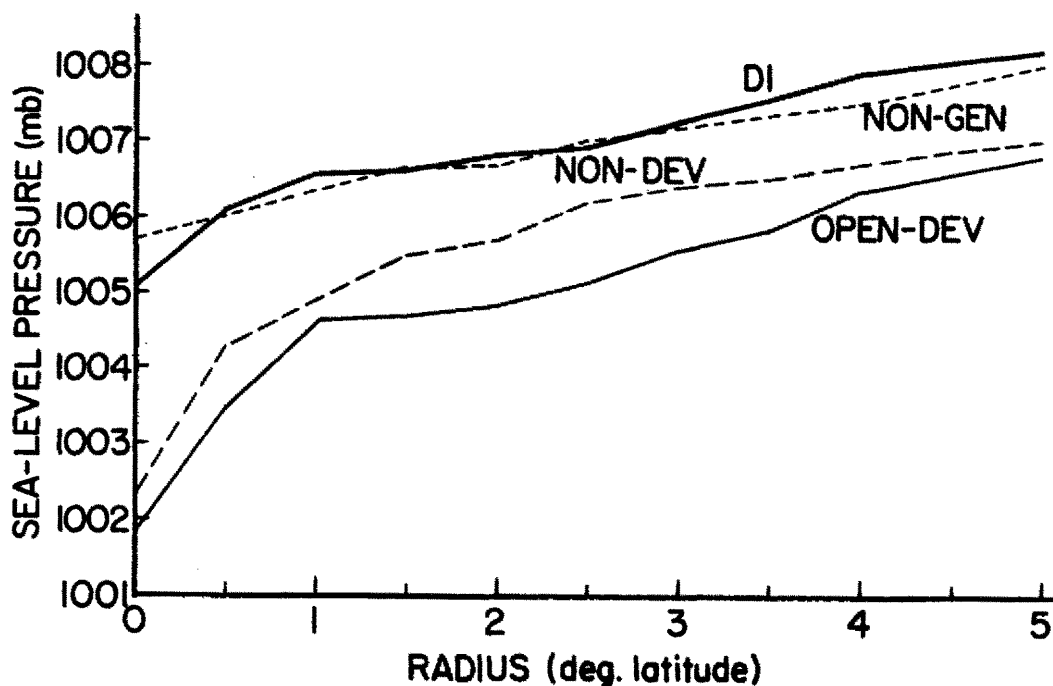


Figure 4.1: Radial profiles of NAT sea-level pressure for the NON-GEN, D1 (early developer), NON-DEV, and OPEN-DEV composites.

4.2.2 Streamlines and Isotachs

Figure 4.2 shows the mean NAT streamlines and isotachs (in knots) for NON-GEN, D1, NON-DEV, and OPEN-DEV. As with all NAT plots, north is up. The large-scale features are much the same in all four. The strongest winds tend to occur about 3° north of the center, except for OPEN-DEV, where even stronger southwesterlies are evident at the southeast fringe of the plot. The strong easterlies north of the center are likely due to the enhanced trade winds that often occur poleward of a tropical disturbance. The lightest winds appear west or southwest of the center. Not surprisingly, this sector is often the hardest part of a disturbance to “close off” on an aircraft invest mission. The streamlines all show well-defined cyclonic circulations, although the streamlines in the NON-GEN composite are not as circular as those in the other composites. At first these results seem to conflict with those of Zehr (1976), whose rawinsonde composites for non-developers did not have closed circulation. But as was pointed out in the previous chapter, the disturbances composited as NON-GEN and NON-DEV in this report are much closer to being developers than Zehr’s non-developers are. In fact, as Fig. 4.2 shows, the composites for D1 and NON-GEN are so similar as to be basically indistinguishable.

4.2.3 Tangential Wind

In Fig. 4.2 above, the radial wind components are quite small compared to the tangential components; hence, the isotachs of total wind in that figure are a close approximation of the NAT tangential winds. The tangential winds shown in Fig. 4.3 are in the ROT system, in which the motion vector of the center points up. In both the D1 and NON-GEN composites the tangential wind is strongest in the right semicircle and weakest in the left. The most noticeable difference is in the right front quadrant, where D1 has a large area of winds in excess of 20 knots that NON-GEN lacks. This is similar to the NAT depiction in Fig. 4.2, where, since tropical disturbances generally move towards the west-northwest, the right front quadrant is north of the center. In contrast to Fig. 4.2, however, the ROT OPEN-DEV composite also has an area of winds above 20 knots while the NON-DEV composite does not. Does this indicate that developing disturbances tend

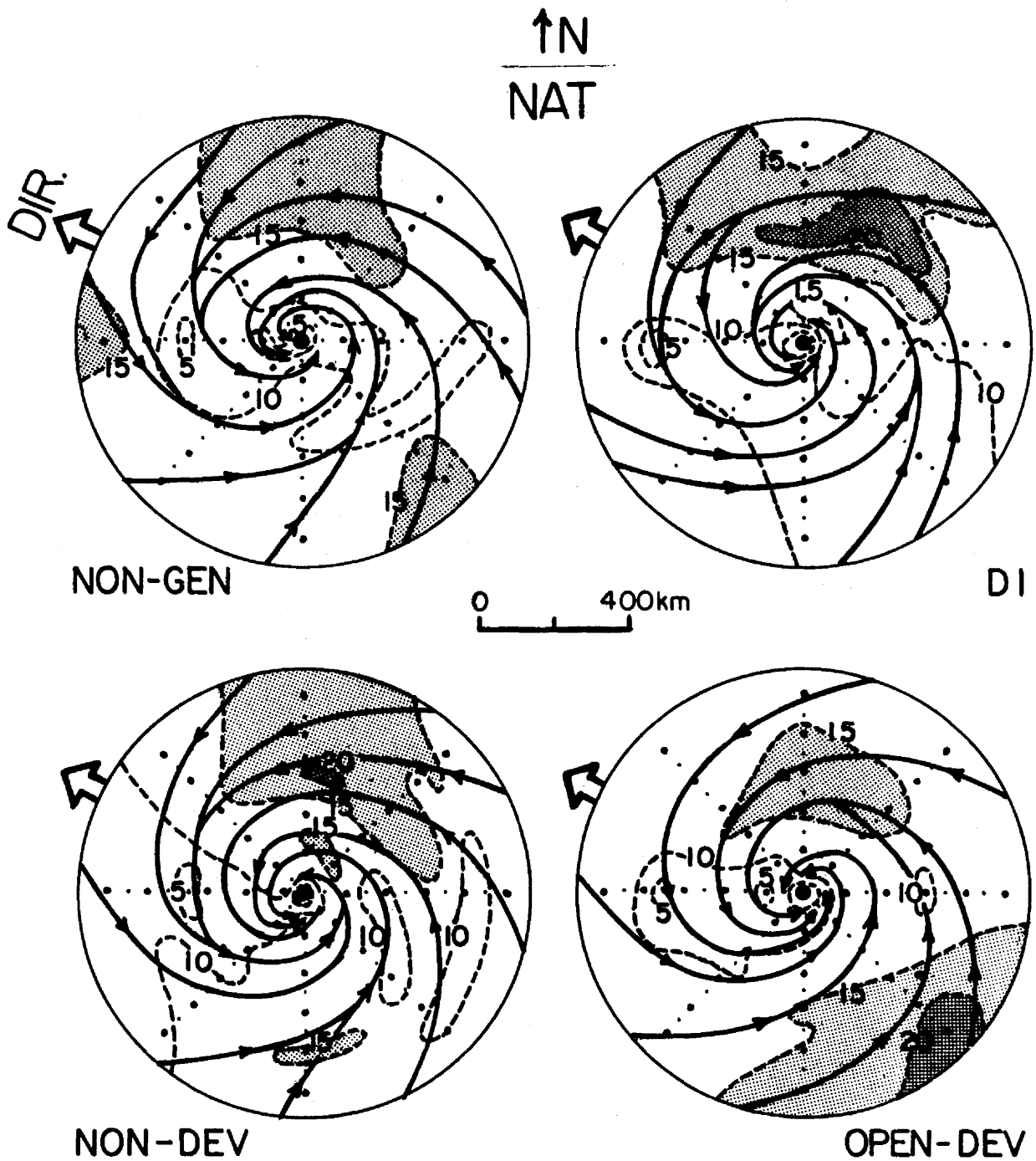


Figure 4.2: NAT streamlines (solid, with arrows) and isotachs (dashed, in knots) out to 5° latitude from the center for NON-GEN, D1 (early developer), NON-DEV, and OPEN-DEV. Grid point spacing is 0.5° latitude (30 n mi), with larger dots at the whole-degree points. North is up. Note: 2 knots = 1 m/s.

to have higher tangential winds in the right front quadrant? While that is a possibility, there are not enough data in that portion of the composite grid to make the results statistically significant.

Figure 4.4 shows the radial profiles of tangential wind. All four profiles are nearly featureless, staying near 9 knots from 0.5° to 5° latitude from the center. There is no sign, either in this figure or in Fig. 4.3, of a maximum wind band near the center in any of the composites.

4.2.4 Relative Vorticity

Previous rawinsonde composite studies (Zehr, 1976; Erickson, 1977; McBride, 1979; Lee, 1986) have shown a large difference in low-level relative vorticity between developing and non-developing disturbances. Erickson, for example, found that within 2° of the center the average low-level (950 mb) relative vorticity was $4 \times 10^{-5} s^{-1}$ for developers, compared with $2 \times 10^{-5} s^{-1}$ for non-developers. For $0-4^\circ$ from the center, his values dropped to $1.8 \times 10^{-5} s^{-1}$ and $0.8 \times 10^{-5} s^{-1}$ for developers and non-developers, respectively. Lee gave similar numbers, and concluded that in order for a cloud cluster to develop into a tropical cyclone there must be a sufficient amount of vorticity accumulated in the vicinity of the cluster. McBride came to a similar conclusion, that pre-typhoon systems are found in large areas that have high values of low-level relative vorticity.

Figure 4.5 shows, on an expanded scale, the relative vorticity fields for the inner 2.5° of each composite. Since NON-DEV and D1 have somewhat stronger tangential winds at 0.5° radius than OPEN-DEV and NON-GEN (see Fig. 4.4), their relative vorticities are higher inside that radius. Otherwise, all four composites are basically the same. The radial profiles in Fig. 4.6 also show that outside of 1° radius the four composites are the same. For comparison with the rawinsonde-derived figures given above, Table 4.1 gives the area-weighted averages of relative vorticity for $0^\circ-2^\circ$ and $0^\circ-4^\circ$ radius for all four composites. The vorticity values in the table for all four of the composites are very close to Erickson's values for developers, indicating once again that the NON-GEN and

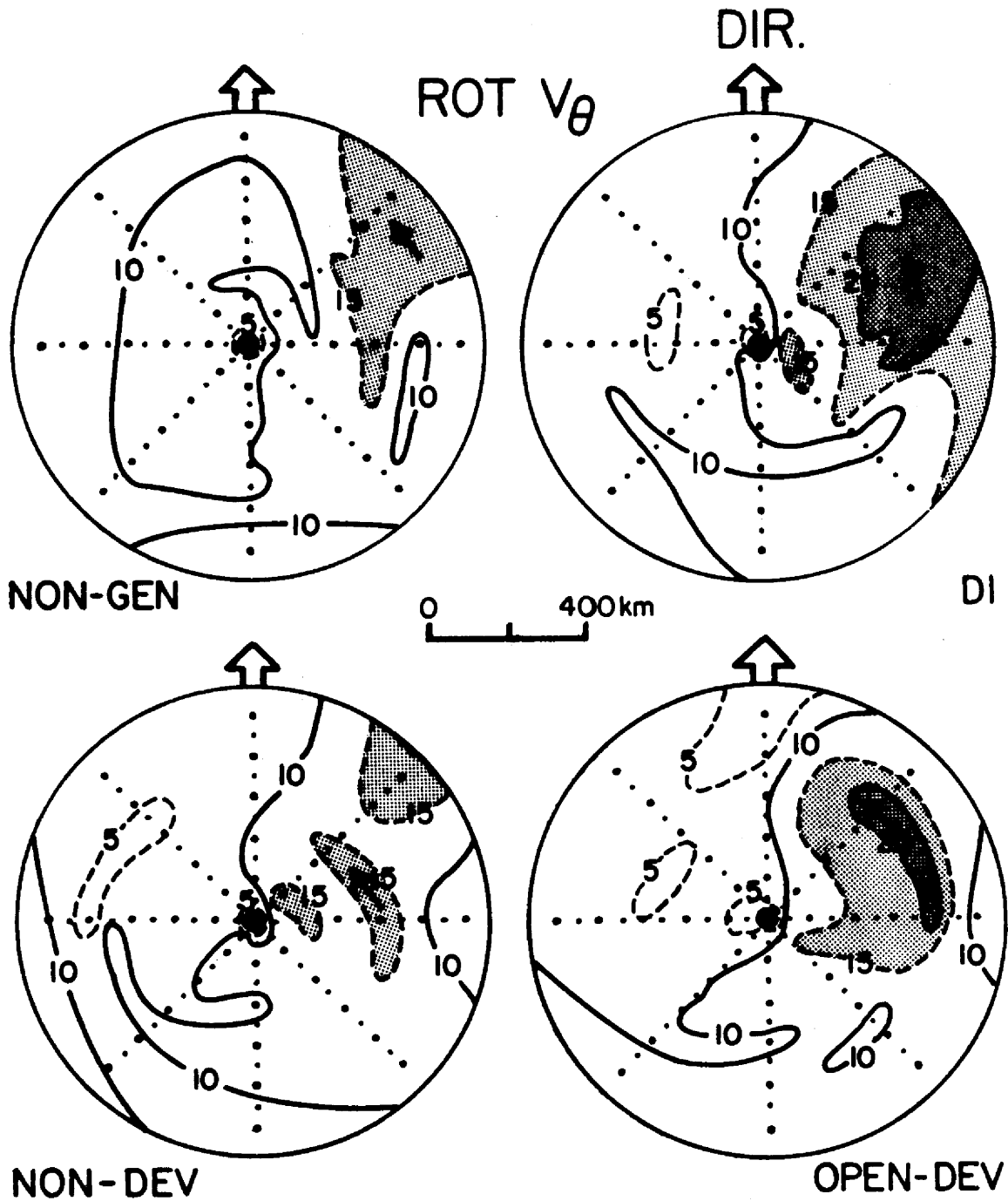


Figure 4.3: Plots of ROT tangential wind, in knots, out to 5° latitude from the center for NON-GEN, D1 (early developer), NON-DEV, and OPEN-DEV. Grid point spacing is 0.5° latitude (30 n mi) with larger dots at the whole-degree points. Direction of movement of system centers is up the page as indicated by arrow. Note: 2 knots = 1 m/s.

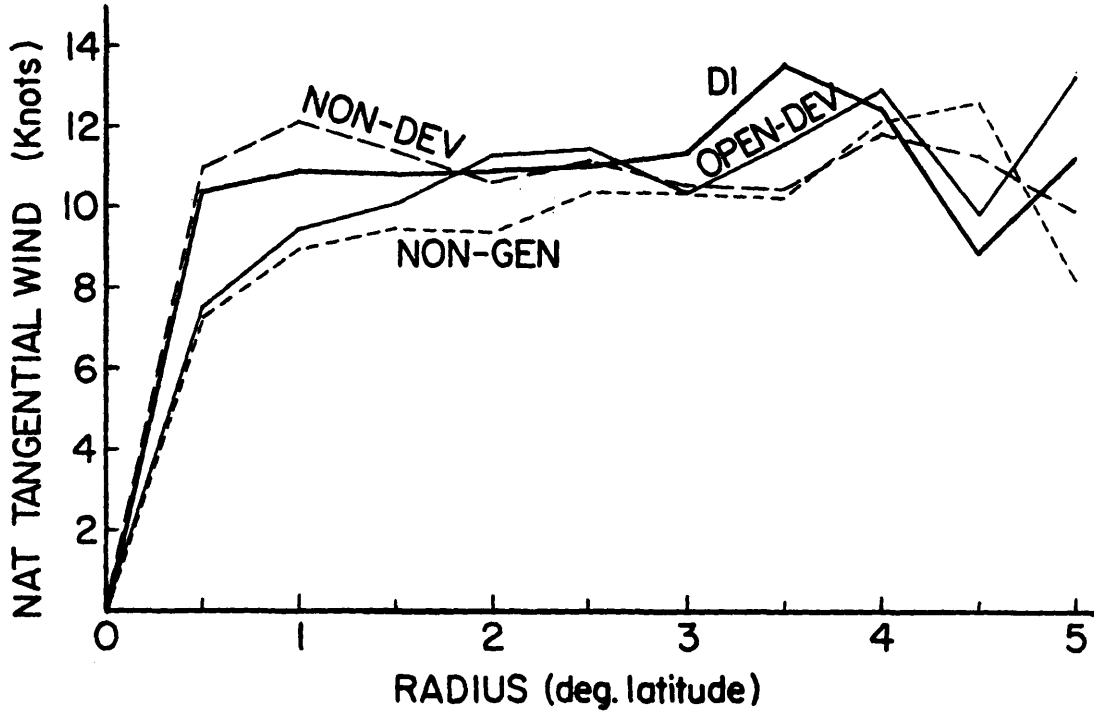


Figure 4.4: Radial profiles of NAT tangential wind, in knots, out to 5° from the center for NON-GEN, D1 (early developer), NON-DEV, and OPEN-DEV. Note: 2 knots = 1 m/s.

NON-DEV composites in this report are not the same as the non-developers of the earlier rawinsonde studies, and are very close to being developers.

Table 4.1: Area-weighted Average Relative Vorticity ($10^{-5}s^{-1}$).

Radius	D1	NON-GEN	OPEN-DEV	NON-DEV
$0^\circ - 2^\circ$	4.7	4.0	4.8	4.6
$0^\circ - 4^\circ$	2.5	2.6	2.6	2.5

The one really noteworthy aspect of the vorticity fields is the strong vorticity that is found near the center in all four plots. Since the Coriolis parameter f is about $3.4 \times 10^{-5}s^{-1}$, we see that for the four composites the relative vorticity is anywhere from 3 to 6 times larger than f . As Schubert and Hack (1982) have shown, such high values for relative vorticity tend to increase resistance to the radial movements of air parcels (i.e., the inertial stability) and hence increase the efficiency of warming near the center due to latent heat release, which in turn results in a faster spin-up of the circulation near the center. While

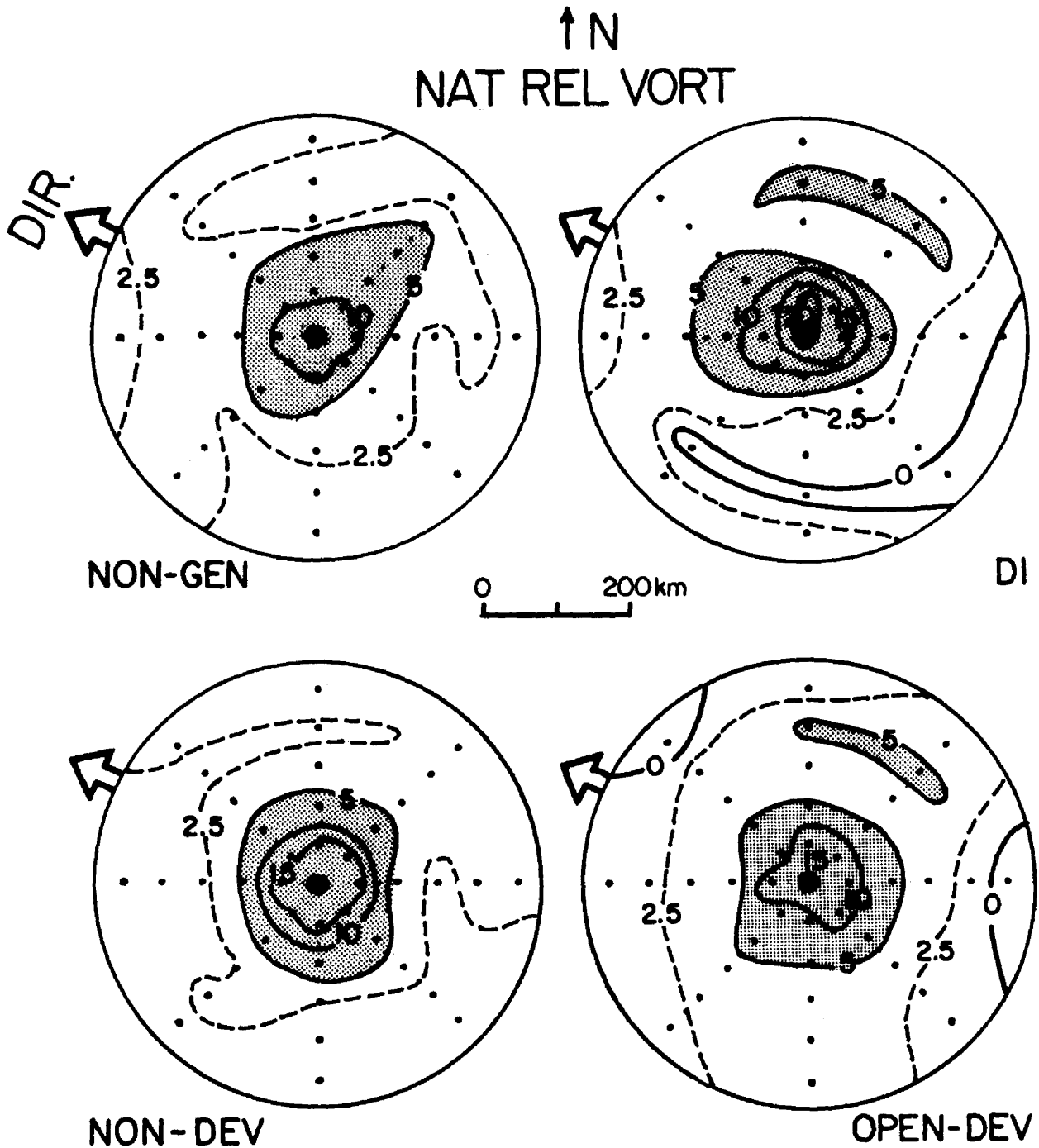


Figure 4.5: Expanded-scale plots of NAT relative vorticity, in units of $10^{-5} s^{-1}$, for NON-GEN, D1 (early developer), NON-DEV, and OPEN-DEV. Grid point spacing is 0.5° latitude (30 n mi) and the plots extend out to just past 2.5° radius. Heavy zero lines separate positive (cyclonic) from negative (anti-cyclonic) areas. The Coriolis parameter f is approximately $3.4 \times 10^{-5} s^{-1}$ for these composites. North is up.

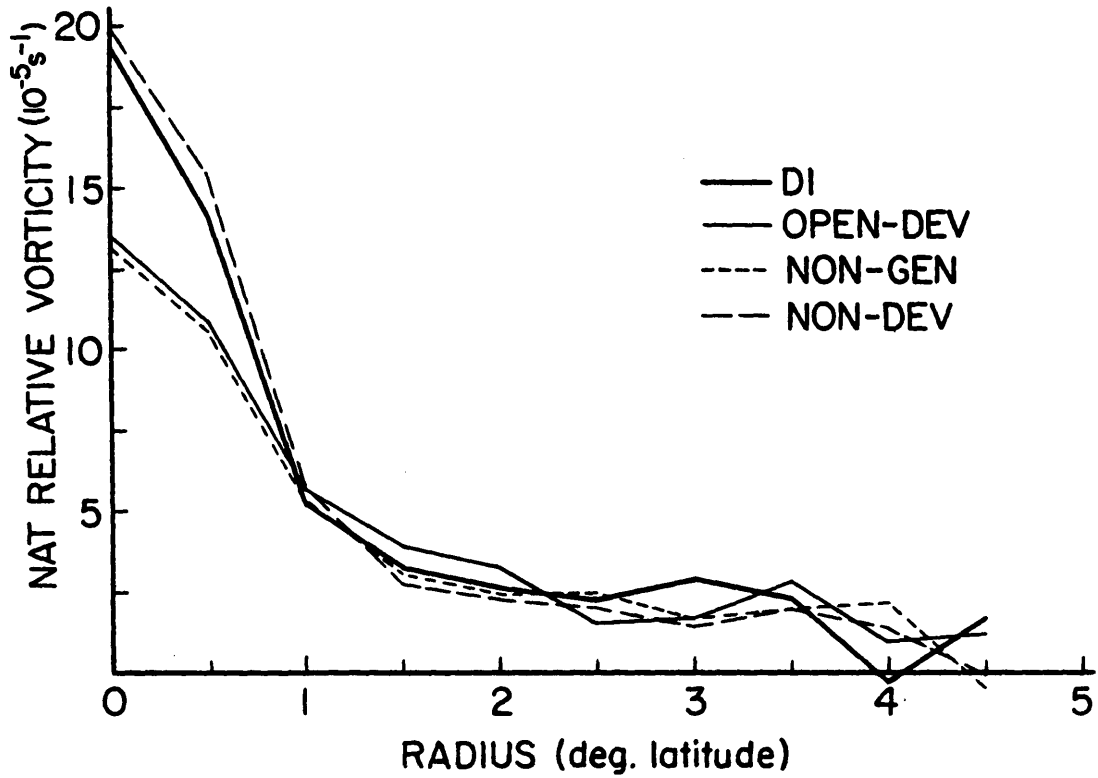


Figure 4.6: Radial profiles of NAT relative vorticity, in units of $10^{-5}s^{-1}$, out to 4.5° latitude from the center for NON-GEN, D1 (early developer), NON-DEV, and OPEN-DEV. The Coriolis parameter f is approximately $3.4 \times 10^{-5}s^{-1}$ for these composites.

NON-GEN has the weakest relative vorticity near the center of the four composites, even it has enough for significant inertial stability.

Earlier rawinsonde studies have shown that large amounts of low-level relative vorticity are necessary for development. Since the NON-GEN composite of this report has the required vorticity, it seems clear that vorticity by itself is not necessarily enough. But given that D1 and NON-GEN disturbances both have the required vorticity, what keeps the NON-GENs from developing?

4.2.5 Radial Wind

None of the rawinsonde studies referenced above has much to say about the low-level radial winds near the centers of either genesis or non-genesis disturbances. McBride (1979) found that his D2 developer composite (which is very close to this report's D1 composite) had a mean radial wind of -2 knots at 4° from the center, compared with about -1 knots for his N1 non-developers. Lee (1986) gives radial profiles of radial wind to within 1° of the center. His non-genesis cases have about -1 knots of radial wind from 1° - 5° , but his GN1 genesis case has radial winds from -1 knot at 1° from the center to a bit over -2 knots at 5° . His GN2 composite, which is a little more developed than this report's D1, shows a radial wind of -3 knots from 1° - 5° .

All of these rawinsonde composites, however, are data-poor within 2° of the center compared with the composites in this report, while from 3° - 5° the two sets of composites have similar numbers of observations. Table 4.2 compares McBride's and Lee's composites with D1, NON-GEN, OPEN-DEV, and NON-DEV of this report. It is clear that inside of 3° the composites of this report have many more observations, and inside of 1° the advantage is especially great. In addition, all of the rawinsonde composites referenced here have a radial grid spacing of 2° latitude, compared with 0.5° in this study. Hence, the composites about to be shown represent the first detailed look at low-level radial winds within 2.5° latitude of the center.

Figure 4.7 shows plots of the NAT radial wind within 2.5° of the centers of the four composites. In some ways, the four composites are roughly similar. All four have areas

Table 4.2: Number of Observations Within Given Radii of Center.

Composite		0 – 1°	1 – 3°	3 – 5°	0 – 5°
	D1	396	769	244	1409
	NON-GEN	286	752	304	1342
	OPEN-DEV	265	699	271	1235
	NON-DEV	585	1157	371	2113
McBride	N1	—	143	224	—
(1979)	D2	20	151	281	452
Lee	PN2	—	—	—	457
(1986)	GN1	—	—	—	421
	GN2	—	—	—	404

of positive (outward) radial wind in their northwest quadrants, and NON-GEN, D1, and OPEN-DEV also have areas of negative (inward) radial wind of -5 knots or stronger in their southwest quadrants. But if D1 is compared closely with NON-GEN, some important differences are apparent within 1.5° of the center. Of the 24 grid points within that radius of the center, NON-GEN has 8 points with radial winds stronger than -2.5 knots, while D1 has 12. For radial winds stronger than -5 knots, NON-GEN has a single grid point while D1 has four. Of the 16 grid points within 1 of the center, radial winds stronger than -2.5 knots occur at four points in NON-GEN, compared with D1's eight. Hence, within 1.5° of the center, and especially within 1°, inward radial winds are stronger in the genesis D1 composite than in the non-genesis NON-GEN composite. Including OPEN-DEV and NON-DEV in this comparison reinforces this conclusion.

Figure 4.7a shows the radial wind difference between D1 and NON-GEN in a different way. These plots are in the motion, or MOT, coordinate system, which means that we are seeing the radial component of the relative wind; that is, the wind relative to the moving center. The most obvious feature of all four plots is that there is inward flow in the western semicircle and most of the northeast quadrant, and outward flow elsewhere. But as in Fig. 4.7, a closer inspection shows that D1 has stronger overall inward radial wind within 1° of the center than does NON-GEN. Not only is D1's inflow stronger than NON-GEN's (D1 has an area of stronger than -10 kt SW of the center), its outflow NE through SE

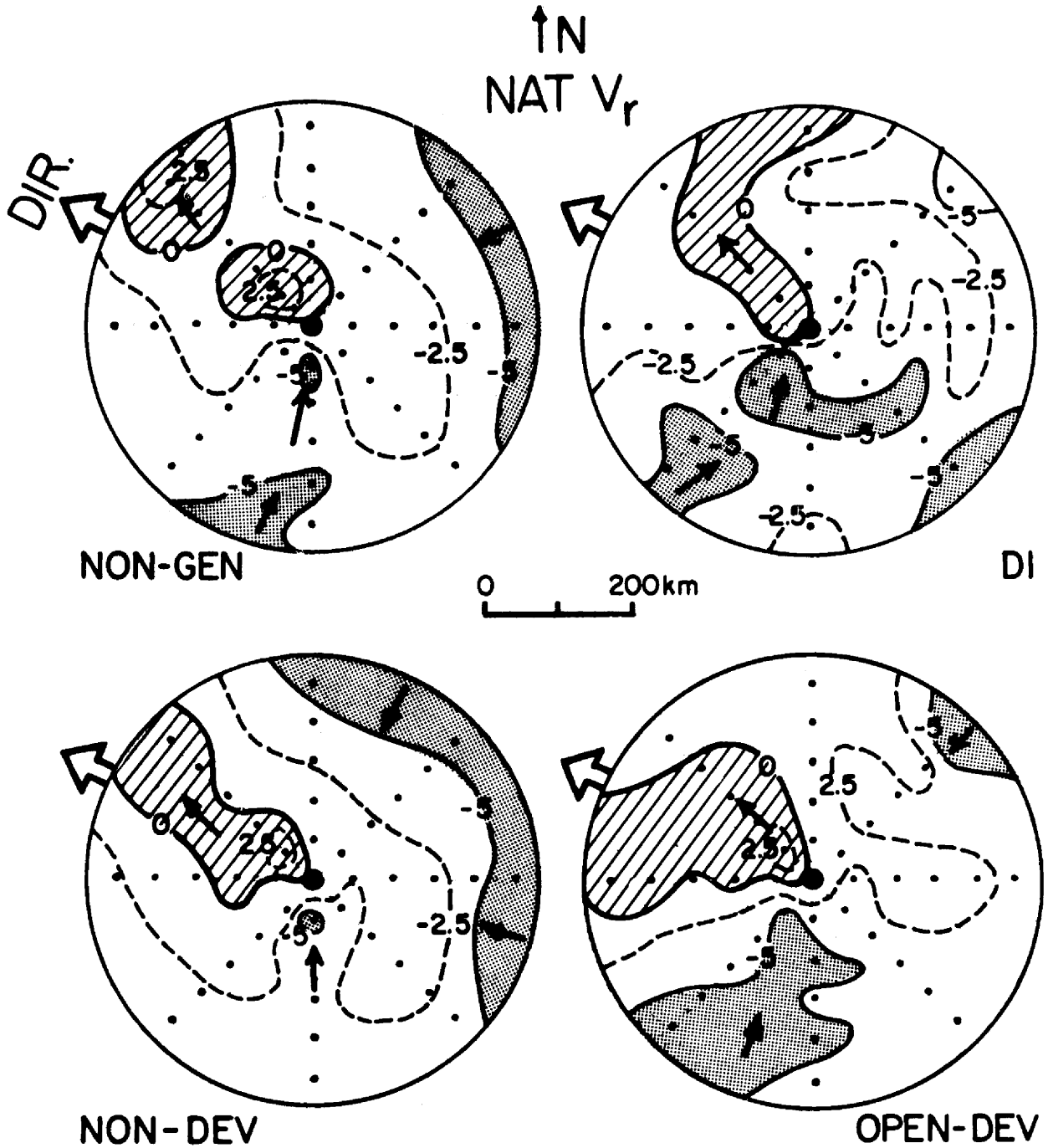


Figure 4.7: Expanded-scale plots of NAT radial wind, in knots, for NON-GEN, D1 (early developer), NON-DEV, and OPEN-DEV. Grid point spacing is 0.5° latitude (30 n mi) and the plots extend out to just past 2.5° radius. Heavy zero lines separate areas of positive (outward) from negative (inward) radial wind. North is up. Note: 2 knots = 1 m/s.

of the center is weaker. The same comparison can be made between OPEN-DEV and NON-DEV.

It is worth noting here that the direction of motion of the centers of all four composite systems is towards the west-northwest. The low-level inflow occurs ahead of the moving centers while the outflow occurs behind them; that is, the systems are overtaking the surrounding air as they move. Indeed, D1 and OPEN-DEV show what might be interpreted as radial wind surges west and southwest of their centers. By comparison, NON-GEN shows a somewhat weaker surge northwest of its center, while NON-DEV shows no surge at all. Such surges may play an important role in transporting momentum to the center. These surges seem strongest in D1.

Figure 4.8 (top) shows radial profiles of the NAT radial wind out to 5° . The azimuthally averaged radial wind is over twice as strong in D1 as in NON-GEN at 0.5° and 1° from the center, and 1.35 times as strong at 1.5° . Within 1° of the center, the OPEN-DEV curve closely follows D1, while NON-DEV stays close to NON-GEN.

Figure 4.8 (bottom) shows the same profiles, but in the MOT system. At 0.5° , the difference between D1 and NON-GEN is slightly less, but further out the radial wind in D1 is over seven times as strong as NON-GEN at 1° , and 1.65 times as strong at 1.5° . These changes in the azimuthal averages may seem strange at first, but such changes are possible due to the fact that many of the disturbances undergo acceleration during a mission, so that not all winds in a given mission necessarily have the same motion vector subtracted from them. Moreover, the distribution of observations about the center changes from mission to mission, so that different grid boxes have different average motion vectors subtracted out.

Here, then, is found the first significant difference between the average genesis and non-genesis disturbances: the inward radial wind out to 1.5° from the center is two or more times stronger in the genesis case. This is particularly true in the MOT coordinate system. In addition, apparent radial wind surges near the center are stronger in D1 (MOT system) than in NON-GEN.

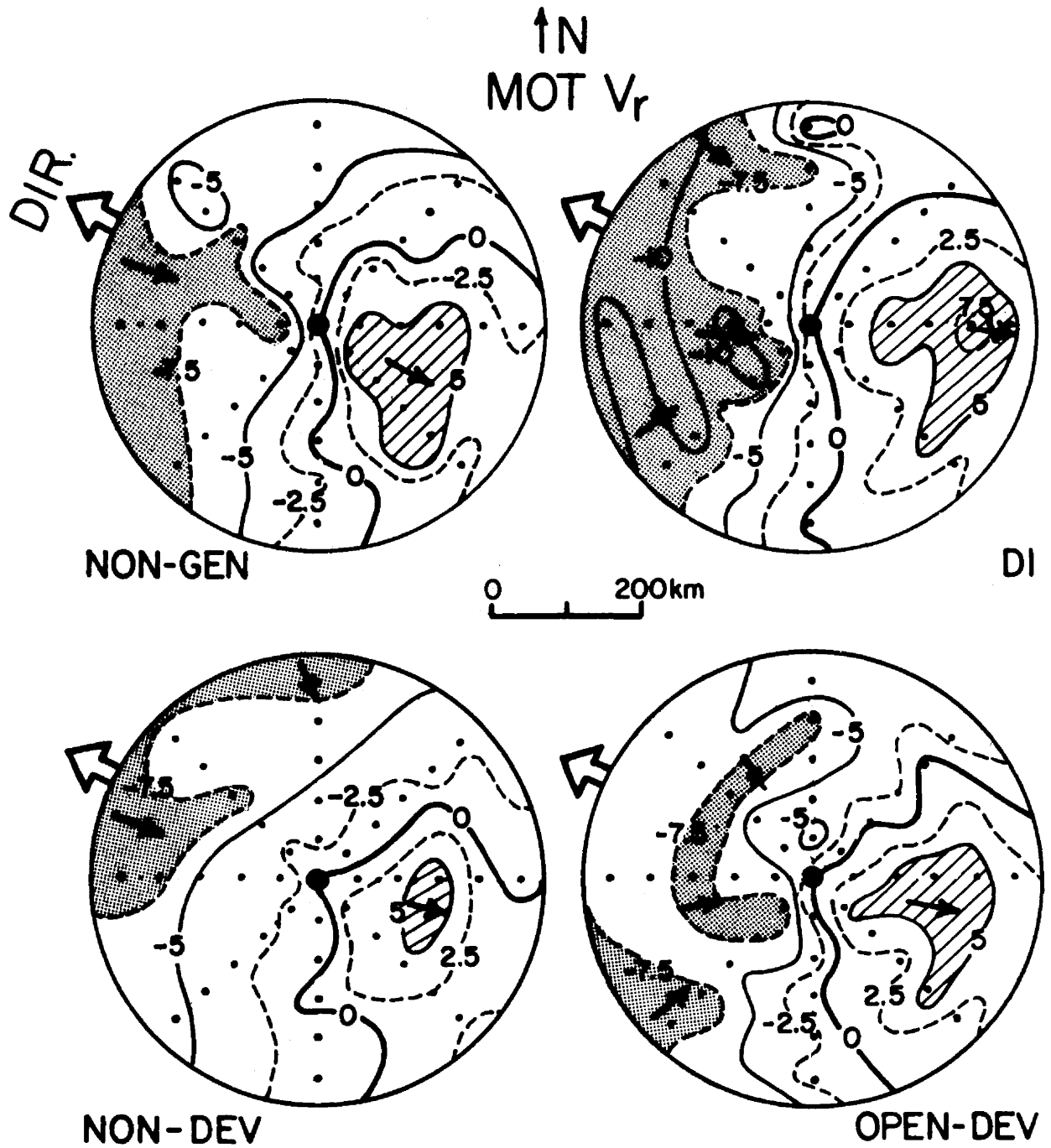


Figure 4.7: a. Same as Fig. 4.7, except MOT radial winds. North is up.

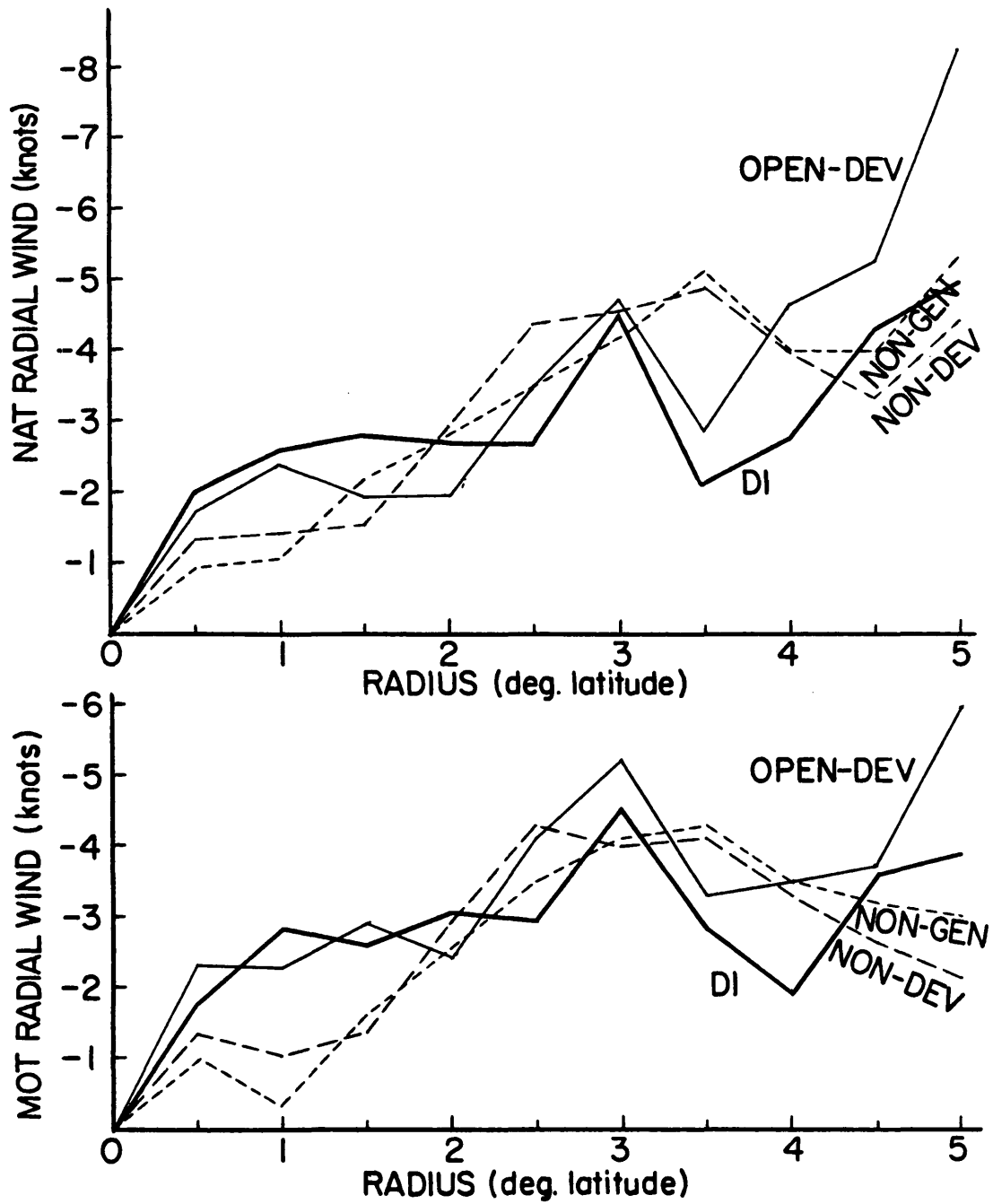


Figure 4.8: Radial profiles of NAT (top) and MOT (bottom) radial wind, in knots, for NON-GEN, D1 (early developer), NON-DEV, and OPEN-DEV. Negative values indicate inward radial winds. Note: 2 knots = 1 m/s.

4.2.6 Divergence

As with radial wind, this section presents the first detailed look at low-level divergence within 2.5° latitude of the center, with radial profiles out to 4.5° from the center.

Figure 4.9 (top) shows the radial profiles of divergence in the NAT system. As one might expect after looking at the radial wind profiles in Fig. 4.8, D1 has over twice the low-level convergence (i.e., negative divergence) at the center and 0.5° from the center that NON-GEN has. At 1° from the center, D1 exceeds NON-GEN by about 50%, but NON-GEN actually exceeds D1 at 1.5° . This result at 1.5° is true because, even though the radial wind at that radius is stronger in D1, NON-GEN has a much larger contribution from the shear term $\partial V_r / \partial r$, as a look at Fig. 4.8 shows. When OPEN-DEV and NON-DEV are added, the results are basically the same, but the differences are not as great. Outside of 1.5° , the four curves stay fairly close to one another.

Again as with radial wind, the MOT system seems to increase the difference between D1 and NON-GEN near the center, as Fig. 4.9 (bottom) shows. Indeed, the D1 and OPEN-DEV curves are little affected, but the convergence at 1° is significantly reduced for both NON-GEN and NON-DEV. From 1.5° on out, the four curves are nearly the same.

The horizontal NAT distributions of divergence within 2.5° of the center for the four composites are displayed in Fig. 4.10. Within 1.5° of the center, it is at once apparent that D1 has a larger and much better organized area of strong convergence than NON-GEN does. Indeed, not only do D1 and OPEN-DEV have larger and stronger areas of convergence, NON-GEN and NON-DEV both have an area of strong positive divergence 0.5° from the center.

Figure 4.11 shows the same plots in the ROT coordinate system. The results are basically the same as the previous figure, but now D1 and OPEN-DEV have no areas of positive divergence within 0.5° of the center, while NON-GEN and NON-DEV still do. For the two genesis composites, the main area of central convergence is centered just ahead of the circulation center.

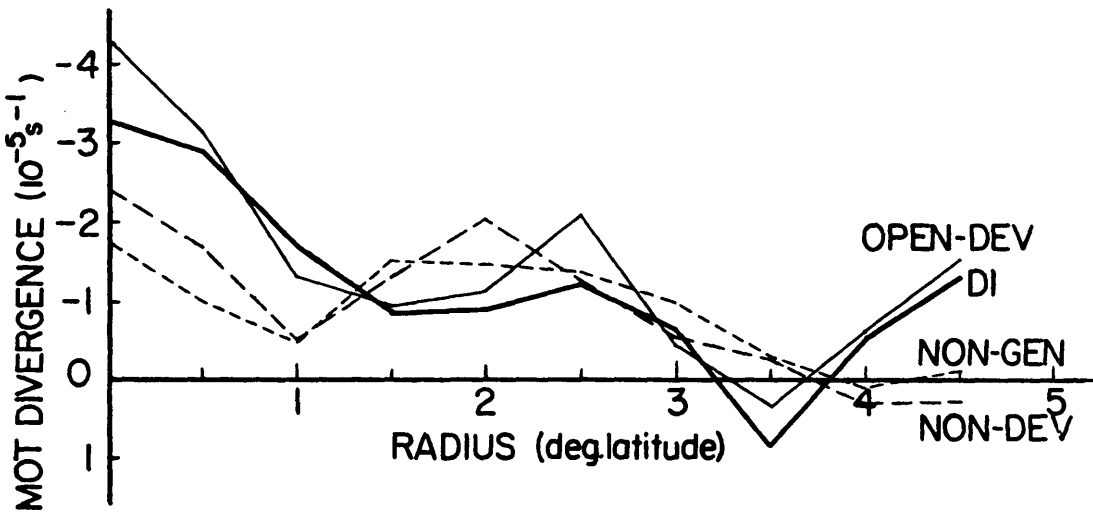
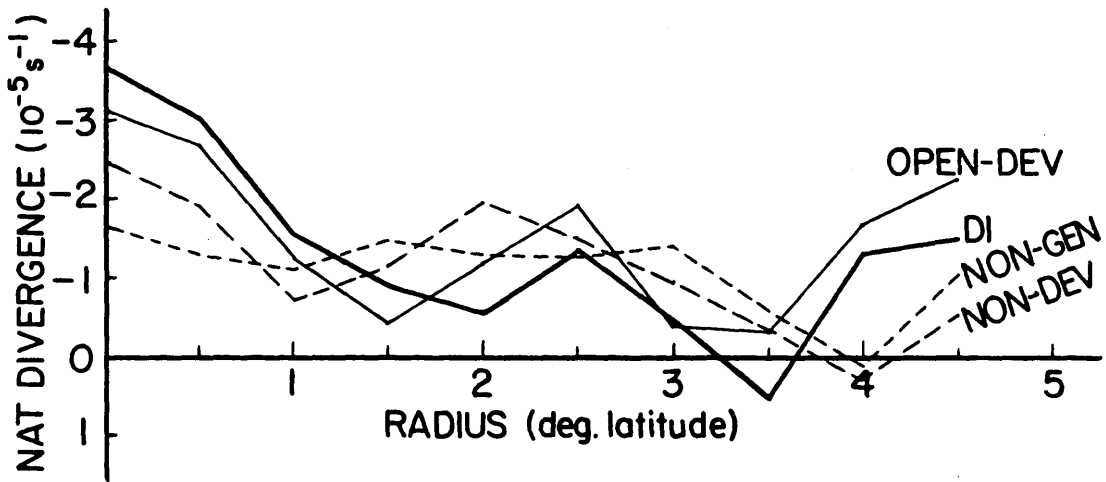


Figure 4.9: Radial profiles of NAT (top) and MOT (bottom) divergence, in units of $10^{-5} s^{-1}$, for NON-GEN, D1 (early developer), NON-DEV, and OPEN-DEV. Negative values indicate positive convergence.

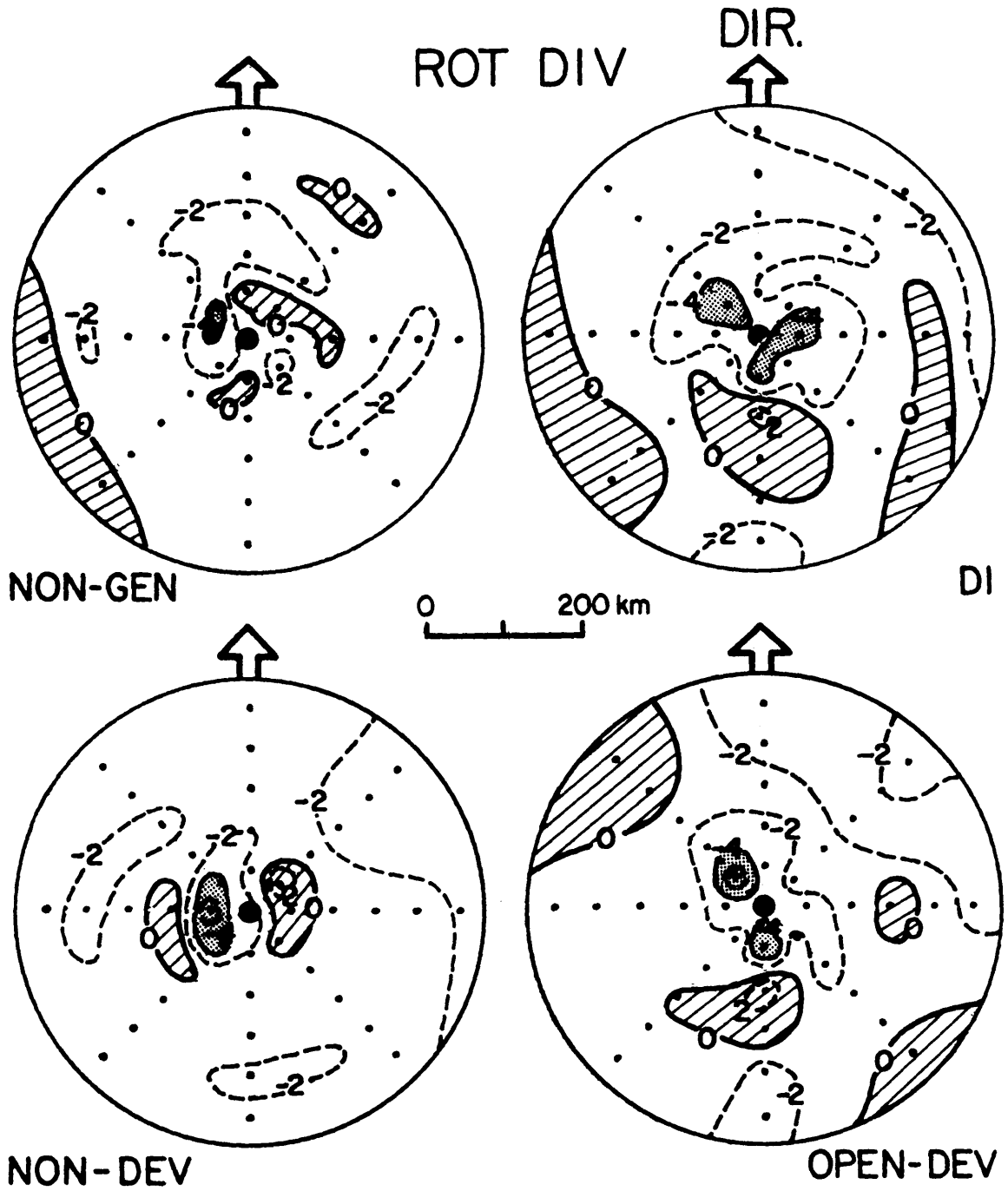


Figure 4.11: Same as Fig. 4.10, except ROT divergence. Direction of system motion is up the page as indicated by arrow.

Finally, Fig. 4.12 shows the same plots in the MOT system. It is noteworthy that all four composites have similar areas of positive divergence just east of the center. They also have areas of convergence just west and north of the center, but the convergence is much stronger in D1 and OPEN-DEV, with magnitudes exceeding $10 \times 10^{-5} s^{-1}$ in D1 and $12 \times 10^{-5} s^{-1}$ in OPEN-DEV.

Since strong low-level convergence in tropical disturbances implies strong upward motion and hence strong moist convection, these divergence results imply that D1 will have significantly stronger convection near the center than NON-GEN. This stronger convection in D1, along with the high inertial stability discussed earlier in the section on vorticity, would result in much stronger warming due to latent heat release and consequently faster spin-up near the center than in NON-GEN. This shows the importance of having the areas of strong low-level convergence near the center, where they can have the strongest effect on the developing vortex.

These divergence results parallel those in the radial wind fields. Hence, it is hypothesized here that strong inward radial wind and a strong and well organized area of convergence near the center of a disturbance are a good indication that development will take place, or is already taking place. See Chapter 6 for similar results that support this hypothesis.

4.2.7 Balance Between Wind and Pressure Gradient

In a cylindrical coordinate system, the equation of motion in the radial direction is:

$$dV_r/dt = (V_\theta^2/r) + fV_\theta - (1/\rho)\partial p/\partial r + Fr \quad (4.1)$$

where V_r is the radial wind, V_θ is the tangential wind, r is radius, f is the Coriolis parameter, ρ is air density, p is surface pressure, and Fr is the radial component of friction. If $dV_r/dt = Fr = 0$, we have the well-known gradient wind equation, in which the centrifugal acceleration, Coriolis acceleration, and pressure gradient force are in balance. If we also define the centrifugal term $Cf = V_\theta^2/r$, the Coriolis term $Co = fV_\theta$, and the pressure

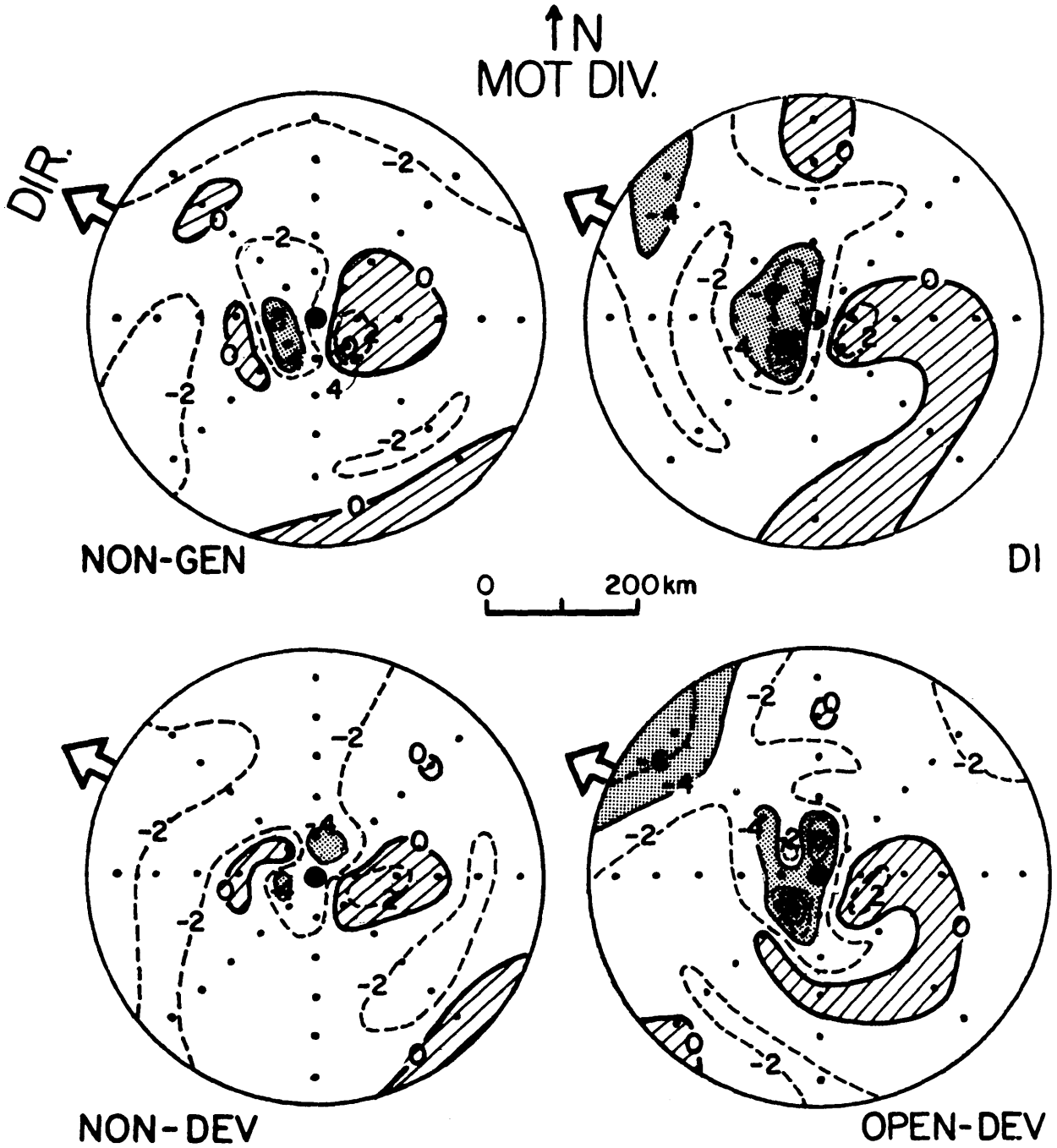


Figure 4.12: Same as Fig. 4.10, except MOT divergence. The value of the innermost contour 0.5° southwest of the center in OPEN-DEV is $-12 \times 10^{-5} s^{-1}$. North is up.

gradient term $Pr = (1/\rho)\partial p/\partial r$, then Eq. 4.1 becomes simply:

$$Cf + Co = Pr \quad (4.2)$$

and a "balance parameter" B can be defined as follows:

$$B = (Cf + Co)/Pr \quad (4.3)$$

Of course, if gradient balance exists, then $B = 1$. Supergradient tangential winds are indicated if $B > 1$, but the tangential wind is subgradient if $B < 1$.

Given radial profiles of surface pressure, tangential wind, and tangential wind squared, Eq. 4.3 can be used to compute B at any of the composite grid-point radii. However, more meaningful results are obtained in practice if Eq. 4.2 is integrated over finite intervals of radius to smooth out local irregularities in the radial profiles, as Gray (1962) did in his investigation of radial wind accelerations in Atlantic hurricanes. When integrated from r_1 to r_2 , the three terms in Eq. 4.2 become:

$$\bar{C}f = \int_{r_1}^{r_2} (V_\theta^2/r) dr = \int_{r_1}^{r_2} V_\theta^2 d(\ln r) = V_\theta^2 \ln(r_2/r_1) \quad (4.4)$$

$$\bar{C}o = \int_{r_1}^{r_2} fV_\theta dr = fV_\theta(r_2 - r_1) \quad (4.5)$$

$$\bar{P}r = \int_{r_1}^{r_2} (1/\rho)(\partial p/\partial r) dr = (1/\rho)(p_2 - p_1) \quad (4.6)$$

and the averaged balance parameter is:

$$\bar{B}(r_1, r_2) = (\bar{C}f + \bar{C}o)/\bar{P}r. \quad (4.7)$$

For the composited radial profiles in this study, the average tangential wind over a finite interval of radius is computed arithmetically, but V_θ^2 is estimated graphically from a plot of V_θ^2 vs. $\ln r$ (see Gray, 1962). For each composite, f is treated as a constant and given the value corresponding to the latitude of the composite center.

Figure 4.13 gives the radial profiles of \bar{B} for D1, NON-GEN, OPEN-DEV and NON-DEV. The interval of integration ($r_2 - r_1$) is 60 n mi (111 km), or 1° latitude, and the value of \bar{B} is assigned to the center of the interval. Thus, the \bar{B} obtained by integrating from

0.5° to 1.5° is plotted at 1° radius, etc. There is a problem at 0.5°, since an integration from 0° to 1° would result in $\bar{C}f$ being undefined. At this radius, Eq. 4.3 was used in finite-difference form, using the point values of V_θ and V_θ^2 at 0.5° instead of integrating. Indeed, when this method is used at the other radii in Fig. 4.13, the results are nearly exactly the same as the ones obtained by integrating. Hence, the values at 0.5° should be trustworthy.

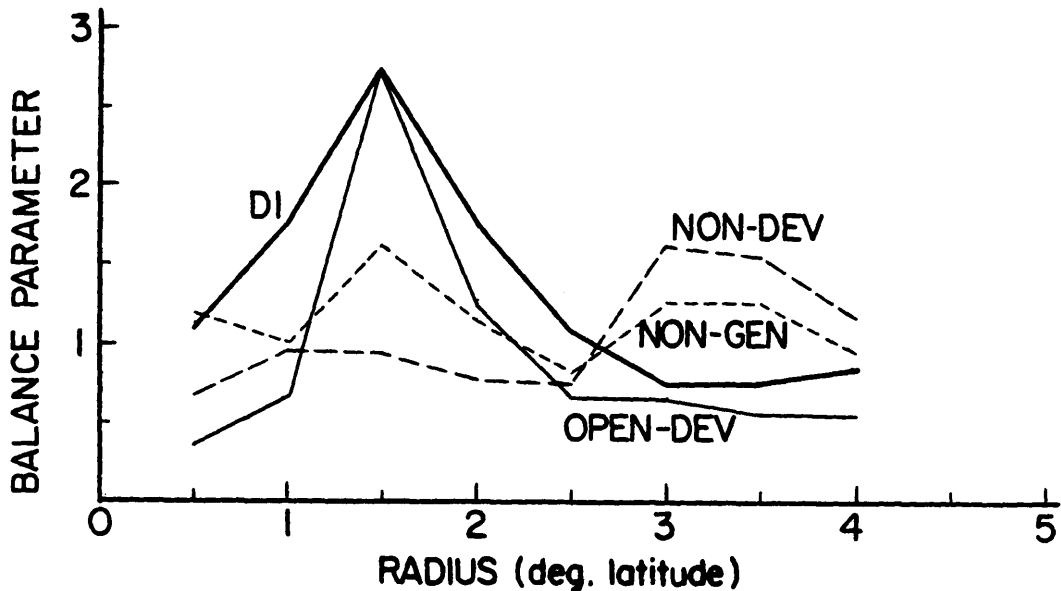


Figure 4.13: Radial profiles of \bar{B} , the averaged balance parameter, calculated over 60 mi intervals of integration, from 0.5° to 4° radius for NON-GEN, D1 (early developer), NON-DEV, and OPEN-DEV. The horizontal line at $\bar{B} = 1$ indicates gradient wind balance.

The most striking feature of Fig. 4.13 is the large peak in \bar{B} at 1.5° in the D1 and OPEN-DEV composites, indicating strongly supergradient tangential winds. NON-GEN has a lesser peak at that radius, while NON-DEV is subgradient all the way out to 2.5°. At 3° to 3.5°, the situation is reversed, with NON-GEN and NON-DEV having mildly supergradient winds while D1 and OPEN-DEV are subgradient.

For comparison with Fig. 4.13, Table 4.3 gives some values of \bar{B} for various radial intervals larger than 1° of latitude. It is evident that as the interval size is increased, the differences between the composites lessen as they approach $\bar{B} = 1$, except for OPEN-DEV.

Table 4.3: \bar{B} Computed Over Differing Intervals of Radius

Composite	1 – 2.5°	1 – 3°	0 – 4.5°
D1	2.54	1.65	1.14
NON-GEN	1.08	1.13	1.07
OPEN-DEV	1.67	1.17	0.68
NON-DEV	0.78	0.85	1.02

Based on Fig. 4.13 and Table 4.3, the strong surge of supergradient tangential winds inside of 2.5° from the center distinguishes the genesis composites D1 and OPEN-DEV from NON-GEN and NON-DEV. OPEN-DEV is especially interesting, because it shows the strong peak near 1.5° radius in spite of the fact that elsewhere within 2.5° of the center its values of \bar{B} are substantially lower than those of D1.

But it is also interesting to note that NON-GEN, while it does not have the strong peak in \bar{B} that distinguishes a genesis composite, does have a weaker version of it, which NON-DEV lacks. This may be yet another indication of how close the NON-GEN composite is to being a genesis composite, in that while it does not in fact undergo genesis, it may be “trying” to do so. NON-DEV, on the other hand, shows no such tendency. This difference is likely due to the fact that NON-DEV contains, in addition to the missions in NON-GEN, many missions flown on former named storms or typhoons that are now dissipating. Certainly a dissipating circulation, even though it may still be quite well defined, has even less of a tendency towards genesis than most of the non-genesis disturbances represented in the NON-GEN file. Since NON-DEV contains more missions flown on dissipating systems than NON-GEN, it might be expected not to display the slight peak at 1.5° that NON-GEN has. Does the strength of the peak, then, correlate with “genesis potential”? More investigation is needed to answer this question.

4.3 Summary of Results

1. Comparisons of sea-level pressure, streamlines and isotachs, tangential wind, and relative vorticity failed to show any significant differences between D1 and NON-GEN at low level.

2. **Radial Wind:** Inside of 1.5° radius, the inward radial wind is at least twice as strong in D1 as in NON-GEN. Differences are even greater in the MOT system. In addition, apparent radial wind surges are evident west and southwest of the center, and are stronger in D1 than in NON-GEN.
3. **Divergence:** Within 1° of the center, low-level convergence (negative divergence) is roughly twice as strong in D1 as in NON-GEN. In addition, areas of strong convergence near the center are larger and better organized in D1 as compared with NON-GEN, implying stronger and better-organized convection near the center in D1. It is hypothesized that for any given disturbance, the strength and organization of the convergence near the center are good indicators of the potential for development.
4. **Balance Parameter:** A very strong peak in \bar{B} appears at 1.5° from the center in the D1 composite, but only a weak peak is present in NON-GEN. More generally, the values of \bar{B} for the radial interval $1-2.5^\circ$ seem to indicate very strongly supergradient tangential winds in D1, compared with approximate gradient balance in NON-GEN (see Table 4.3).
5. In general, the OPEN-DEV composite displays the same genesis features present in D1, while NON-DEV displays the same lack of such features characteristic of NON-GEN.

Chapter 5

DEVELOPMENT

5.1 Data Sets Being Compared

The D1, D2, and D3 composites, or data sets, represent three progressive stages in the development of a typical western North Pacific tropical cyclone, from the minimal depression stage D1, with maximum tangential winds of about 20 knots, to the minimal tropical storm stage D3, with maximum tangential winds of about 35 knots. The D2 composite is an intermediate stage between the other two, perhaps somewhat closer to D1 than to D3 in degree of development. Using these three composites, this chapter presents a brief look at the changes that occur in the low-level wind and pressure fields of a newly forming tropical cyclone as it develops to minimal tropical storm intensity.

5.2 Development at Low Level

5.2.1 Sea-Level Pressure

Composite radial profiles of sea-level pressure for D1, D2, and D3 are shown in Fig. 5.1. Outside of 2° latitude from the center all the way to 5° , the pressure drop is nearly uniform from one stage to the next—about 2 mb from D1 to D2 and slightly more than 2 mb from D2 to D3. It is especially noteworthy that the pressure gradient in the 2° - 5° interval remains roughly the same in all three composites. Inside of 2° , however, the pressure gradient steepens dramatically from D1 to D3, especially near the center. From D1 to D2, and from D2 to D3, pressure drops are about 5 mb and 9 mb, respectively, at the center, while at a radius of 0.5° the drops are about 4 mb and 6 mb, respectively.

Certainly these results are no great surprise, as the pressure drop near the center of a developing tropical cyclone is a well-known phenomenon. For example, the recent results

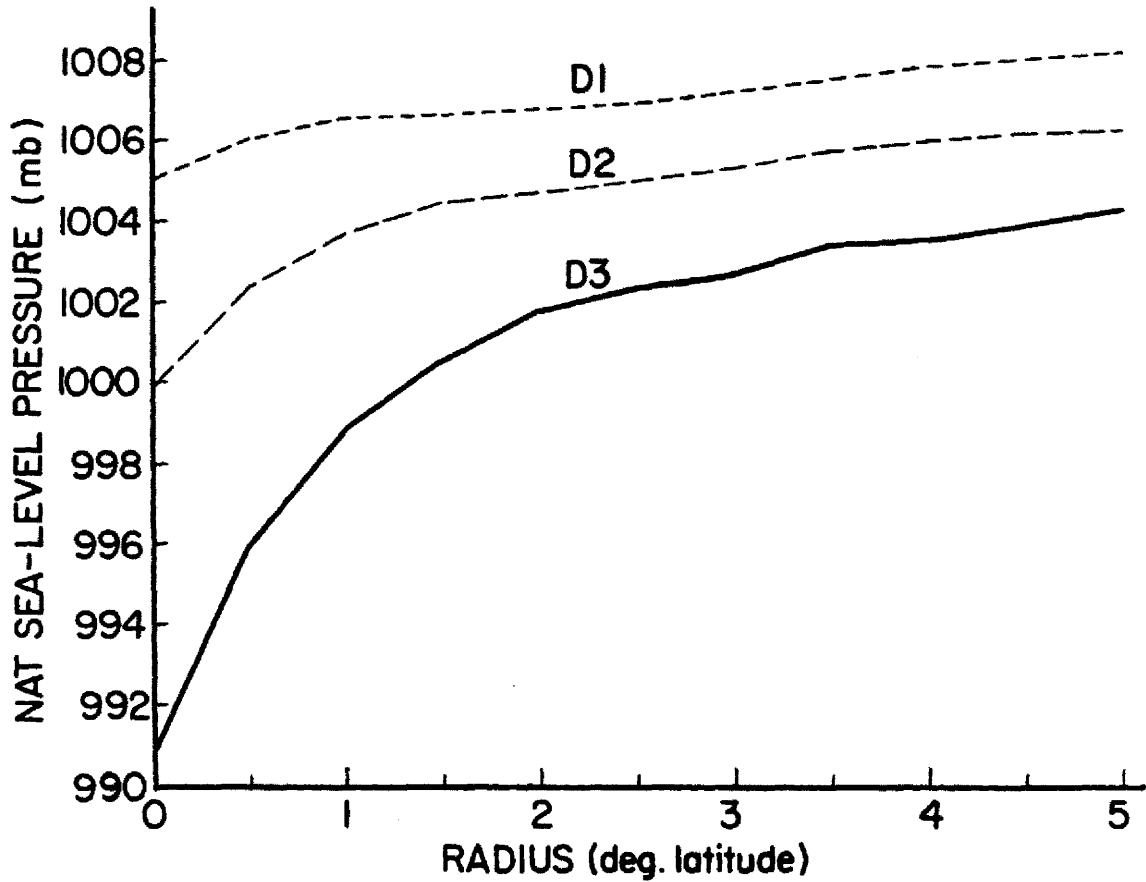


Figure 5.1: Radial profiles of NAT sea-level pressure out to 5° latitude from the center for the D1 (early developer), D2 (middle developer), and D3 (late developer) composites.

of Lee (1986) also show a concentrated pressure drop near the center (Figs. 19 and 20 in his report). However, whereas Lee's profiles seem to show an inward-propagating zone of stronger pressure gradient, the results of this report show no evidence of it. Instead, steeper gradients seem to spread out from the center.

5.2.2 Tangential Wind

In keeping with the results of the previous section, one would expect the tangential winds to increase near the center in going from D1 to D2 to D3. As Fig. 5.2 shows, this is exactly the case. Since these profiles are azimuthal averages, however, the highest tangential winds tend to be averaged out, so that a distinct wind maximum near the center is not evident until stage D3 is reached.

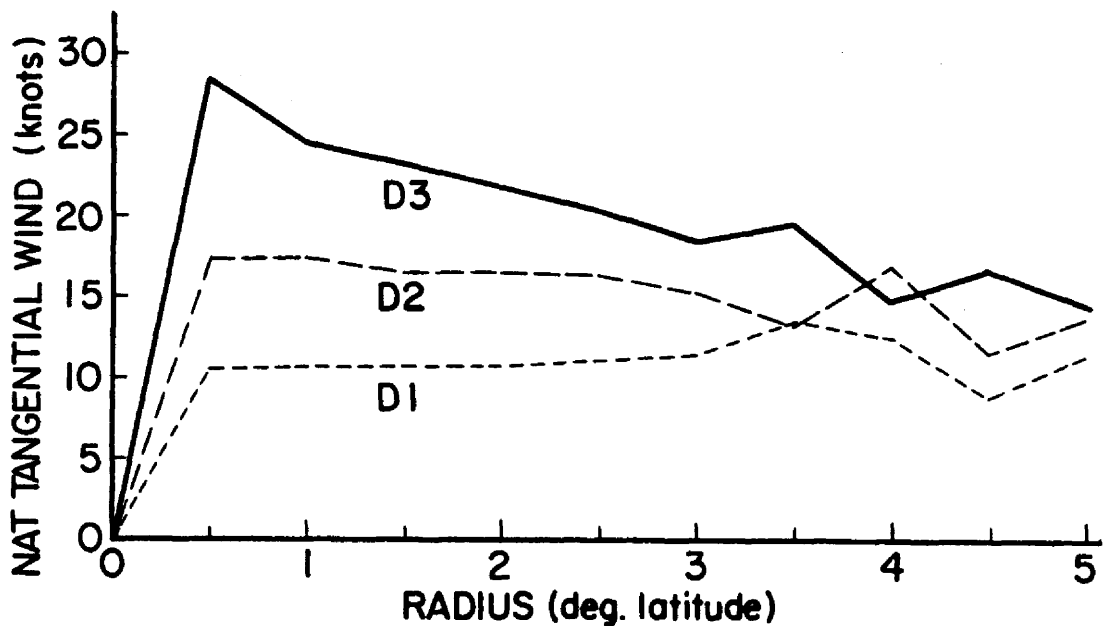


Figure 5.2: Radial profiles of NAT tangential wind, in knots, out to 5° latitude from the center for the D1 (early developer), D2 (middle developer), and D3 (late developer) composites. Note: 2 knots = 1 m/s.

The development of a maximum wind band near the center is much better displayed in Fig. 5.3, where ROT system plots of the tangential wind are shown. In the D1 composite the highest tangential winds are well away from the center, but in the D2 plot the 15-knot isotach has nearly wrapped itself around the center, and an area of over 20 knots has

appeared to the right of the center. In the D3 composite, a band of 25-knot winds nearly circles the center, and a maximum wind of 35 knots is just to the right of the center.

The difference plots in Fig. 5.4 give a detailed look at how the tangential wind field changes from one stage to the next. The first plot, for D2 - D1 (i.e., D2 minus D1), shows the wind actually dropping off significantly in the right-front quadrant 4° to 5° from the center. The main area of increased wind, amounting to a 5-knot or greater increase, encompasses a large area that is centered in the left semicircle, giving D2 a more symmetrical wind field than D1 (see Fig. 5.3). In the composite for D3-D2, increases of 10-15 knots are clustered right around the center and in an area far out in the right rear quadrant. Here, the right semicircle has larger areas of increased wind than the left, with the result that the wind field in D3 is more asymmetric than in D2, or about as asymmetric as D1. Indeed, as the composite for D3-D1 shows, the total change in tangential wind from D1 to D3 is remarkably symmetric about the center. The difference isotach for plus 10 knots is nearly circular about the center, varying in radius between 2° and 3° of latitude.

These difference plots, then, appear to bring out three main features of early tropical cyclone intensification:

1. On the whole, it appears that in a developing cyclone the basic asymmetry in the tangential wind field, as shown by the stronger winds in the right semicircle in the ROT system, is maintained as the cyclone intensifies.
2. The greatest increase in tangential wind takes place within 1° of the center. This is especially apparent in the D3-D1 composite.
3. Prior to the development of a maximum wind band near the center, a newly-formed cyclone's strongest winds tend to be $3-5^{\circ}$ from the center and in the right-front quadrant. As the cyclone develops further this area of strong winds seems to collapse as the maximum wind band begins to appear near the center (see plot for D2-D1). Is this due to the trade wind surges which often appear north of a disturbance's center? Further study is needed to determine the reality of this phenomenon.

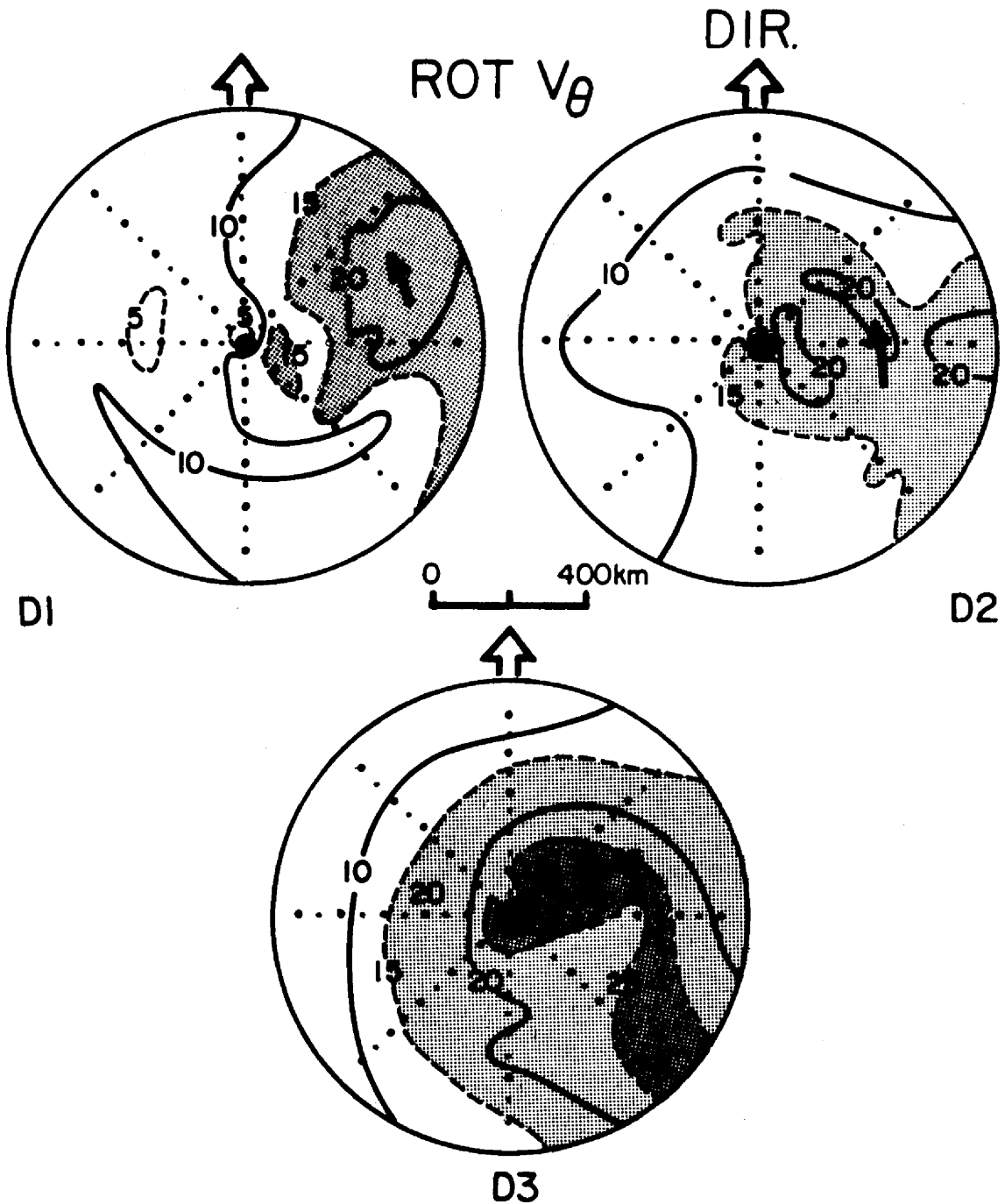


Figure 5.3: Plots of ROT tangential wind, in knots, out to 5° latitude from the center for the D1 (early developer), D2 (middle developer), and D3 (late developer). Grid point spacing is 0.5° latitude (30 n mi) and larger dots mark whole-degree points. Direction of storm motion is up the page. In the D3 plot, isotachs inside the unlabelled 20-knot isotach around the center are omitted. Note: 2 knots = 1 m/s.

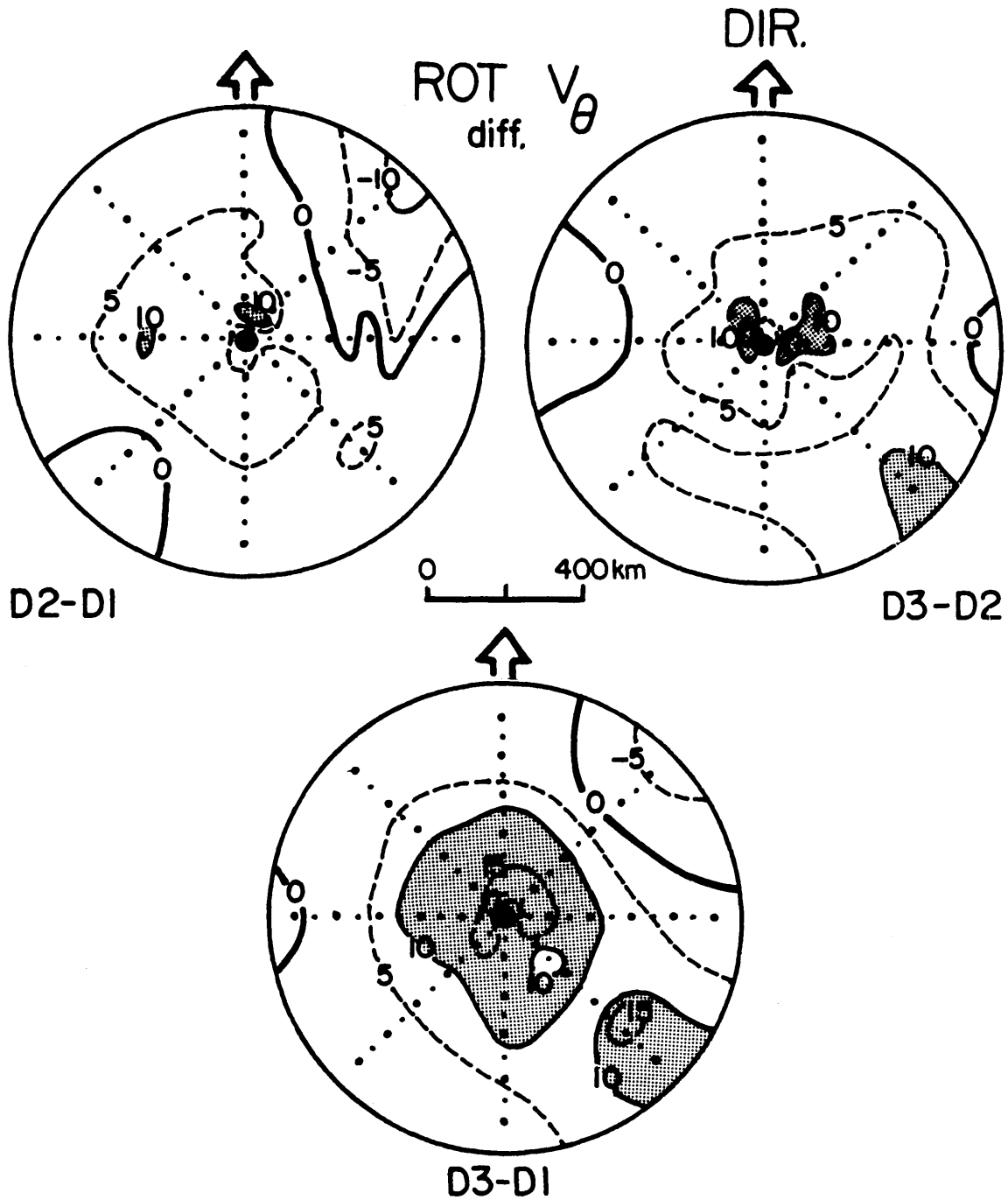


Figure 5.4: Difference plots for ROT tangential wind, in knots, derived from the plots in Fig. 5.3, for D2 - D1 (D2 minus D1), D3 - D2, and D3 - D1. Grid point spacing is 0.5° latitude (30 n mi) and the plots extend out to 5° from the center. Larger dots mark whole-degree points. The heavy zero lines separate positive from negative differences. Direction of storm motion is up the page. Note: 2 knots = 1 m/s.

5.2.3 Relative Vorticity

Figure 5.5 shows radial profiles of relative vorticity in the NAT system. As might be expected from an inspection of Fig. 5.2, vorticity increases rapidly near the center, while there is no real change outside of 2° from the center. Within 1° of the center, the relative vorticity increases from five times the Coriolis parameter f in D1 to nearly $12 \times f$ in D3. Thus, the inertial stability (Schubert and Hack, 1982) increases rapidly as development proceeds, leading to more and more efficient use of latent heat released near the center, so that the storm can continue to intensify even in the absence of any further intensification of the convection near the center.

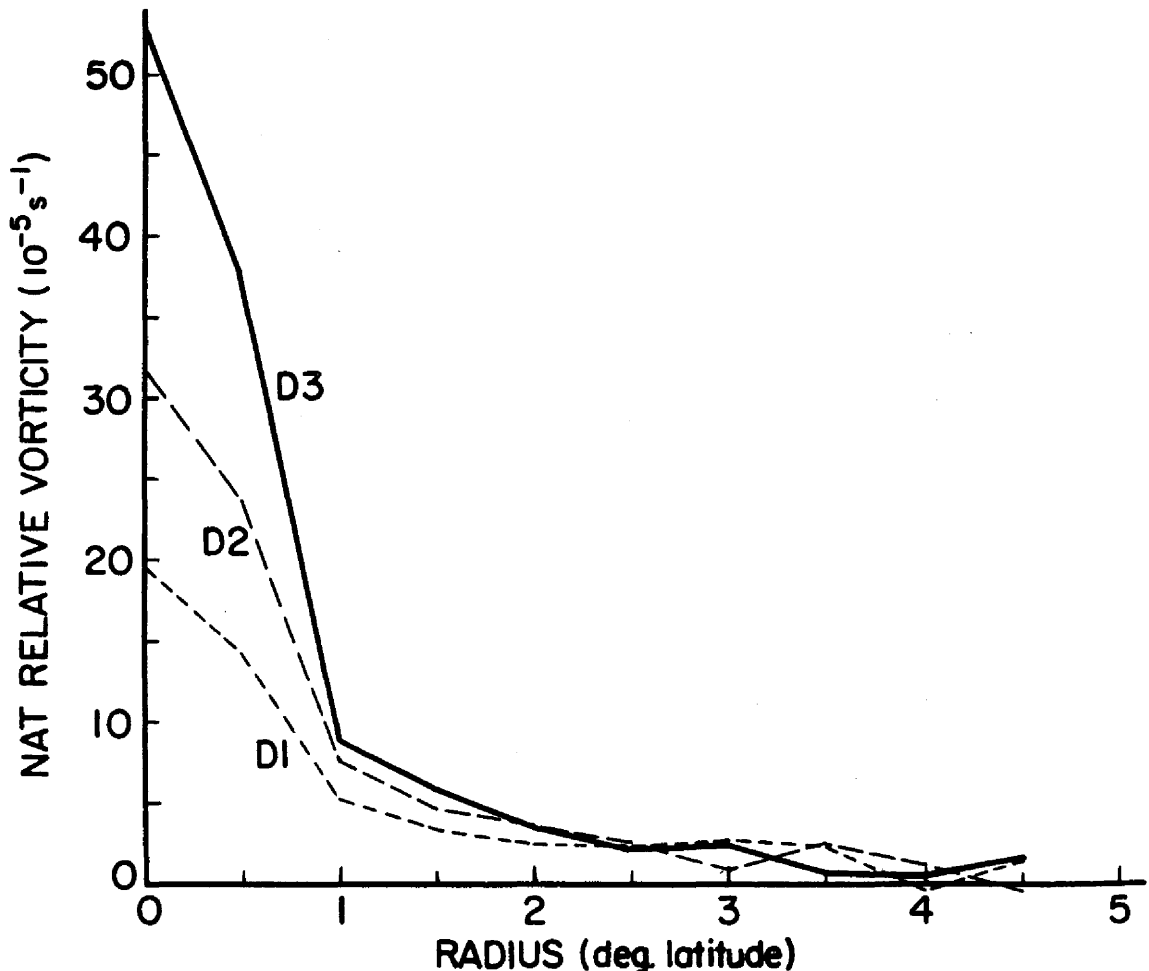


Figure 5.5: Radial profiles of NAT relative vorticity out to 4.5° latitude from the center for the D1 (early developer), D2 (middle developer), and D3 (late developer) composites, in units of $10^{-5} s^{-1}$. The Coriolis parameter f is approximately $3.4 \times 10^{-5} s^{-1}$ for D1 and D2, and approximately $4.5 \times 10^{-5} s^{-1}$ for D3.

5.2.4 Radial Wind

Radial profiles of NAT radial wind are shown in Fig. 5.6. The clear-cut differences between stages of development that were evident in the sea-level pressure and tangential wind profiles are not evident here. It is noteworthy, however, that both D2 and D3 everywhere exceed D1. In addition, D3 has generally stronger inward-directed radial wind inside of 2 from the center, but at 0.5° D2 actually has slightly stronger inflow. Outside of 2° , radial winds in D2 and D3 generally increase, but the profiles are fairly noisy.

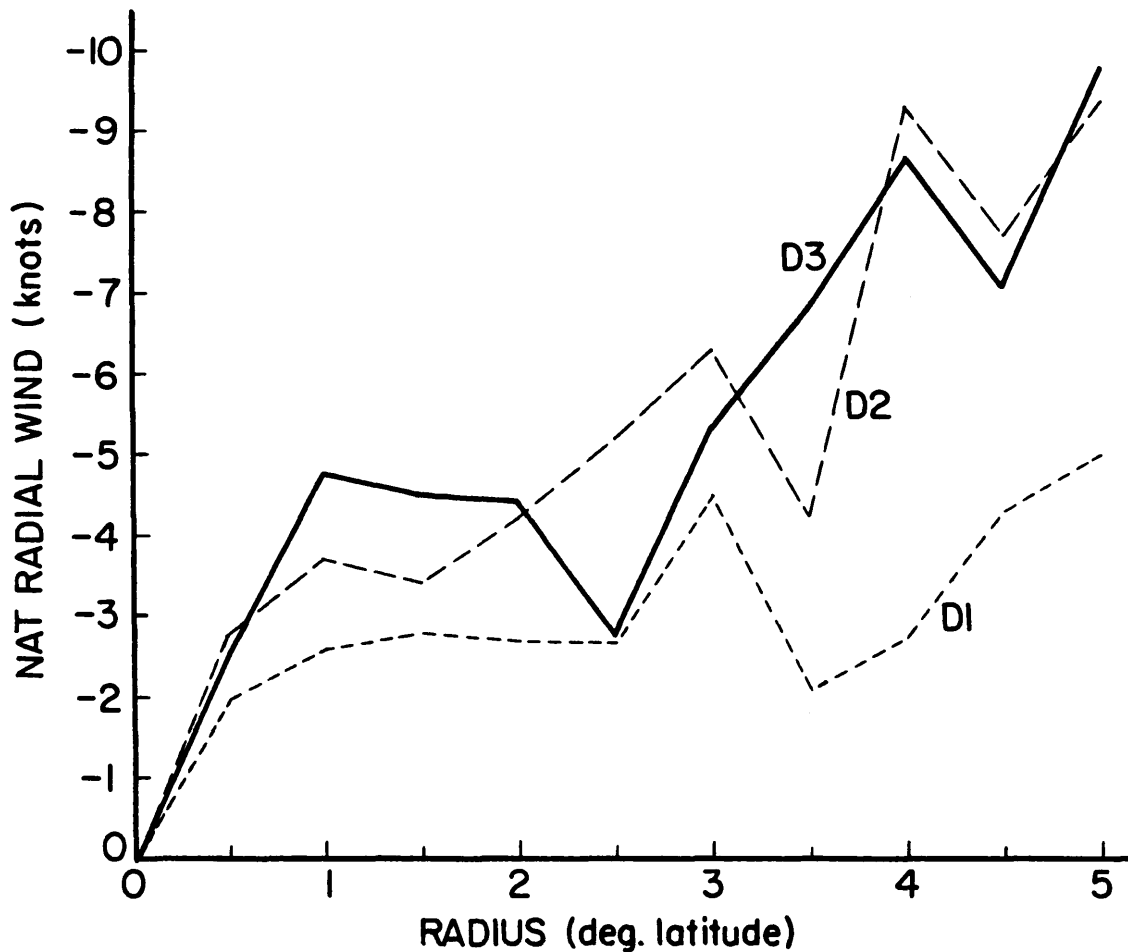


Figure 5.6: Radial profiles of NAT radial wind, in knots, out to 5° latitude from the center for D1 (early developer), D2 (middle developer), and D3 (late developer). Negative values indicate inward-directed radial wind. Note: 2 knots = 1 m/s.

A much more detailed portrayal of the NAT radial wind fields within 2.5° of the center appears in Fig. 5.7. Basic features common to all three composites include the

area or areas of positive radial wind west through north of the center, and the areas of strong negative radial wind southeast through southwest of the center. The area of positive radial wind decreases from D1 to D2, then almost vanishes in D3. At the same time, negative radial wind strengthens significantly in the southern semicircle of D2 as compared with D1, but in going from D2 to D3 little if any additional strengthening occurs there. But the shrinkage of the area of positive radial wind northwest of the center in going from D2 to D3 does result in the stronger negative azimuthally averaged radial wind near the center in D3, previously noted in Fig 5.6.

If these same composites are done in the ROT coordinate system, as shown in Fig. 5.8, the larger-scale features are basically the same, but the areas of positive radial wind, now in the right-front quadrant, are similar in size in all three composites. Instead of the shrinking positive area, a kind of radial wind “dipole” appears, in which an area of positive radial wind and an area of strong negative radial wind oppose each other across the center at radii of 0.5° from the center. The strength of this dipole appears to increase as the composite cyclone develops. Only more investigation can determine if this dipole is real or just an artifact of the ROT system.

Finally, Fig. 5.8a shows the MOT radial winds within 2.5° of the center. The large area of positive radial wind that occupies most of the eastern half of D1 becomes much smaller in D2, and actually breaks up in D3. Meanwhile, the areas of inflow in the western halves of the three composites change very little. Thus, the degree of asymmetry in the MOT radial wind field decreases as the composite system develops and inflow spreads into the eastern half of the storm.

5.2.5 Divergence

The radial profiles of NAT divergence within 2.5° of the center are shown in Fig. 5.9. As expected, the low-level convergence (negative divergence) is highest at the centers of all three composites. Just as in Chapter 4 we saw that D1 had significantly higher convergence than NON-GEN within 1° of the center, here we see that convergence continues to increase in this region in going from D1 through D2 to D3. However, it also appears that this

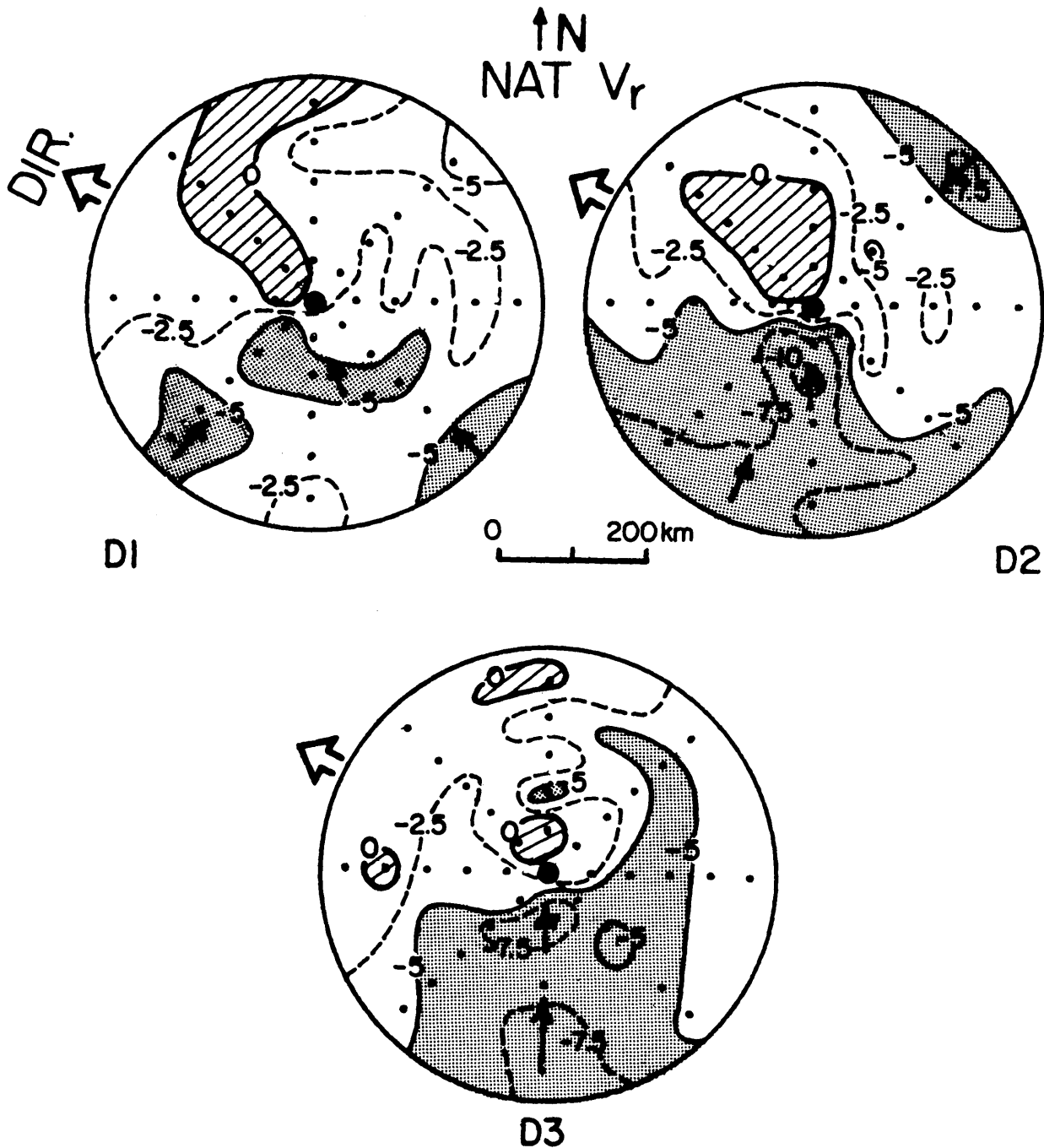


Figure 5.7: Expanded-scale plots of NAT radial wind, in knots, for the D1 (early developer), D2 (middle developer), and D3 (late developer) composites. Grid point spacing is 0.5° latitude (30 n mi), and the plots extend out to just past 2.5° radius. Heavy zero lines separate positive (outward) from negative (inward) radial wind. North is up. Note: 2 knots = 1 m/s.

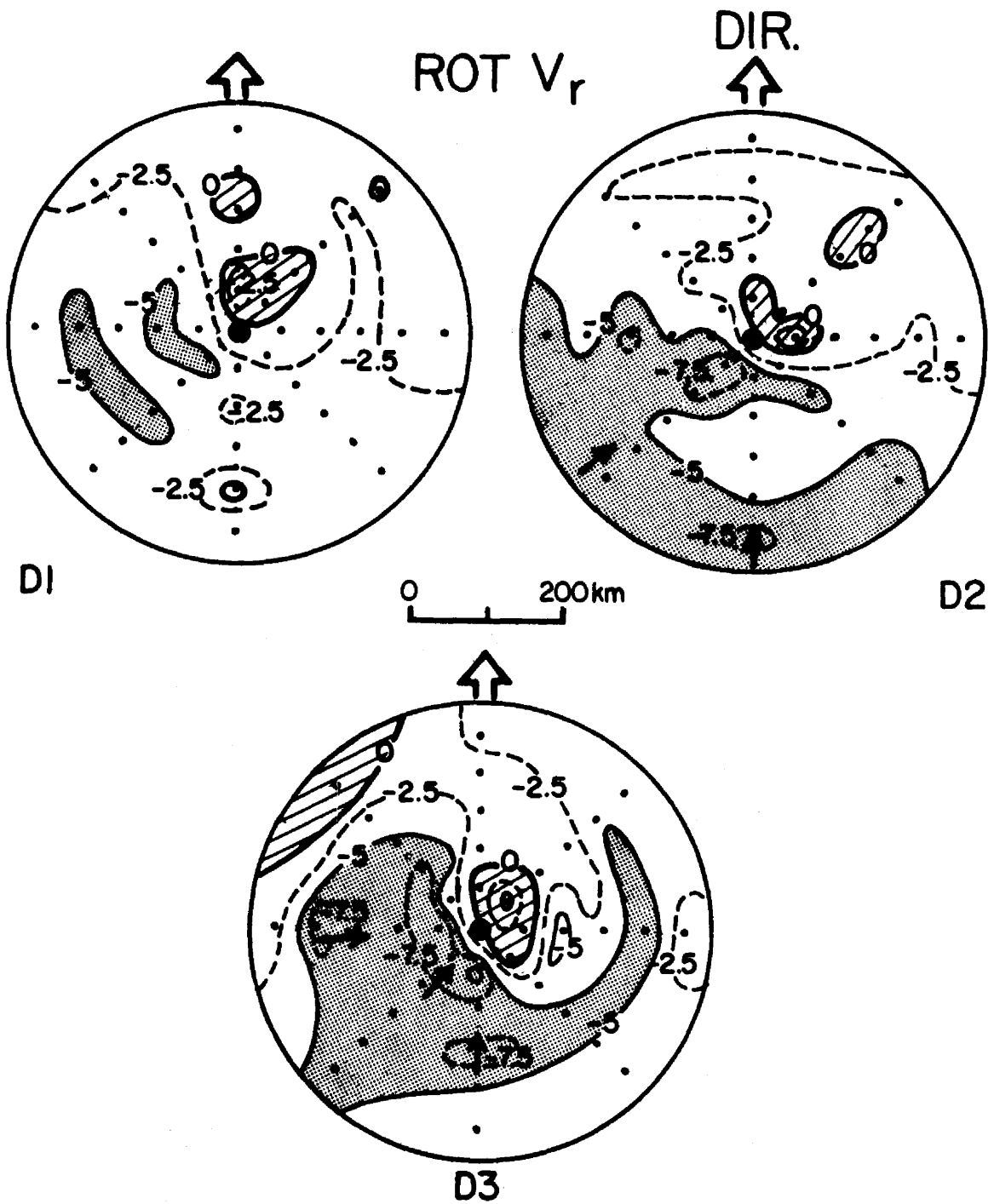


Figure 5.8: Same as Fig. 5.7, except ROT radial winds. Direction of storm motion is up the page.

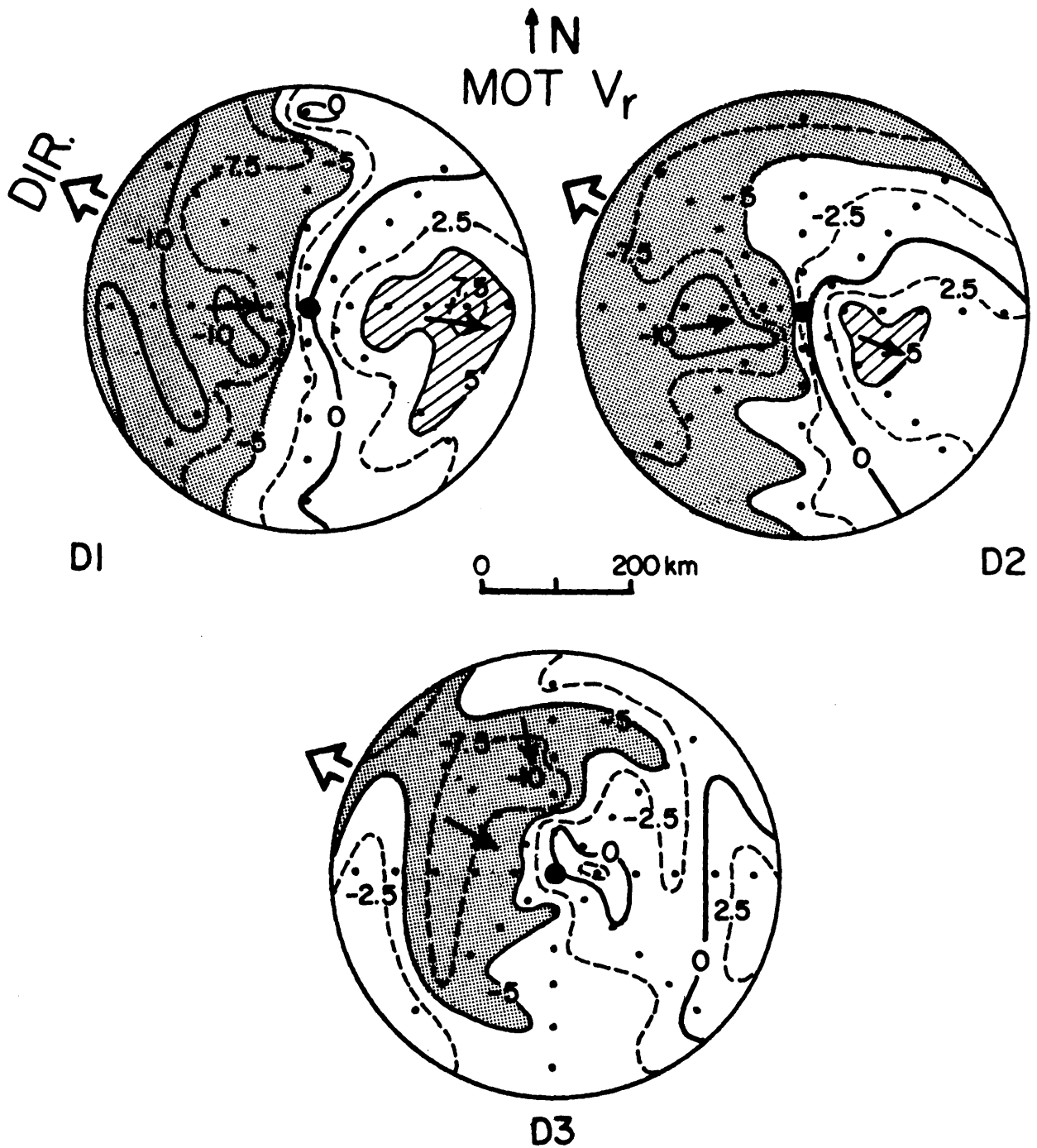


Figure 5.8: a. Same as Fig. 5.7, except MOT radial winds. North is up.

increase starts to level off between D2 and D3, in spite of the large changes that are occurring in the tangential wind and pressure fields at the same time.

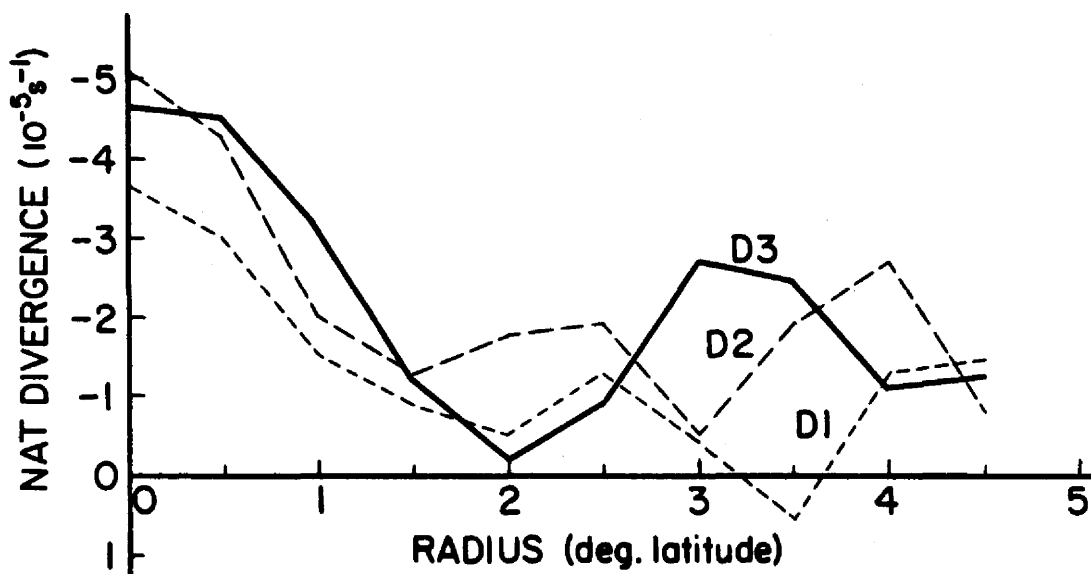


Figure 5.9: Radial profiles of NAT divergence, in units of $10^{-5} s^{-1}$, out to 4.5° latitude from the center, for D1 (early developer), D2 (middle developer), and D3 (late developer). Negative values indicate positive convergence.

These increases in the convergence are shown in detail in Fig. 5.10, where plan views of NAT divergence out to 2.5° from the center are given. In D1 the strongest convergence is 0.5° southwest of the center, with a secondary maximum just north of the center. The northern maximum vanishes in D2, but very strong convergence, exceeding $10^{-4} s^{-1}$, is now due south of the center. This southern maximum changes little in going to D3, but the northern area reappears, so that the area of convergence exceeding $4 \times 10^{-5} s^{-1}$ expands somewhat from D2 to D3. Thus, as the composite cyclone develops, the convergent area around the center strengthens and expands, but again this trend seems to be slowing down by the time stage D3 is reached.

Interestingly enough, this apparent slowing down in the increase of the low-level convergence at stage D3 seems to be confirmed by the recent work of Lee (1986). Within 1° of the centers of his rawinsonde composites, he found that mid-tropospheric upward vertical motion increases between his Stage 2 (roughly the same as D2 here) and Stage

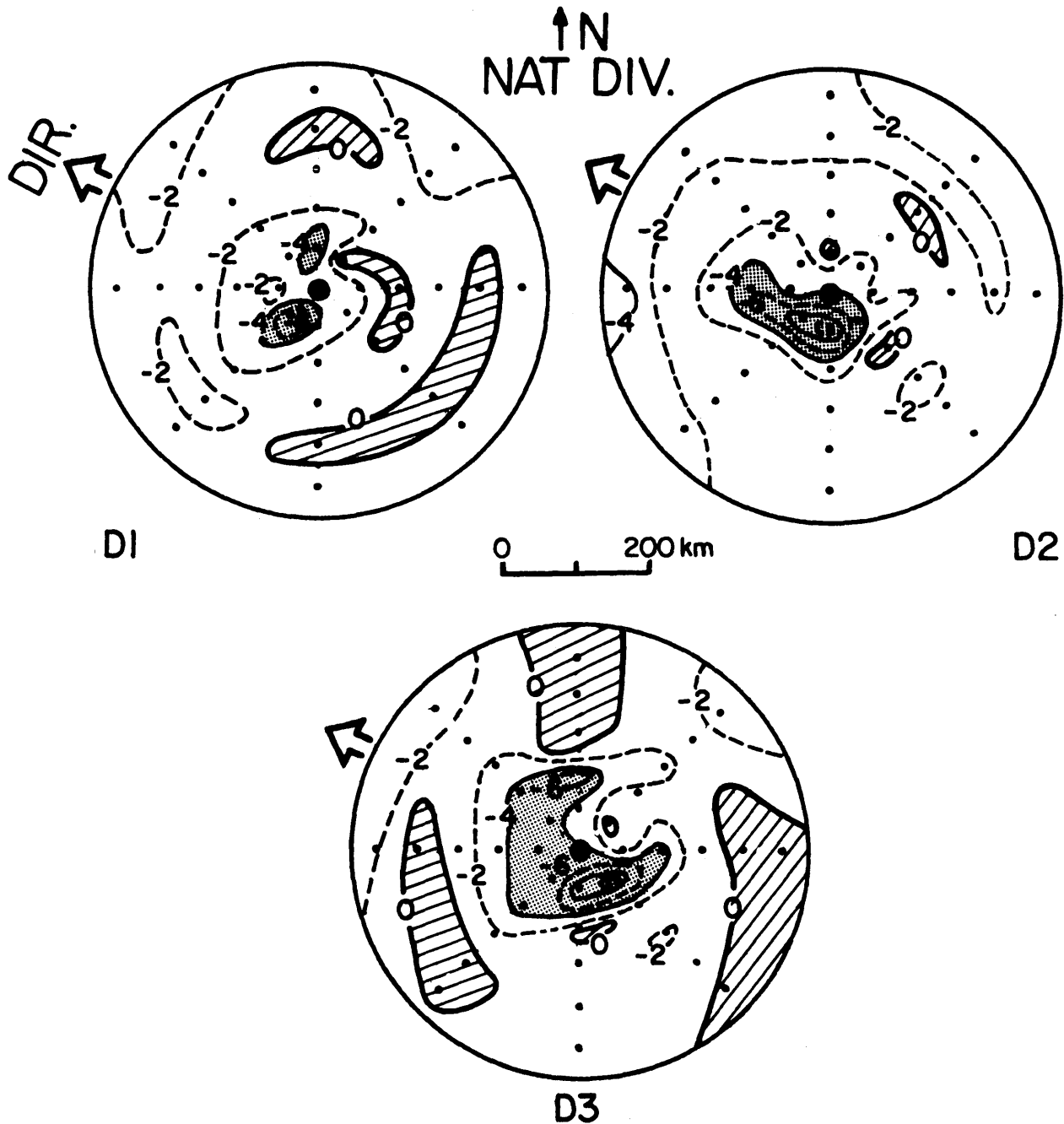


Figure 5.10: Expanded-scale plots of NAT divergence, in units of $10^{-5} s^{-1}$, for the D1 (early developer), D2 (middle developer), and D3 (late developer) composites. Grid point spacing is 0.5° (30 n mi) and the plots extend out to 2.5° radius. Heavy zero lines separate positive from negative (convergent) areas. Values of unlabelled contours can be easily inferred from the surrounding labelled contours. North is up.

3 (between this report's D2 and D3, but closer to D3). But from his Stage 3 to Stage 4 (somewhat more intense than this report's D3), this upward vertical motion actually declines somewhat. Since it is well-known that a close relationship exists between low-level convergence and upward vertical motion in developing tropical cyclones, it is likely that the slowing down seen in this report corresponds to Lee's vertical motion decline; indeed, the convergence in D3 may already be declining! Since upward vertical motion is strongly tied to moist convection, a study of satellite imagery might reveal this decline as a corresponding temporary decline in convection near the center. Lee notes that Arnold (1977) did find that the radial extent of cloudiness decreases somewhat at the depression stage (Lee's Stage 3), before increasing again later as the system reaches tropical storm intensity (Lee's Stage 4). But as was noted earlier in the discussion of vorticity, the storm can continue to intensify even though the convection (already quite strong) stays the same or even declines a bit, because of the increasing inertial stability and warming efficiency near the center.

5.2.6 Balance Between Wind and Pressure Gradient

The averaged balance parameter \bar{B} is defined and explained in Chapter 4. Radial profiles of \bar{B} calculated with an interval of integration of 60 nautical miles are shown for D1, D2, and D3 in Fig. 5.11. The large peak at a radius of 1.5° latitude for the D1 composite was noted in Chapter 4. In the D2 and D3 composites, the peak appears to move away from the center as it declines in amplitude. Indeed, except for the small rise in the D3 profile at 4°, the composite cyclone seems to be getting closer to gradient wind balance as it develops towards tropical storm intensity.

5.3 Summary of Results

1. **Sea-Level Pressure:** As expected, as the cyclone develops, sea-level pressure drops rapidly near the center, inside 2° radius, while outside that radius the pressure drops much more slowly. Pressure gradients steepen quickly near the center, but change little outside of 2°, at least up to the level of development represented by D3.

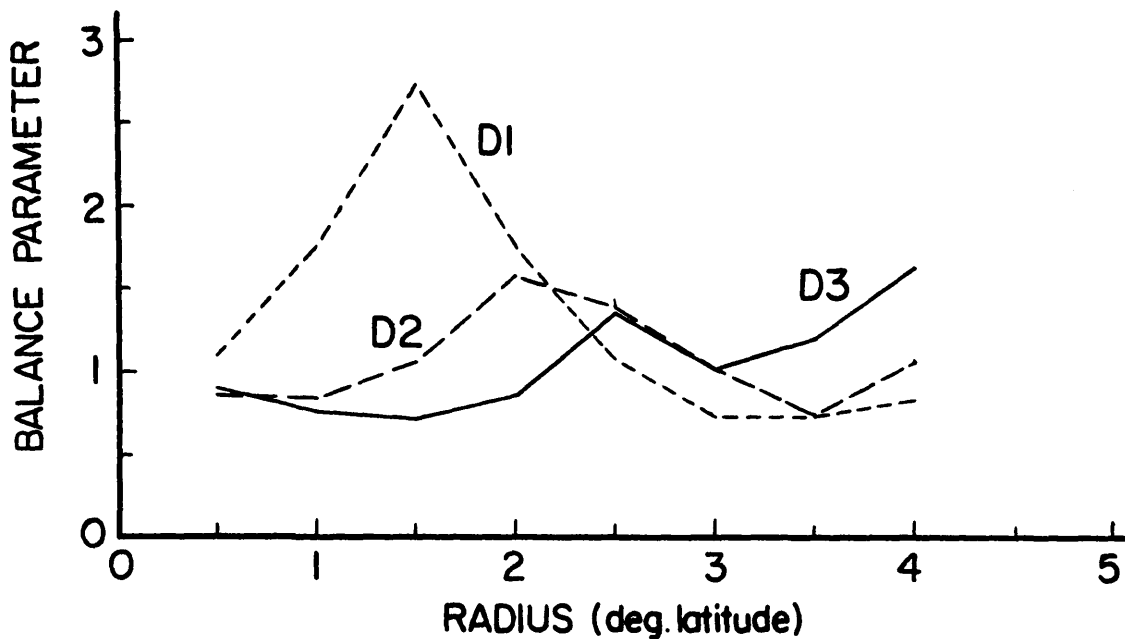


Figure 5.11: Radial profiles of \bar{B} , the averaged balance parameter, calculated over 60 n mi intervals of integration, from 0.5° to 4° radius for D1 (early developer), D2 (middle developer), and D3 (late developer). The horizontal line at $\bar{B} = 1$ indicates gradient wind balance.

2. Tangential Wind: Tangential wind increases the most within about 1° of the center. Overall, the winds increase fairly symmetrically about the center, maintaining the strongest winds to the right of the center.
3. Relative Vorticity: Vorticity increases greatly near the center, but very little outside of 2° from the center. Inertial stability increases very rapidly within 1° of the center, allowing more and more efficient use of available latent heat in that region.
4. Radial Wind and Divergence: Inward radial wind and low-level convergence both increase near the center as the cyclone develops, but the increase seems to be slowing between D2 and D3. Indeed, as Lee's work (1986) indicates, inward radial wind and convergence near the center may already be declining temporarily at the D3 stage. Nevertheless, the increasing inertial stability near the center allows the storm to continue its intensification.

- 5. Balance Parameter: The apparent surge of supergradient winds at 1.5° in D1 appears to move out from the center and decline in D2 and D3 as the composite cyclone tends toward approximate gradient balance.**

Chapter 6

PRE-STORM VS. PRE-TYPHOON

6.1 Data Sets Being Compared

This short chapter will continue the general methodology of the preceding two chapters. In Chapter 4, D1 and NON-GEN were compared with an emphasis of the factors which allowed D1 to achieve genesis. Little thought was given as to how the further development process proceeded. The question of what happens as a new cyclone develops from the incipient cyclone stage to minimal tropical storm intensity was taken up in Chapter 5, where D1, D2, and D3 were examined.

In this chapter, only developing systems are under consideration, yet the primary emphasis is not on the development process itself, but on what factors might determine whether or not a developing system ultimately reaches typhoon intensity (here defined as maximum surface wind 75 knots) or tropical storm intensity. The PRE-STM composite represents the typical developer that never develops beyond the tropical storm stage, while PRE-TY represents the typical developer that goes on to become a full-blown typhoon. Just as earlier we considered the question of why D1 goes on to be a tropical storm and NON-GEN does not, here we try to discover why PRE-TY goes on to be a typhoon and PRE-STM does not.

6.2 Comparing PRE-STM and PRE-TY

6.2.1 Sea-Level Pressure

Radial profiles of NAT sea-level pressure (SLP) are shown for PRE-STM and PRE-TY in Fig. 6.1. The two profiles are quite similar, never differing by as much as a millibar, but it is PRE-STM that has the lower SLP, all the way out to 5° latitude from the center. Both composites have about the same pressure gradients as well, except that PRE-TY has a slightly steeper gradient from the center to 1° radius.

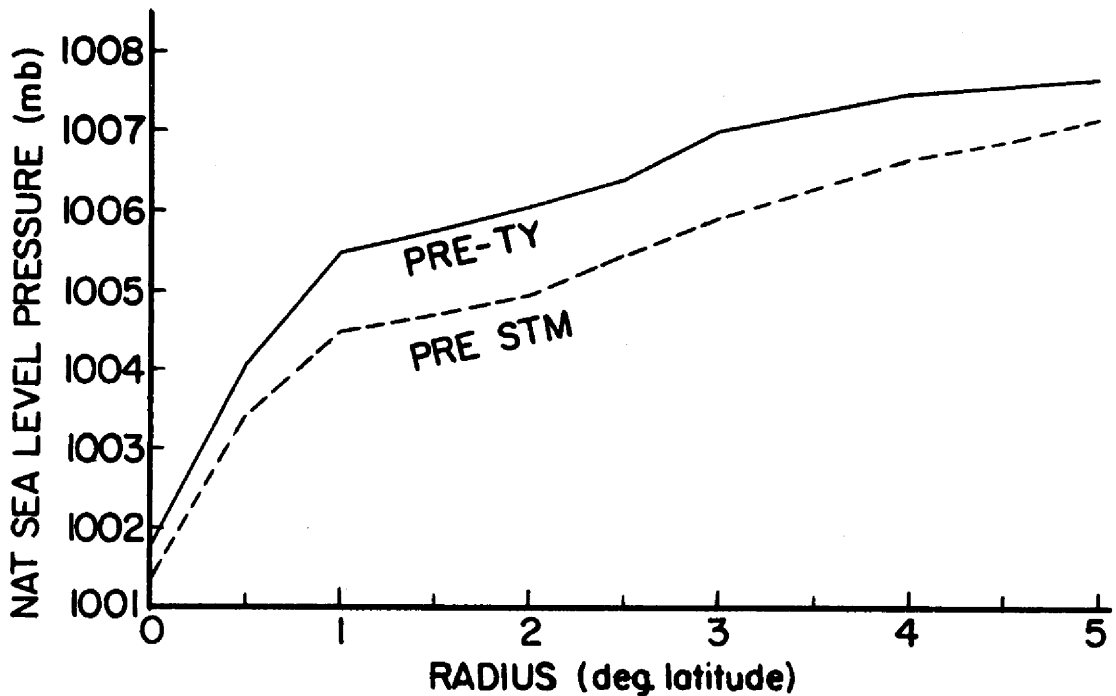


Figure 6.1: Radial profiles of NAT sea-level pressure out to 5° latitude from the center for the PRE-STM and PRE-TY composites.

6.2.2 Tangential Wind and Vorticity

Since the SLP profiles for the two composites are so similar, it comes as no surprise that the NAT tangential wind profiles are also nearly the same. As Fig. 6.2 shows, this is indeed the case. PRE-TY has slightly stronger tangential winds out to about 3.5° from

the center, but PRE-STM is only one or two knots weaker. Since both composites have winds between 12 and 15 knots out to 4° , this slight difference is not very significant.

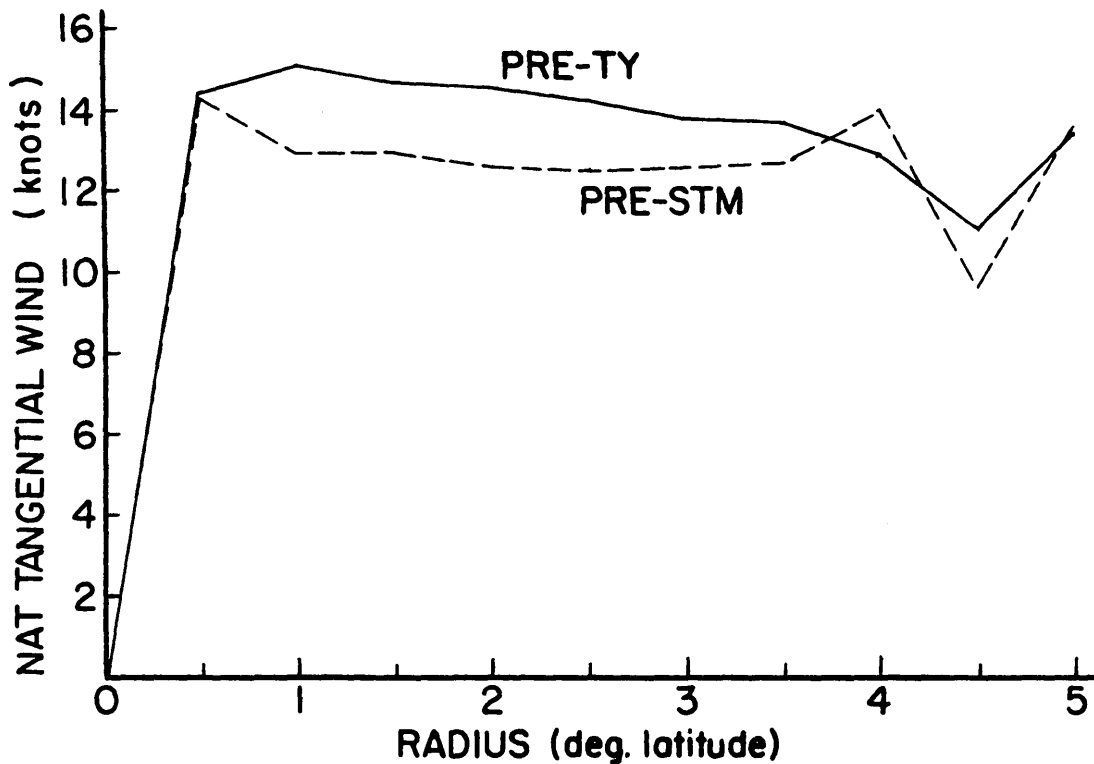


Figure 6.2: Radial profiles of NAT tangential wind, in knots, for the PRE-STM and PRE-TY composites. Note: 2 knots = 1 m/s.

Radial profiles of NAT relative vorticity are presented in Fig. 6.3. As expected, these profiles are virtually identical, with strong peaks at the center.

6.2.3 Radial Wind and Divergence

Figure 6.4 presents the radial profiles of NAT radial wind for PRE-STM and PRE-TY. In contrast to the SLP and tangential wind results, these radial wind profiles do show an important difference between the two composites. Furthermore, this difference is qualitatively the same as that between D1 and NON-GEN back in Chapter 4, as shown in Fig. 4.8 (top); that is, PRE-TY has a much stronger inward radial wind than PRE-STM inside 1.5° from the center. The difference is greatest at 1° radius, where the inward radial wind is twice as strong in the PRE-TY composite as in PRE-STM.

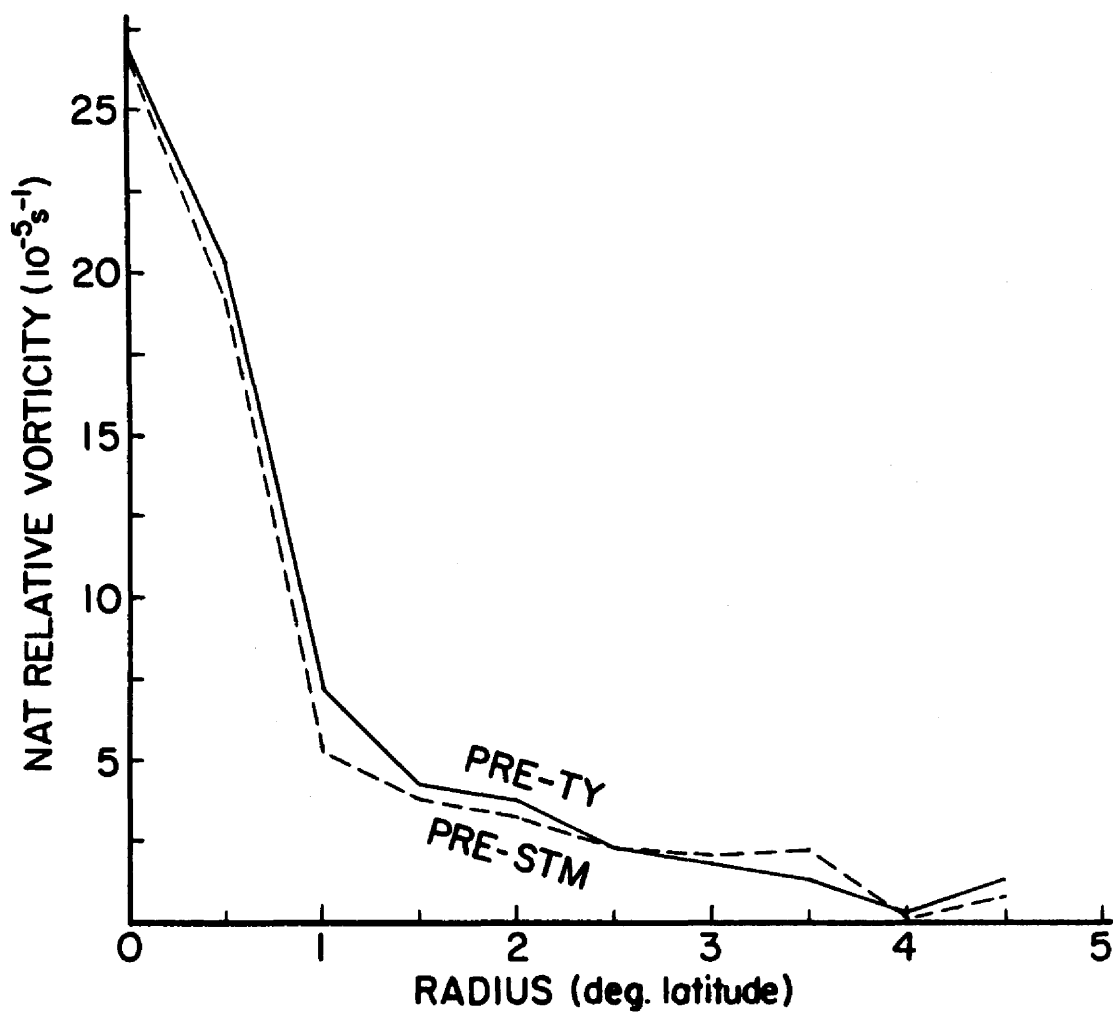


Figure 6.3: Radial profiles of NAT relative vorticity out to 4.5° latitude from the center for the PRE-STM and PRE-TY composites. The Coriolis parameter f is approximately $3.4 \times 10^{-5} s^{-1}$ for these composites.

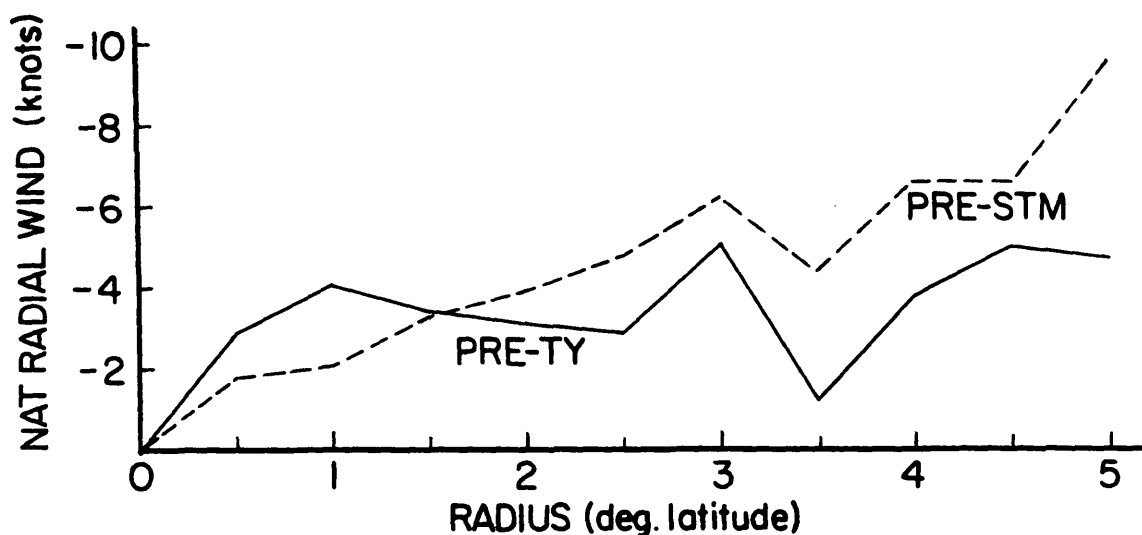


Figure 6.4: Radial profiles of NAT radial wind in knots for PRE-STM and PRE-TY. Negative values indicate inward-directed radial wind. Note: 2 knots = 1 m/s.

The corresponding profiles of NAT divergence appear in Fig. 6.5, where they show that PRE-TY has significantly stronger low-level convergence inside 1° from the center. Again, the relationship shown between PRE-TY and PRE-STM here is qualitatively the same as that between D1 and NON-GEN in Chapter 4 (see Fig. 4.9).

Detailed views of the horizontal distributions of NAT radial wind within 2.5° of the center are shown in Fig. 6.6 (upper plots). Both composites show an area of positive (outward) radial wind northwest of the center. PRE-STM has its strongest inward radial wind, exceeding 7.5 knots, in a band extending from 2° SSW of the center eastward to 2.5° SE of the center. On the other hand, the strongest inward radial wind in PRE-TY is in a concentrated area just south of the center, with magnitudes exceeding 10 knots.

Plots of the radial winds in the MOT system are appended in Fig. 6.6a. PRE-TY has a somewhat larger area of outflow in its eastern half than PRE-STM, but it also has stronger inflow coming in from the west than PRE-STM. Otherwise, there is not much to distinguish one from the other.

The plots of NAT divergence, given in the lower half of Fig. 6.6, reveal that PRE-TY has a much stronger and better-organized area of low-level convergence near the center than PRE-STM. Again, this result is similar to that for D1 and NON-GEN in chapter

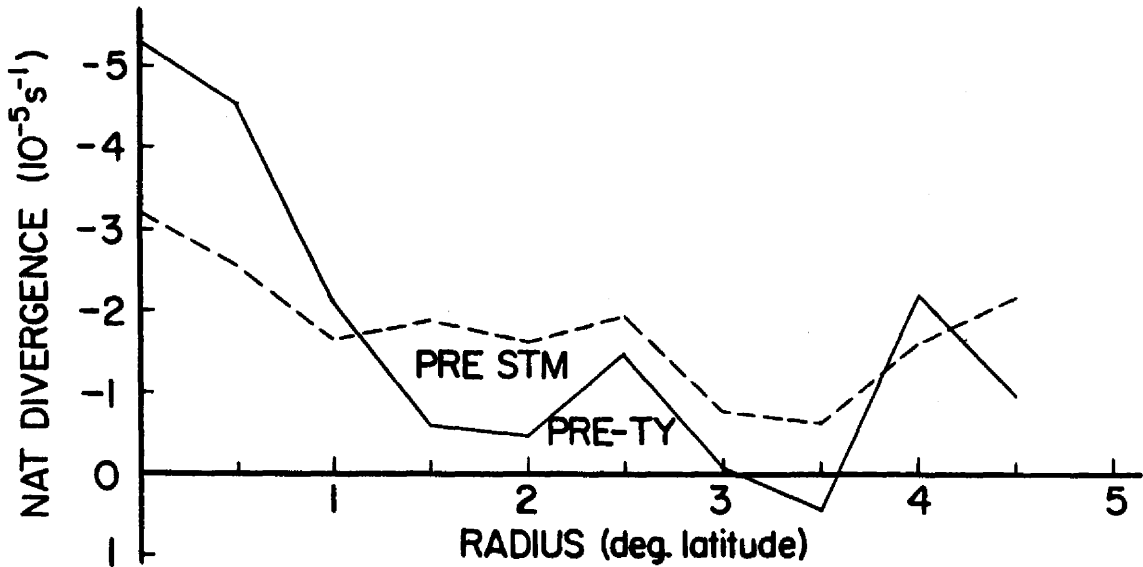


Figure 6.5: Radial profiles of NAT divergence for the PRE-STM and PRE-TY composites. Negative values indicate positive convergence.

4 (see Fig 4.10), but it should be emphasized that here even PRE-STM has an area of low-level convergence near the center that is about as strong and well-organized as D1 in Fig. 4.10. Hence, while PRE-STM may have weaker low-level convergence near the center than PRE-TY, it still has enough to distinguish it as a developer.

What is perhaps most compelling about these results is the fact that they are so consistent with the analogous results in Chapter 4 for D1 and NON-GEN. Thus, the results here support those in Chapter 4, and vice versa. Therefore, a similar conclusion can be drawn. The low-level convergence field near the center of a developing, newly-formed tropical cyclone serves as an indicator of how likely the system is to develop into a typhoon. The better-organized and stronger the convergence is, the more likely the system is to achieve typhoon status (i.e., max. surface winds 75 knots).

It cannot be said here that strong convergence at low level actually causes a system to develop past a certain intensity, but only that the convergence serves as an indicator that such development will probably take place, or is already in progress.

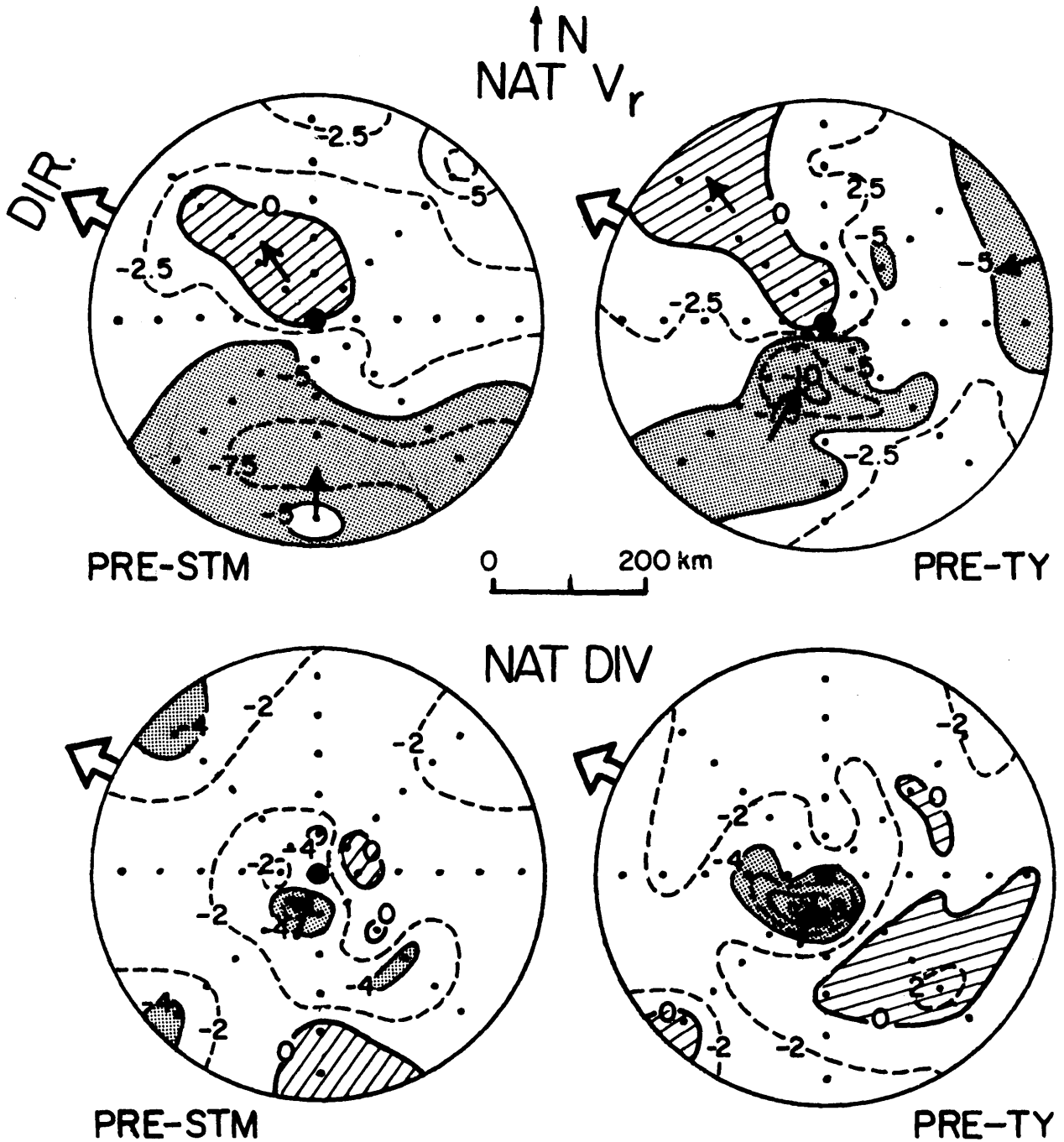


Figure 6.6: Expanded-scale plots of NAT radial wind in knots (top) and NAT divergence in units of $10^{-5}s^{-1}$ (bottom) for PRE-STM and PRE-TY. Grid point spacing is 0.5° latitude, or 30 n mi, and the plots extend out to just past 2.5° radius. In all plots, north is up and the heavy curves are zero lines, separating positive from negative areas. The values of contours left unlabelled can be easily inferred from the surrounding labelled contours.

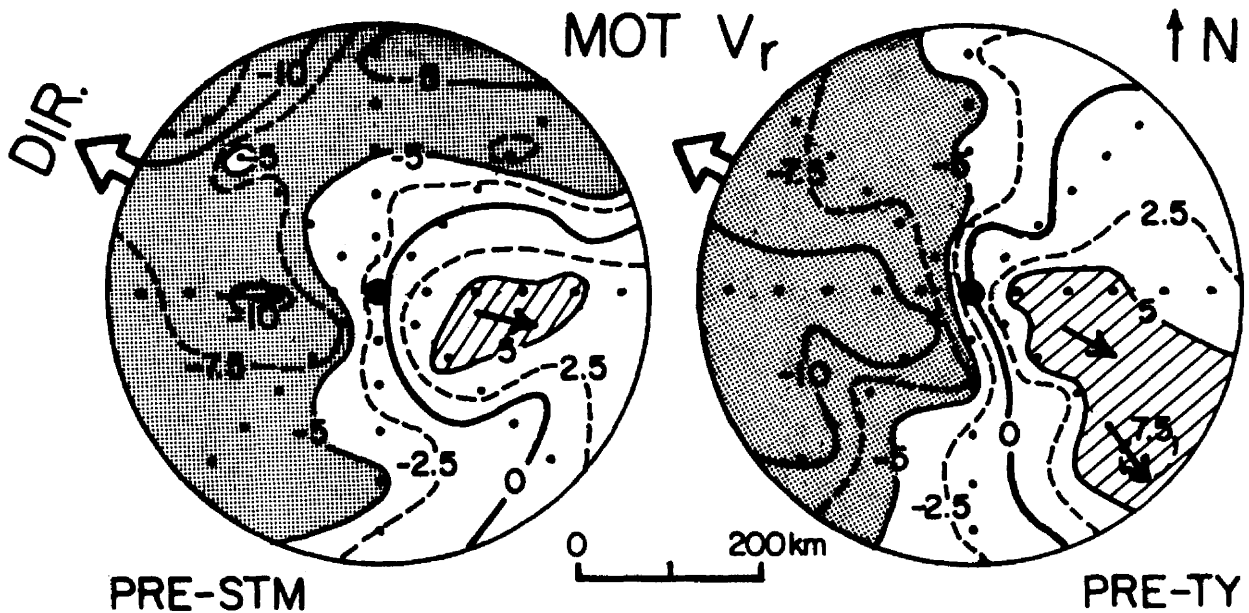


Figure 6.6: a. Expanded-scale plots of MOT radial wind in knots for PRE-STM and PRE-TY. Grid point spacing is 0.5° latitude, or 30 n mi, and the plots extend out to just past 2.5° radius. Heavy zero lines separate positive (outward) from negative (inward) radial winds. North is up.

6.2.4 Balance Between Wind and Pressure Gradient

As in the previous two chapters, the averaged balance parameter B is calculated for this chapter with a 60 nautical mile interval of integration. The radial profiles of \bar{B} for PRE-STM and PRE-TY are given in Fig. 6.7. Unlike the results of previous chapters, the two profiles here are very much the same. Both have moderate peaks at a radius of 1.5° , then drop off out to 3° from the center. Beyond that they rise slightly, with PRE-TY having a somewhat stronger rise out to 4° . If these profiles are compared with those in Fig. 5.11 in Chapter 5, the PRE-STM profile is seen to be very similar to D1. PRE-TY, on the other hand, shows signs of starting the transition to a D2 type of profile; its peak at 1.5° is smaller, a new peak may be forming at 2° , and B is increasing at 4° . But these indications, suggestive as they may be, are still very slight in magnitude and can hardly be considered conclusive, since the profiles for PRE-STM and PRE-TY are still basically identical.

6.3 Summary

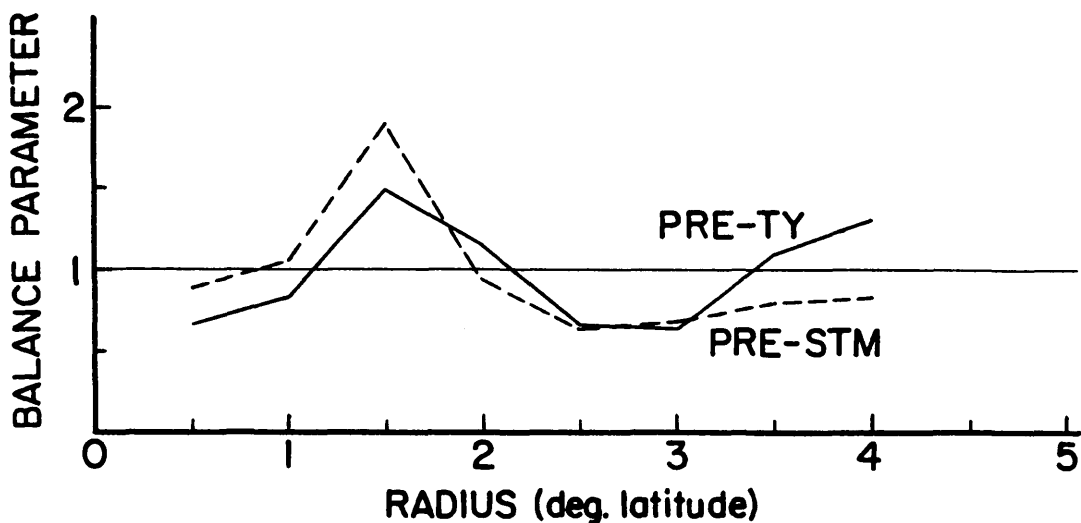


Figure 6.7: Radial profiles of \bar{B} , the averaged balance parameter, calculated over 60 n mi intervals of integration, from 0.5° to 4° radius for PRE-STM and PRE-TY. The horizontal line at $\bar{B} = 1$ indicates gradient wind balance.

1. Sea-Level Pressure: PRE-STM had slightly lower SLP at all radii; otherwise the profiles for PRE-STM and PRE-TY were virtually the same.
2. Tangential Wind and Vorticity: Again, the two composites had virtually identical profiles of both tangential wind and relative vorticity.
3. Radial Wind and Divergence: PRE-TY had significantly stronger inward radial winds than PRE-STM inside 1.5° from the center, and had a stronger and better-organized area of low-level convergence near the center as well. Significantly, these results are consistent with the corresponding results of Chapter 4 regarding D1 and NON-GEN. It is hypothesized that for a system at the stage of development represented by both PRE-STM and PRE-TY, the strength and organization of the low-level convergence field near the center are good indicators of the system's likelihood of developing into a full-blown typhoon (max. surface winds ≥ 75 knots).
4. Balance Parameter: Both profiles are about the same, and resemble the profile of D1 in Chapter 4.

Chapter 7

SUMMARY AND DISCUSSION

7.1 Summary of Results

7.1.1 Genesis vs. Non-Genesis

Ever since Gray (1975, 1979) set forth the basic climatological requirements for tropical cyclone genesis, many rawinsonde compositing studies have been conducted in an effort to identify the specific factors that determine whether or not a given class of disturbances will develop or not. Given two similar disturbances in an environment that meets Gray's conditions, why does Disturbance A undergo cyclogenesis while Disturbance B does not?

At low level, one of the most consistent results of rawinsonde composite research has been that genesis disturbances have significantly more relative vorticity over a large area (see, for example, Lee, 1986 or McBride, 1979). In this report's flight data composites, however, even the special class of non-genesis composite (NON-GEN) has such required low-level vorticity. In fact, the low-level vorticity field is virtually the same for both NON-GEN and the genesis composite D1.

It was pointed out in Chapter 4 that this is because the disturbances that went into the non-genesis composite were generally very close to being developers. But this also shows that the presence of the required vorticity, while necessary, is not sufficient as an indicator that cyclogenesis is imminent or already underway.

In the flight data composites, the only really significant differences between D1 and NON-GEN are found in the radial wind and divergence fields within 1.5° radius latitude of the center. The inward radial wind inside of 1.5° is over twice as strong in D1 as in NON-GEN, with the result that D1 has a much stronger and better-organized low-level convergence field within 1° of the center. It is worth noting that this result is beyond

the reach of rawinsonde compositing because it involves the wind field very close to the center, where rawinsonde composites are at their worst.

7.1.2 Development

While nothing very new is uncovered concerning early development at low level, the D1, D2, and D3 composites do give the first really detailed look at how the wind and pressure fields change near the center as development proceeds. Within 2° of the center, the sea-level pressure drops rapidly as development progresses from D1 to D3, while tangential wind and relative vorticity both more than double in magnitude. By contrast, radial wind and divergence undergo much smaller changes, with only a mild increase in the inward radial wind and a slight enlargement of the area of strong convergence near the center. Both of these changes seem to be slowing down in going from D2 to D3.

7.1.3 Pre-storm vs. Pre-typhoon

Although PRE-STM has slightly lower sea-level pressure overall, the tangential wind and relative vorticity fields of the two composites are virtually indistinguishable. But just as D1 has stronger inward radial winds near the center than NON-GEN, so PRE-TY has stronger radial winds than PRE-STM. PRE-TY's convergence near the center is correspondingly stronger and better-organized than PRE-STM's. In general, the similarities and differences between PRE-TY and PRE-STM parallel those between D1 and NON-GEN.

7.2 The Presence and Probable Role of Low-Level Surges

7.2.1 Radial Wind, Convergence, and Low-Level Surges

The most significant results of this study have been the large differences in the inner-core (inside of 1.5°) radial wind and convergence fields between D1 and NON-GEN, and between PRE-TY and PRE-STM. As was pointed out in Chapters 4 and 6, these results imply that D1 has stronger, better-organized convection near the center than NON-GEN, and similarly for PRE-TY over PRE-STM. Indeed, Lunney's recent work (1988) with

DMSP satellite imagery has shown that while D1 and NON-GEN have similar amounts of convection within 4° of the center, D1 has nearly twice as many convective elements in the $0\text{-}2^\circ$ range; i.e., convection is much more strongly concentrated near the center in D1 than in NON-GEN. So it appears that the question posed at the beginning of this chapter, that is, why Disturbance A achieves cyclogenesis while the similar Disturbance B does not, can be answered. Something acts on Disturbance A to enhance the low-level radial wind/convergence field near its center, which in turn strengthens the deep convection there. This then can give rise to a nonlinear, unstable intensification process in the inner core (Lee, 1986; Lunney, 1988). But what exactly is the enhancement mechanism itself?

Lee (1986) and Lunney (1988) have recently given strong evidence for the existence of environmentally induced low-level wind surges, which force mass into the disturbance's central region (inside of 1.5°). Lunney points out that these surges are not accelerated into the center by the radial pressure gradient, which is typically weak, but are driven in from the outside by large-scale environmental forces. The influx of mass, which is manifested by the increased low-level convergence near the center, results in stronger upward motion and enhanced convection. Lee (1986) notes that such surges are often observed acting on a disturbance immediately before the central convection is enhanced and the disturbance develops into a cyclone. On the other hand, as Lunney (1988) points out, such surges are generally not observed in the non-genesis cases.

In this report, the main evidence for surges appears in Chapter 4. In Fig. 4.7, both D1 and OPEN-DEV have strong NAT radial winds blowing into the center from the south and southwest, while NON-GEN and NON-DEV both lack this feature. In the MOT system (see Fig. 4.7a), strong radial winds penetrate into the centers of D1 and OPEN-DEV from the west. Finally, the profiles of the balance parameter \bar{B} in Fig. 4.13 give a good indication of supergradient tangential winds within 2° of the center in D1 and OPEN-DEV, which tends to confirm Lunney's finding that the surges are not locally pressure-driven. Hence, it appears that these momentum surges are indeed the key factor

in determining which disturbances will develop, inasmuch as they act to enhance deep convection near the center.

7.2.2 Surges and Inertial Stability

Lee (1986) has shown that not only do environmentally forced surges enhance the low-level convergence near the center, they also bring about large inward eddy vorticity fluxes. Such fluxes are necessary to account for the observed increase of tangential wind in the presence of surface frictional energy loss. Hence, the surges act simultaneously to enhance the low-level convergence near the center and to bring in the cyclonic vorticity needed to begin the spin-up of the tangential winds. The surge, being a transient phenomenon, then typically fades away as the new cyclone continues to intensify.

The early development of the new cyclone, shown both in Lee (1986) and in Chapter 5 of this report, is characterized by a radial wind/convergence field near the center that strengthens little if at all, yet the tangential wind near the center continues to increase, along with the relative vorticity. (See Figs. 5.3, 5.5, 5.6, 5.7, 5.7a, and 5.9 in Chapter 5 of this report.) It appears likely that these tangential winds and relative vorticity increases near the center are in part a response to the larger inertial stability near the center (Schubert and Hack, 1982). The center is warmed more efficiently by the latent heat released in the deep convection in that region. This in turn leads to hydrostatically induced pressure falls at low level in response to the wind increases. As inertial stability continues to increase, this warming becomes more and more efficient, until the surface pressure-falls near the center are large enough to bring the pressure field into approximate balance with the tangential wind field. Figure 5.1 shows the large pressure drops near the center, and the balance parameter plots in Fig. 5.11 show how the tangential wind comes more and more into balance with the radial pressure gradient as development proceeds.

7.3 Genesis and Development

The results of this paper support those of Lee (1986) and Lunney (1988) in identifying environmentally forced low-level surges as the most probable mechanism (once other

required large-scale favorable environmental conditions have been satisfied) for the triggering of tropical cyclogenesis in a large majority of cases in the western North Pacific. It seems especially clear that during formation and early development the low-level wind field near the center does not develop in response to the changing pressure field; rather, it is the pressure field that eventually adjusts to the wind. Thus, a typical sequence of formation/development might run as follows:

1. A tropical cloud cluster, or disturbance, forms in a region where conditions are generally favorable for tropical cyclone formation. A weak low-level cyclonic circulation forms in many cases.
2. A low-level surge (e.g., monsoon surge, cross-equatorial surge, or trade-wind surge; see Lee, 1986) penetrates to the inner region of the disturbance. (Without this surge, the disturbance typically rains itself out in a day or two, ending up as a non-genesis case.)
3. Low-level convergence and deep convection near the center are both enhanced, and eddy vorticity flux begins to spin up the vortex. At this stage, radial pressure gradients are too weak to account for the tangential winds near the center.
4. As the vortex intensifies, the surge fades, but increasing inertial stability allows intensification to proceed. The center is warmed more and more efficiently even though the convection and low-level convergence may be strengthening very little if at all.
5. Warming-induced pressure falls at the center eventually bring the pressure and tangential wind fields into approximate balance.

Of course, this scenario is somewhat simplified, if not indeed a little bit simplistic. Many details remain to be worked out as to exactly how surge disturbance interaction brings about cyclone formation and sets the stage for the subsequent early development process. It is this author's hope that much more research will be focused on this problem in the near future.

This research has shown that the divergence and vorticity fields of the early stage tropical cyclone can be quite decoupled from each other. Previous TC development theories and modeling efforts which assumed a relationship between divergence-vorticity (i.e.—the typically CISK and some of the other parameterization scheme) appear not to be physically valid in this regard. This paper may also help explain why so many of the early tropical cyclone PE modeling spin-up times have been too slow. The type of low level surge action here reported has yet to be incorporated in the numerical modeling simulations.

Chapter 8

AFTERWORD

It was with great sadness when I learned that the 54th Weather Reconnaissance Squadron and Detachment 3, 1st Weather Wing, which together comprise the Typhoon Chasers of Andersen AFB, Guam, were deactivated in August, 1987. This unfortunate action is made necessary by ever-tightening federal budget constraints; there simply isn't enough money to continue flying the storms anymore. Not only will this deprive the forecasters at the Joint Typhoon Warning Center of a vital source of data, making their already difficult job even harder, it will cut off an invaluable source of data for tropical cyclone research.

As a former ARWO who flew with the 54th for three years, I am well acquainted with the proud tradition of safe mission accomplishment that has always characterized the Typhoon Chasers. I am very sorry to see them go, but at the same time I feel fortunate indeed that I was permitted to share their adventures for three wonderful years.

Michael G. Middlebrooke

7 September, 1987

ACKNOWLEDGEMENTS

The author would like to thank Professor William M. Gray for his guidance and strong encouragement in this research endeavor. I would also like to thank Captains Roger Edson and Candis Weatherford for many beneficial discussions on this topic and to William Thorson and Ms. Barbara Brumit for very valuable programming and manuscript preparation support.

The author is grateful to the US Air Force for support of the author's graduate studies at CSU. The National Science Foundation Grants No. ATM-8419116 and ATM-8418204 gave necessary financial support to various aspects of this observational study.

REFERENCES

- Arnold, C. P., 1977: Tropical cyclone cloud and intensity relationships. Dept. of Atmos. Sci. Paper No. 277, Colo. State Univ. Fort Collins, CO, 154 pp.
- Colon, J. A. and Staff, NHRP, 1961: On the structure of Hurricane Daisy (1958). NHRP Report No. 48, 102 pp.
- Colon, J. A. and Staff, NHRP, 1964: On the structure of Hurricane Helene (1958). NHRP Report No. 72, 50 pp.
- Erickson, S. L., 1977: Comparison of developing vs. non-developing tropical disturbances. Dept. of Atmos. Sci. Paper No. 274, Colo. State Univ., Fort Collins, CO, 81 pp.
- Frank, W. M., 1977: The structure and energetics of the tropical cyclone, I: Storm structure. *Mon. Wea. Rev.*, 105, 1119-1135.
- Frank, W. M., 1984: Composite analysis of the core of Hurricane Frederick 1979. *Mon. Wea. Rev.*, 112, 2401-2420.
- Gray, W. M., 1962: On the balance of forces and radial accelerations in hurricanes. *Quart. J. Roy. Meteor. Soc.*, 378, 430-458.
- Gray, W. M., 1968: Global view of the origin of tropical disturbances and storms. *Mon. Wea. Rev.*, 96, 669-700.
- Gray, W. M., 1975: Tropical cyclone genesis. Dept. of Atmos. Sci. Paper No. 234, Colo. State Univ., Fort Collins, CO, 119 pp.
- Gray, W. M., 1979: Hurricanes: their formation, structure and likely role in the tropical circulation. Supplement to *Meteorology Over the Tropical Oceans*. Published by RMS, James Glaisher House, Grenville Place, Bracknell, Berkshire, RG 12 1BX, D. B. Shaw, ed., 155-218.
- Gray, W. M., 1981: Recent advances in tropical cyclone research from rawinsonde composite analysis. Paper prepared for the WMO Committee of Atmospheric Science, Geneva, Switzerland, 407 pp.
- Hawkins, H. F., 1971: Comparison of results of the Hurricane Debbie (1969) modification experiments with those from Rosenthal's numerical model simulation experiments. *Mon. Wea. Rev.*, 99, 427-434.
- Hawkins, H. F. and S. M. Imbembo, 1976: The structure of a small intense hurricane—Inez 1966. *Mon. Wea. Rev.*, 104, 418-442.

- Hawkins, H. F. and D. T. Rubsam, 1968: Hurricane Hilda, 1964. I: Genesis, as revealed by satellite photographs conventional and aircraft data. *Mon. Wea. Rev.*, 96, 428-452.
- Henderson, R. S., 1978: USAF Aerial Weather Reconnaissance using the Lockheed WC-130 Aircraft. *Bull. Amer. Meteor. Soc.*, 59, 1136-1143.
- Hughes, L. A., 1952: On the low-level wind structure of tropical cyclones. *J. Meteor.*, 9, 422-428.
- Joint Typhoon Warning Center (JTWC), 1977: Annual typhoon report. US Naval Oceanography Command Center, Joint Typhoon Warning Center, COMNAVMARIANAS Box 17, FPO San Francisco, 96630.
- Joint Typhoon Warning Center (JTWC), 1978: Annual typhoon report. US Naval Oceanography Command Center, Joint Typhoon Warning Center, COMNAVMARIANAS Box 17, FPO San Francisco, 96630.
- Joint Typhoon Warning Center (JTWC), 1979: Annual typhoon report. US Naval Oceanography Command Center, Joint Typhoon Warning Center, COMNAVMARIANAS Box 17, FPO San Francisco, 96630.
- Joint Typhoon Warning Center (JTWC), 1980: Annual tropical cyclone report. US Naval Oceanography Command Center, Joint Typhoon Warning Center, COMNAVMARIANAS Box 17, FPO San Francisco, 96630, NTIS AD A094668, 185 pp.
- Joint Typhoon Warning Center (JTWC), 1981: Annual tropical cyclone report. US Naval Oceanography Command Center, Joint Typhoon Warning Center, COMNAVMARIANAS Box 17, FPO San Francisco, 96630, NTIS AD A112002, 194 pp.
- Joint Typhoon Warning Center (JTWC), 1982: Annual tropical cyclone report. US Naval Oceanography Command Center, Joint Typhoon Warning Center, COMNAVMARIANAS Box 17, FPO San Francisco, 96630, NTIS AD A124860, 236 pp.
- Joint Typhoon Warning Center (JTWC), 1983: Annual tropical cyclone report. US Naval Oceanography Command Center, Joint Typhoon Warning Center, COMNAVMARIANAS Box 17, FPO San Francisco, 96630, 195 pp.
- Joint Typhoon Warning Center (JTWC), 1984: Annual tropical cyclone report. US Naval Oceanography Command Center, Joint Typhoon Warning Center, COMNAVMARIANAS Box 17, FPO San Francisco, 96630, 219 pp.
- Jordan, C. L., D. A. Hurt and C. A. Lowry, 1960: On the structure of Hurricane Daisy of 27 August 1958. *J. Meteor.*, 17, 337-348.
- Jorgensen, D. P., 1984: Mesoscale and convective scale characteristics of mature hurricanes. I. General observations by research aircraft. *J. Atmos. Sci.*, 41, 1268-1285.
- Lee, C.-S., 1986: An observational study of tropical cloud cluster evolution and cyclogenesis in the western North Pacific. Dept. of Atmos. Sci. Paper No. 403, Colo. State Univ., Fort Collins, CO, 250 pp.
- Lunney, P. A., 1988: Environmental and convective influence on tropical cyclone development vs. non-development. Forthcoming Dept. of Atmos. Sci. Paper, Colo. State Univ., Ft. Collins, CO, 95 pp.

- McBride, J. L., 1979: Observational analysis of tropical cyclone formation. Dept. of Atmos. Sci. Paper No. 308, Colo. State Univ., Fort Collins, CO, 230 pp.
- Riehl, H., and J. Malkus, 1961: Some aspects of Hurricane Daisy, 1958. *Tellus*, 13, 181-213.
- Schubert, W. H. and J. J. Hack, 1982: Inertial stability and tropical cyclone development. *J. Atmos. Sci.*, 39, 1687-1697.
- Sheets, R. C., 1967a: On the structure of Hurricane Janice (1958). NHRL Report No. 76, 38 pp.
- Sheets, R. C., 1967b: On the structure of Hurricane Ella (1962). NHRL Report No. 77, 33 pp.
- Sheets, R. C., 1968: On the structure of Hurricane Dora (1964). NHRL Report No. 83, 64 pp.
- Weatherford, C. L., 1985: Typhoon structural variability. Dept. of Atmos. Sci. Paper No. 391, Colo. State Univ., Fort Collins, CO, 75 pp.
- Weatherford, C., and W. M. Gray, 1988a: Typhoon structure as revealed by aircraft reconnaissance: Part I: Data analysis and climatology. *Mon. Wea. Rev.*, June issue.
- Weatherford, C., and W. M. Gray, 1988b: Typhoon structure as revealed by aircraft reconnaissance: Part II: Structural variability. *Mon. Wea. Rev.*, June issue.
- Zehr, R., 1976: Tropical disturbance intensification. Dept. of Atmos. Sci. Paper No. 259, Colo. State Univ., Fort Collins, CO, 91 pp.

Appendix A

W. M. GRAY'S FEDERALLY SUPPORTED RESEARCH PROJECT REPORTS SINCE 1967

CSU Dept. of
Atmos. Sci.

<u>Report No.</u>	<u>Report Title, Author, Date, Agency Support</u>
104	The Mutual Variation of Wind, Shear and Baroclinicity in the Cumulus Convective Atmosphere of the Hurricane (69 pp.). W. M. Gray. February 1967. NSF Support.
114	Global View of the Origin of Tropical Disturbances and Storms (105 pp.). W. M. Gray. October 1967. NSF Support.
116	A Statistical Study of the Frictional Wind Veering in the Planetary Boundary Layer (57 pp.). B. Mendenhall. December 1967. NSF and ESSA Support.
124	Investigation of the Importance of Cumulus Convection and ventilation in Early Tropical Storm Development (88 pp.). R. Lopez. June 1968. ESSA Satellite Lab. Support.
Unnumbered	Role of Angular Momentum Transports in Tropical Storm Dissipation over Tropical Oceans (46 pp.). R. F. Wachtmann. December 1968. NSF and ESSA Support.
Unnumbered	Monthly Climatological Wind Fields Associated with Tropical Storm Genesis in the West Indies (34 pp.). J. W. Sartor. December 1968. NSF Support.
140	Characteristics of the Tornado Environment as Deduced from Proximity Soundings (55 pp.). T. G. Wills. June 1969. NOAA and NSF Support.
161	Statistical Analysis of Trade Wind Cloud Clusters in the Western North Pacific (80 pp.). K. Williams. June 1970. ESSA Satellite Lab. Support.
—	A Climatology of Tropical Cyclones and Disturbances of the Western Pacific with a Suggested Theory for Their Genesis/Maintenance (225 pp.). W. M. Gray. NAVWEARSCHFAC Tech. Paper No. 19-70. November 1970. (Available from US Navy, Monterey, CA). US Navy Support.

CSU Dept. of
Atmos. Sci.

<u>Report No.</u>	<u>Report Title, Author, Date, Agency Support</u>
179	A diagnostic Study of the Planetary Boundary Layer over the Oceans (95 pp.). W. M. Gray. February 1972. Navy and NSF Support.
182	The Structure and Dynamics of the Hurricane's Inner Core Area (105 pp.). D. J. Shea. April 1972. NOAA and NSF Support.
188	Cumulus Convection and Larger-scale Circulations, Part I: A Parametric Model of Cumulus Convection (100 pp.). R. E. Lopez. June 1972. NSF Support.
189	Cumulus Convection and Larger-scale Circulations, Part II: Cumulus and Meso-scale Interactions (63 pp.). R. E. Lopez. June 1972. NSF Support.
190	Cumulus Convection and Larger-scale Circulations, Part III: Broadscale and Meso-scale Considerations (80 pp.). W. M. Gray. July 1972. NOAA-NESS Support.
195	Characteristics of Carbon Black Dust as a Tropospheric Heat Source for Weather Modification (55 pp.). W. M. Frank. January 1973. NSF Support.
196	Feasibility of Beneficial Hurricane Modification by Carbon Black Seeding (130 pp.). W. M. Gray. April 1973. NOAA Support.
199	Variability of Planetary Boundary Layer Winds (157 pp.). L. R. Hoxit. May 1973. NSF Support.
200	Hurricane Spawned Tornadoes (57 pp.). D. J. Novlan. May 1973. NOAA and NSF Support.
212	A Study of Tornado Proximity Data and an Observationally Derived Model of Tornado Genesis (101 pp.). R. Maddox. November 1973. NOAA Support.
219	Analysis of Satellite Observed Tropical Cloud Clusters (91 pp.). E. Ruprecht and W. M. Gray. May 1974. NOAA/NESS Support.
224	Precipitation Characteristics in the Northeast Brazil Dry Region (56 pp.). R. P. L. Ramos. May 1974. NSF Support.
225	Weather Modification through Carbon Dust Absorption of Solar Energy (190 pp.). W. M. Gray, W. M. Frank, M. L. Corrin, and C. A. Stokes. July 1974.
234	Tropical Cyclone Genesis (121 pp.). W. M. Gray. March 1975. NSF Support.

CSU Dept. of
Atmos. Sci.

<u>Report No.</u>	<u>Report Title, Author, Date, Agency Support</u>
—	Tropical Cyclone Genesis in the Western North Pacific (66 pp.). W. M. Gray. March 1975. US Navy Environmental Prediction Research Facility Report. Tech. Paper No. 16-75. (Available from the US Navy, Monterey, CA). Navy Support.
241	Tropical Cyclone Motion and Surrounding Parameter Relationships (105 pp.). J. E. George. December 1975. NOAA Support.
243	Diurnal Variation of Oceanic Deep Cumulus Convection. Paper I: Observational Evidence, Paper II: Physical Hypothesis (106 pp.). R. W. Jacobson, Jr. and W. M. Gray. February 1976. NOAA-NESS Support.
257	Data Summary of NOAA's Hurricanes Inner-Core Radial Leg Flight Penetrations 1957-1967, and 1969 (245 pp.). W. M. Gray and D. J. Shea. October 1976. NSF and NOAA Support.
258	The Structure and Energetics of the Tropical Cyclone (180 pp.). W. M. Frank. October 1976. NOAA-NHEML, NOAA-NESS and NSF Support.
259	Typhoon Genesis and Pre-typhoon Cloud Clusters (79 pp.). R. M. Zehr. November 1976. NSF Support.
Unnumbered	Severe Thunderstorm Wind Gusts (81 pp.). G. W. Walters. December 1976. NSF Support.
262	Diurnal Variation of the Tropospheric Energy Budget (141 pp.). G. S. Foltz. November 1976. NSF Support.
274	Comparison of Developing and Non-developing Tropical Disturbances (81 pp.). S. L. Erickson. July 1977. US Army Support.
—	Tropical Cyclone Research by Data Compositing (79 pp.). W. M. Gray and W. M. Frank. July 1977. US Navy Environmental Prediction Research Facility Report. Tech. Paper No. 77-01. (Available from the US Navy, Monterey, CA). Navy Support.
277	Tropical Cyclone Cloud and Intensity Relationships (154 pp.). C. P. Arnold. November 1977. US Army and NHEML Support.
297	Diagnostic Analyses of the GATE A/B-scale Area at Individual Time Periods (102 pp.). W. M. Frank. November 1978. NSF Support.
298	Diurnal Variability in the GATE Region (80 pp.). J. M. Dewart. November 1978. NSF Support.
299	Mass Divergence in Tropical Weather Systems, Paper I: Diurnal Variation; Paper II: Large-scale Controls on Convection (109 pp.). J. L. McBride and W. M. Gray. November 1978. NOAA-NHEML Support.

CSU Dept. of

Atmos. Sci.

Report No.

Report Title, Author, Date, Agency Support

- New Results of Tropical Cyclone Research from Observational Analysis (108 pp.). W. M. Gray and W. M. Frank. June 1978. US Navy Environmental Prediction Research Facility Report. Tech. Paper No. 78-01. (Available from the US Navy, Monterey, CA). Navy Support.
- 305 Convection Induced Temperature Change in GATE (128 pp.). P. G. Grube. February 1979. NSF Support.
- 308 Observational Analysis of Tropical Cyclone Formation (230 pp.). J. L. McBride. April 1979. NOAA-NHEML, NSF and NEPRF Support.
- Tropical Cyclone Origin, Movement and Intensity characteristics Based on Data Compositing Techniques (124 pp.). W. M. Gray. August 1979. US Navy Environmental Prediction Research Facility Report. Tech. Paper No. CR-79-06. (Available from the US Navy, Monterey, CA). Navy Support.
- Further Analysis of Tropical Cyclone Characteristics from Rawinsonde Compositing Techniques (129 pp.). W. M. Gray. March 1981. US Navy Environmental Prediction Research Facility Report. Tech. Paper No. CR-81-02. (Available from the US Navy, Monterey, CA). Navy Support.
- 333 Tropical Cyclone Intensity Change—A Quantitative Forecasting Scheme. K. M. Dropco. May 1981. NOAA Support.
- Recent Advances in Tropical Cyclone Research from Rawinsonde Composite Analysis (407 pp.). WMO Publication. W. M. Gray. 1981.
- 340 The Role of the General Circulation in Tropical Cyclone Genesis (230 pp.). G. Love. April 1982. NSF Support.
- 341 Cumulus Momentum Transports in Tropical Cyclones (78 pp.). C. S. Lee. May 1982. ONR Support.
- 343 Tropical Cyclone Movement and Surrounding Flow Relationships (68 pp.). J. C. L. Chan and W. M. Gray. May 1982. ONR Support.
- 346 Environmental Circulations Associated with Tropical Cyclones Experiencing Fast, Slow and Looping Motions (273 pp.). J. Xu and W. M. Gray. May 1982. NOAA and NSF Support.
- 348 Tropical Cyclone Motion: Environmental Interaction Plus a Beta Effect (47 pp.). G. J. Holland. May 1982. ONR Support.
- Tropical Cyclone and Related Meteorological Data Sets Available at CSU and Their Utilization (186 pp.). W. M. Gray, E. Buzzell, G. Burton and Other Project Personnel. February 1982. NSF, ONR, NOAA, and NEPRF Support.

CSU Dept. of
Atmos. Sci.

<u>Report No.</u>	<u>Report Title, Author, Date, Agency Support</u>
352	A Comparison of Large and Small Tropical Cyclones (75 pp.). R. T. Merrill. July 1982. NOAA and NSF Support.
358	On the Physical Processes Responsible for Tropical Cyclone Motion (200 pp.). Johnny C. L. Chan. November 1982. NSF, NOAA/NHRL and NEPRF Support.
363	Tropical Cyclones in the Australian/Southwest Pacific Region (264 pp.). Greg J. Holland. March 1983. NSF, NOAA/NHRL and Australian Government Support.
370	Atlantic Seasonal Hurricane Frequency, Part I: El Nino and 30 mb QBO Influences; Part II: Forecasting Its Variability (105 pp.). W. M. Gray. July 1983. NSF Support.
379	A Statistical Method for One- to Three-Day Tropical Cyclone Track Prediction (201 pp.). Clifford R. Matsumoto. December, 1984. NSF/NOAA and NEPRF support.
—	Varying Structure and Intensity Change Characteristics of Four Western North Pacific Tropical Cyclones. (100 pp.). Cecilia A. Askue and W. M. Gray. October 1984. US Navy Environmental Prediction Research Facility Report No. CR 84-08. (Available from the US Navy, Monterey, CA). Navy Support.
—	Characteristics of North Indian Ocean Tropical Cyclone Activity. (108 pp.). Cheng-Shang Lee and W. M. Gray. December 1984. US Navy Environmental Prediction Research Facility Report No. CR 84-11. (Available from the US Navy, Monterey, CA). Navy Support.
391	Typhoon Structural Variability. (77 pp.). Candis L. Weatherford. October, 1985. NSF/NOAA Support.
392	Global View of the Upper Level Outflow Patterns Associated with Tropical Cyclone Intensity Change During FGGE. (126 pp.). L. Chen and W. Gray. October, 1985. NASA support.
394	Environmental Influences on Hurricane Intensification. (156 pp.). Robert T. Merrill. December, 1985. NSF/NOAA Support.
403	An Observational Study of Tropical Cloud Cluster Evolution and Cyclogenesis in the Western North Pacific. (250 pp.). Cheng-Shang Lee. September, 1986. NSF/NOAA support.
—	Factors Influencing Tropical Cyclone Genesis as Determined from Aircraft Investigative Flights into Developing and Non-Developing Tropical Disturbances in the Western North Pacific. (94 pp.). Michael Middlebrooke. June, 1988. NSF/NOAA support.

CSU Dept. of

Atmos. Sci.

Report No.

Report Title, Author, Date, Agency Support

- | | |
|-----|---|
| — | Recent Colorado State University Tropical Cyclone Research of Interest to Forecasters. (115 pp.). William M. Gray. June, 1987. US Navy Environmental Prediction Research Facility Contractor Report CR 87-10. Available from US Navy, Monterey, CA. Navy support. |
| 428 | Tropical Cyclone Observation and Forecasting With and Without Aircraft Reconnaissance. (105 pp.) Joel D. Martin. May, 1988. USAF, NWS, ONR support. |
| — | Environmental and convective influence on tropical cyclone development vs. non-development. Patrick A. Lunney. June, 1988. |
| — | Typhoon structural evolution. Candis Weatherford. June, 1988. |

Author: Michael G. Middlebrooke
(P.I.: William M. Gray)

INVESTIGATION OF TROPICAL CYCLONE GENESIS AND
DEVELOPMENT USING LOW-LEVEL AIRCRAFT FLIGHT DATA

Colorado State University
Department of Atmospheric Science
Fort Collins, CO 80523

Subject Headings
Tropical cyclones
Aircraft flight data
Tropical cyclone genesis

US Air Force
NSF/NOAA Grant No. ATM-8419116

Low-level wind and pressure observations from aircraft weather reconnaissance missions flown in the western North Pacific were composited on a polar coordinate grid. The observations are from eight years of US Air Force investigative and center-fix missions flown into both developing and non-developing tropical disturbances in the western North Pacific during the period 1977-1984. The missions were separated into various categories depending on the type of disturbance that were flown in; e.g., genesis vs. non-genesis, or development stage 1, 2, or 3, or pre-tropical storm vs. pre-typhoon. Data composites were made for each category.

Author: Michael G. Middlebrooke
(P.I.: William M. Gray)

INVESTIGATION OF TROPICAL CYCLONE GENESIS AND
DEVELOPMENT USING LOW-LEVEL AIRCRAFT FLIGHT DATA

Colorado State University
Department of Atmospheric Science
Fort Collins, CO 80523

Subject Headings
Tropical cyclones
Aircraft flight data
Tropical cyclone genesis

US Air Force
NSF/NOAA Grant No. ATM-8419116

Low-level wind and pressure observations from aircraft weather reconnaissance missions flown in the western North Pacific were composited on a polar coordinate grid. The observations are from eight years of US Air Force investigative and center-fix missions flown into both developing and non-developing tropical disturbances in the western North Pacific during the period 1977-1984. The missions were separated into various categories depending on the type of disturbance that were flown in; e.g., genesis vs. non-genesis, or development stage 1, 2, or 3, or pre-tropical storm vs. pre-typhoon. Data composites were made for each category.

Author: Michael G. Middlebrooke
(P.I.: William M. Gray)

INVESTIGATION OF TROPICAL CYCLONE GENESIS AND
DEVELOPMENT USING LOW-LEVEL AIRCRAFT FLIGHT DATA

Colorado State University
Department of Atmospheric Science
Fort Collins, CO 80523

Subject Headings
Tropical cyclones
Aircraft flight data
Tropical cyclone genesis

US Air Force
NSF/NOAA Grant No. ATM-8419116

Low-level wind and pressure observations from aircraft weather reconnaissance missions flown in the western North Pacific were composited on a polar coordinate grid. The observations are from eight years of US Air Force investigative and center-fix missions flown into both developing and non-developing tropical disturbances in the western North Pacific during the period 1977-1984. The missions were separated into various categories depending on the type of disturbance that were flown in; e.g., genesis vs. non-genesis, or development stage 1, 2, or 3, or pre-tropical storm vs. pre-typhoon. Data composites were made for each category.

Author: Michael G. Middlebrooke
(P.I.: William M. Gray)

INVESTIGATION OF TROPICAL CYCLONE GENESIS AND
DEVELOPMENT USING LOW-LEVEL AIRCRAFT FLIGHT DATA

Colorado State University
Department of Atmospheric Science
Fort Collins, CO 80523

Subject Headings
Tropical cyclones
Aircraft flight data
Tropical cyclone genesis

US Air Force
NSF/NOAA Grant No. ATM-8419116

Low-level wind and pressure observations from aircraft weather reconnaissance missions flown in the western North Pacific were composited on a polar coordinate grid. The observations are from eight years of US Air Force investigative and center-fix missions flown into both developing and non-developing tropical disturbances in the western North Pacific during the period 1977-1984. The missions were separated into various categories depending on the type of disturbance that were flown in; e.g., genesis vs. non-genesis, or development stage 1, 2, or 3, or pre-tropical storm vs. pre-typhoon. Data composites were made for each category.